The Institute of Paper Science and Technology

Atlanta, Georgia

Doctor's Dissertation

Polyelectrolyte Adsorption Kinetics

Matthew H. Lang

January, 1994

POLYELECTROLYTE ADSORPTION KINETICS

A thesis submitted by

Matthew H. Lang

B.S. 1988, St. Norbert College
DePere, Wisconsin

M.S. 1990, Institute of Paper Science and Technology
Atlanta, Georgia

in partial fulfillment of the requirements
for the degree of Doctor of Philosophy from
the Institute of Paper Science and Technology
Atlanta, Georgia

January 1994

TABLE OF CONTENTS

LIST OF FIGURES

LIST OF TABLES

ABSTRACT

Polyelectrolytes are used in many industrial applications to improve product quality, increase productivity, and decrease environmental impact. Adsorption of polyelectrolytes is essential for their effectiveness, and often there is only a short time within which the polyelectrolyte must adsorb. Therefore, the rate of polyelectrolyte adsorption is very important.

The main goals of this thesis were to measure the rate of polyelectrolyte adsorption, and to study the impact of several variables on the rate of adsorption. The rate of polyelectrolyte adsorption was studied using a model system consisting of polyallylamine as the polyelectrolyte and polystyrene latex as the adsorbent. The rate of adsorption was measured by monitoring the electrophoretic mobility of the latex as the polyelectrolyte adsorbed. Data were collected under perikinetic, laminar and turbulent flow conditions. Under perikinetic conditions, the electrophoretic mobility of the latex was measured continuously, and a linear relationship was established between the adsorption rate constant and the strength of the superimposed electric field.

A second-order kinetic model was developed using collision theory considerations, and the model was verified through the experiments. The results of the experiments showed that the rate of polyelectrolyte adsorption was first-order in polyelectrolyte concentration, and first-order with respect to the amount of adsorbent surface area available for adsorption. Comparisons were made between

the observed adsorption rate constants and those calculated using von Smoluchowski's equations for rapid coagulation.

It was concluded that the rate of adsorption decreased as the molecular weight of the polyelectrolyte increased. This trend was observed for high and low polyelectrolyte charge densities, under perikinetic, laminar, and turbulent conditions. The rate of adsorption was found to be greater for the high charge density polyelectrolyte as compared to the low charge density polyelectrolyte.

The surface charge density of the adsorbent was varied, and was not found to have a significant effect on the rate of adsorption. A fifty-fold change in the ionic strength of the system did not have a significant effect on the rate of polyelectrolyte adsorption. The implications of this work were discussed with regard to the adsorption of retention aids in the manufacture of paper.

INTRODUCTION

Polymers play a very important role in many industrial applications. With paper manufacture as an example, water-soluble polymers are used to enhance the performance properties of the final product, and are also used to increase the efficiency of the manufacturing process. Product enhancements through the use of polymers include wet and dry strength improvements, and improved sizing. Applications for improved efficiency can lead to higher production rates, reduced energy consumption, and decreased environmental impact.

In all of these applications, adsorption of the soluble polymer to the surface of the targeted substrate is essential. In several applications, polymer adsorption must take place within a time frame of several seconds. Therefore, the rate of polymer adsorption is very important. Despite the importance of polymer adsorption kinetics, very little attention has been given to this area of research. Recently, an increasing amount of work has been performed on the adsorption and desorption kinetics of uncharged polymers from non-polar solvents, but these results do not lend themselves to comparison with water-soluble polyelectrolytes. There is need for fundamental understanding of the factors affecting the rate of polyelectrolyte adsorption.

BACKGROUND

Before reviewing the pertinent literature regarding polymer adsorption

kinetics, it will be helpful to review some basic concepts regarding characteristics of the systems of interest. The main topics to be covered here are: characteristics of polymers in solution; theory of the electric double layer; electrokinetic phenomena; and the work of M. von Smoluchowski regarding the collision frequency of colloidal species.

Polymers in Solution

Polymers are large molecules consisting of many covalently bonded repeating units called monomers. In the following discussion we will be concerned with linear polymers. Polymers are generally described by their degree of polymerization (DP), and their molecular weight. The DP is simply the number of monomer units in the molecule, and the DP can be multiplied by the molecular weight of the repeating monomer unit to get the polymer molecular weight. The molecular weights of polymers may range from several hundred to several million.

Polyelectrolytes are a class of polymers which have charged functional groups along the length of the chain when dissolved in a polar solvent such as water. The fraction of charged monomer units on a polyelectrolyte is referred to as the degree of substitution or charge density (α).

Polymer molecules in solution generally take on a flexible coil configuration.[1] The size of a flexible polymer molecule in solution is often characterized by its radius of gyration,[2] R_g. In general, the radius of gyration of a

polymer in a good solvent depends upon the length of the polymer chain, the flexibility of the chain, the amount of interaction among different portions of the chain, and the amount of interaction between the polymer segments and the solvent. Due to an increase in chain length, the radius of gyration of a given polymer increases as the degree of polymerization increases.

In general, when the charge density of a polyelectrolyte increases, the radius of gyration will increase due to the increased repulsion between the charged segments of the polymer molecule.[3] When the ionic strength of the polymer solution is increased, at moderate levels, the polymer radius of gyration will decrease due to increased shielding between the charged groups within the polymer molecule.[3] According to Flory and Fox, the radius of gyration of a polymer in solution can be calculated from the following equation.[4]

$$R_g = \frac{1}{\sqrt{6}} \left(\frac{[\eta] M}{\Phi} \right)^{\frac{1}{3}} \qquad (1)$$

Where:
$[\eta]$= intrinsic viscosity
M = molecular weight
Φ = Flory constant, 2.5×10^{23}

The radius of gyration of a polymer in solution has a direct influence on its rate of diffusion. According to the Stokes-Einstein equation (2), the diffusion coefficient is inversely proportional to the hydrodynamic radius of a suspended particle.[5]

$$D = \frac{k\,T}{6\,\pi\,\eta_o\,R_t} \qquad (2)$$

where,
D = diffusion coefficient
k = Boltzmann's constant
T = absolute temperature
η_o = viscosity of pure solvent
R_t = hydrodynamic radius of diffusing species

It has been observed experimentally that the radius of gyration and the hydrodynamic radius (determined from diffusion or sedimentation) differ slightly.[6] The ratio of the radii determined from viscosity (R_η) and diffusion (R_t) is found to be in the range of 1.1 to 1.3.[3] Diffusion coefficients of polyelectrolytes can be estimated from intrinsic viscosity data using equations (1) and (2).

Electric Double Layer

The surface of most substances acquires an electric charge when immersed in a polar medium such as water. This charge may arise from any of several mechanisms which include ionization, ion adsorption, and ion dissolution.[5] Examples of ionization include deprotonation of acidic functional groups such as $-SO_4H$ and protonation of weakly basic groups such as $-NH_2$. Adsorption of charged ions to the surface *via* van der Waals forces is an example of surface charge resulting from ion adsorption. Unequal dissolution of oppositely charged ions which compose the surface is an example of the third mechanism of charge acquisition.

In the bulk of an electrolyte solution there is typically a homogeneous distribution of positive and negative ions. When a charged surface is introduced to

the system, the charge on the solid surface results in an excess of oppositely charged counter-ions close to the solid-liquid interface. This region adjacent to the interface where the ion distribution is not homogeneous is called the electric double layer. Though there is a net excess of counter-ions near the interface, electric neutrality exists in the electric double layer such that the sum of the charges on the surface plus the co-ion charge is equal to the counterion charges. Electric double layer theory was advanced by the work of several investigators over decades, and several reviews have been written regarding the development of this theory.[7,8] Therefore, only a brief summary will be presented here.

The work of Helmholtz and Smoluchowski recognized the fact that the distribution of solvated ions near charged surfaces was not homogeneous. The first theories regarding the structure of the electric double layer were developed independently by Gouy and Chapman. The theories of Gouy and Chapman hypothesize that the double layer is diffuse because the counter-ions possess thermal energy while they are simultaneously attracted to the oppositely charged surface. This thermal energy prevents the solvated ions from having specific interactions with the surface. It was recognized that within the double layer, there was a higher concentration of counter-ions and a lower concentration of co-ions with respect to the bulk and that these concentration gradients were more extreme closer to the surface.

The theories of Gouy and Chapman considered the ions as dimensionless

point charges. The contributions of Stern attempted to account for the specific adsorption of ions to the surface, and the finite size of the ions in the double layer. Therefore, according to the contributions of Stern, the electric double layer can be divided into two regions: the inner and outer regions. The inner region consists of specifically adsorbed counter-ions, called the Stern layer, while the outer region consists of diffuse ions, as in the theories of Gouy and Chapman.

Because of the charged surface, an electric potential (ψ_o) is established with respect to the bulk of the solution. The potential within the double layer decreases in magnitude as the distance from the surface increases as a result of the greater separation and screening by the counter-ions. At some distance, just outside the Stern plane, is a transition region called the slip plane. Material inside the slip plane moves with the surface, while material outside moves with the bulk fluid. The electric potential at the slip plane is called the electrokinetic or zeta potential (ζ), and this quantity can be obtained through electrokinetic measurements. A schematic of the electric double layer and the corresponding potential distribution can be found in figure 1.

The thickness of the electric double layer is generally expressed as κ^{-1} where κ is the Debye-Huckel parameter defined by equation 3.

$$\kappa = \left[\frac{e^2 N_A \sum c_i z_i^2}{\varepsilon \varepsilon_o kT} \right]^{\frac{1}{2}} \qquad (3)$$

where:
e = electron charge

N_A = Avogadro's number
c_i = concentration of ion i
z_i = valence of ion i
ε = dielectric constant
ε_o = permittivity of vacuum

For the special case of a 1:1 electrolyte in water at 25°C, the double layer thickness (in nm) is given by equation 4 where c is the electrolyte concentration in moles/liter.

$$\kappa^{-1} = \frac{0.306}{\sqrt{c}} \qquad (4)$$

Electrokinetic Measurements

In general, there are four methods of measuring electrokinetic potential: electroosmosis; electrophoresis; streaming potential; and sedimentation potential.[9] Of these four methods, electroosmosis and electrophoresis will be briefly described.

Electroosmosis is observed when the charged surface is fixed, but the ions adjacent to the surface are induced to migrate because of an externally applied electric field. Because the ions are solvated, the suspending medium is forced to flow with the ions, resulting in net movement of the liquid. Electrokinetic potential information is gained by measuring the liquid velocity per unit current flow.

Electrophoresis is generally used when attempting to measure the zeta potential of the surface of a solid particle suspended in a liquid, typically water. In this technique an electric field is applied across the liquid in which the particles of interest are suspended. Measuring the migrational velocity of the particles in the electric field of known strength gives information about the electrokinetic potential

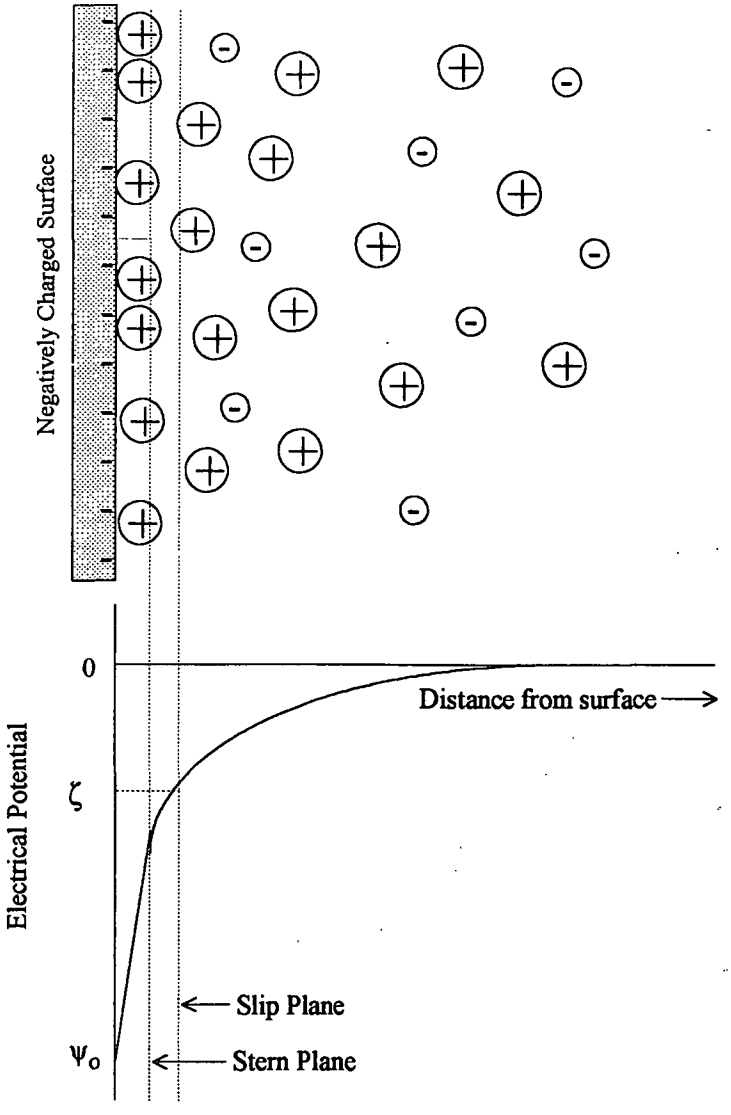

Figure 1. The Electric Double Layer. The top section demonstrates the distribution of ions with respect to the charged surface; the bottom section demonstrates the potential as a function of distance from the surface.

with respect to the bulk. The numerical value resulting from this measurement is called the electrophoretic mobility (E.M.), and it is expressed in terms of velocity per unit electric field strength. It should be noted here that particle electrophoresis is an absolute technique; the data obtained are not derived, but are specifically measured.

The zeta potential can be calculated from electrophoretic mobility data using the Helmholtz-Smoluchowski equation.[10] Depending on the value of κa, where a is the radius of curvature of the particle surface, the Helmholtz-Smoluchowski equation takes two forms. For large values of κa:

$$\zeta = \frac{(E.M.)4\pi\eta}{\varepsilon\varepsilon_o} \tag{5}$$

and for small values of κa,

$$\zeta = \frac{(E.M.)6\pi\eta}{\varepsilon\varepsilon_o} \tag{6}$$

Particle electrophoresis was used throughout this work to evaluate electrokinetic properties of dispersed particles.

Smoluchowski Theory of Coagulation

When considering the rate of coagulation of a colloidal system, the work of von Smoluchowski[11,12] is often cited as the fundamental theory against which more advanced treatments must be compared. Reviews of this work are offered by several authors,[13,14,15] and a brief synopsis will be offered here for the special case of rapid coagulation.

Smoluchowski's simplified system of rapid coagulation is characterized by the following assumptions: transport of the spherical colloids is due to Brownian motion only; there is no repulsion between colliding spheres; and each particle has a sphere of action surrounding it such that when another particle enters this sphere of

action, the two will coalesce irreversibly. The objective of this treatment was to determine the rate of coagulation of the colloidal system.

By first considering a single fixed particle surrounded by a diffusional field of other particles, Smoluchowski determined that the number of particles colliding with the central particle is given by:

$$J = 4\pi R \nu_o D \tag{7}$$

where:
J = collision frequency
R = sum of radii of central and colliding particles
ν_o = number concentration of particles
D = diffusion coefficient of the approaching particles

Removing the condition that the central particle is fixed is accounted for by replacing D (in equation (7)) by the sum of the diffusion coefficients of the reference and approaching particles. Therefore, the collision frequency is given by:

$$J = 4\pi R \nu_o (D_1 + D_2) \tag{8}$$

or if the particles are all of the same size (D_1=D_2),

$$J = 8\pi R \nu_o D \tag{9}$$

Since it is assumed that every collision results in permanent coalescence, the rate of disappearance of the primary particles (singlets) is given by:

$$-\frac{d\nu}{dt} = 8\pi R D \nu^2 \tag{10}$$

When the concentrations are expressed in terms of molar concentrations:

$$-\frac{dC}{dt} = 8\pi RD\mathrm{N_A}C^2 \qquad (11)$$

with a rate constant, k, equal to $8\pi RD\mathrm{N_A}$.

The above treatment is sufficient for describing the initial rate of rapid coagulation of a colloidal system where essentially all collisions are among singlets. Smouchowski further developed this treatment to account for the contributions of collisions among coalesced aggregates of particles, and also extended this treatment to uniformly sheared suspensions.

If this theoretical treatment is applied to a system of colloidal particles and dissolved polymer molecules, there are some notable implications. If we substitute the size of the colliding particle with the polymer radius of gyration, the size of the polymer will have a direct influence on the terms R and D. As $\mathrm{R_g}$ is increased, the term R will increase. At the same time, the diffusion coefficient should decrease according to the Stokes-Einstein equation (2), thus decreasing the collision rate. According to the above arguments, if the polymer radius of gyration is increased under diffusion controlled conditions, the rate of polymer adsorption should decrease.

LITERATURE REVIEW

Several factors may independently affect the rate of polymer adsorption in a given system. Mainly due to instrumentation limitations, there have been relatively few studies which have investigated the kinetics of polymer adsorption.

However, some experimental and theoretical results have been published concerning the impact of different variables on the rate of polymer adsorption.

The emphasis of this review will be on the adsorption of polyelectrolytes from aqueous solution onto an oppositely charged surface of a dispersed adsorbent. While there are some unique factors to be considered for polyelectrolyte adsorption, many aspects of the process are the same as in the adsorption of uncharged polymers. Therefore, useful information will also be drawn from work regarding adsorption of uncharged polymers.

The introductory discussion will be concerned with the various steps in the adsorption process, possible rate-limiting steps, and the existence of different regimes of adsorption kinetics. After a discussion of the impact that several different variables have on the rate of adsorption, the development of kinetic models will be reviewed.

Steps to Adsorption

Polymer adsorption is a complex process, but some general agreement exists on how this process may be divided into steps. Most often, the process is viewed as consisting of the following three steps: 1) transport of the dissolved polymer to the solid-liquid interface through convection and/or diffusion; 2) initial attachment of polymer chains to the solid surface; and 3) reconformation of the adsorbed polymer chains to an equilibrium configuration. The initial attachment of a

single segment of the chain to the surface is considered the adsorption, and subsequent attachment of other segments of the same molecule is considered the reconformation.

Additional steps to the adsorption process are sometimes recognized to account for characteristics unique to the system at hand. When the polymer sample has a broad molecular weight distribution, a fourth step of adsorption consists of competition between molecules of different nature or molecular weight.[16] In the case of adsorption of a polydisperse sample of polymer, the smaller molecules may adsorb more quickly, but the higher molecular weight polymers are thermodynamically favored, and may eventually replace them. This is generally only a concern over longer adsorption times, with a polydisperse polymer sample. When porous substrates such as cellulosic fibers are used, another step of adsorption is recognized. When the pores are larger than, or on the order of the size of the polymer molecules, diffusion into the pores of the adsorbent may occur.[17]

The first two steps of transport to the solid-liquid interface and actual adsorption are most often mentioned as the steps controlling the overall rate of polymer adsorption. However, when a porous material has been used as the adsorbent, reconformation of the polymer on the surface,[17] and diffusion into the pores of the substrate[18] have been considered to be the rate controlling steps in the adsorption.

Occurrence of Different Kinetic Regimes

In most studies of polymer adsorption kinetics, two distinct regions of adsorption rate are found. Typically there is an initial region of rapid adsorption which is characterized by a nearly linear increase of adsorbed polymer with time. As surface saturation is approached, the rate of adsorption begins to level off and eventually becomes zero at saturation. This type of two-regime behavior has been demonstrated for the adsorption of cationic polyelectrolytes onto porous cellulosic substrates,[19,20,21] as well as for adsorption of uncharged polymers onto nonporous charged and uncharged substrates.[22,23,24]

Several explanations for the different regimes have been given, depending on the conditions of the system and the specific materials being used. Perhaps the most common explanation is that as the adsorbed amount increases, it becomes progressively more difficult for the molecules to find space for attachment to the surface. This explanation is sufficient for the adsorption of non-ionic polymers onto nonporous substrates.

In the adsorption of polyelectrolytes, the dramatic rate decrease may also be due to repulsion between the like charges of the adsorbed and unadsorbed molecules. For the adsorption of polyelectrolytes to a porous substrate, it has been suggested that the decreasing rate may be the result of diffusion of polyelectrolyte to the internal surfaces of the adsorbent.[18] When a polydisperse sample of polymer is used, the exchange of adsorbed low molecular weight molecules with unadsorbed

molecules of higher molecular weight is sometimes used to explain the drastically reduced rate of adsorption.[25] As the degree of surface coverage increases, and interactions between adsorbed and unadsorbed polymers become more significant, polymer reconformation rates may become more important.

Rates of Polymer Reconformation

At very high levels of surface coverage with high molecular weight polymers, the dramatic adsorption rate decrease has been attributed to the slow reconformation of the adsorbed polymer.[20] There have been very few studies dealing with the rate of polymer reconformation. Because of the possible effect on the rate of adsorption, the limited conclusions regarding the rate of polymer reconformation will be briefly reviewed here.

For uncharged polymers adsorbing to a charged surface, the rate of reconformation is typically on the order of several minutes.[26] The reconformation of polyelectrolytes on an oppositely charged surface is generally faster than for uncharged polymers, and some conclusions have been drawn regarding the effects of degree of substitution and molecular weight. Reconformation is faster for low molecular weight, high charge density polyelectrolytes than for high molecular weight, low charge density polyelectrolytes.[27] For polyelectrolytes of the same molecular weight, increasing the charge density has been shown to result in slower reconformation.[28] Therefore, polymer molecular weight appears to have an important influence. It has also been shown that the reconformation is faster at lower surface

coverages.[29] The rate of reconformation also depends upon the adsorbent surface properties; reconformation is faster on latex than cellulose.[28]

Polymer adsorption becomes more complex at higher surface coverages, where there are fewer available adsorption sites, and polymer-polymer interactions are more significant. Studies have shown that the rate of adsorption does not begin to decrease due to higher surface coverage until after 50% of surface saturation has been reached.[30] In most applications of polymers, complete surface coverage is not approached. The amount of polymer required to induce flocculation is generally less than half the maximum surface coverage.[31] For the often very short contact times between the furnish and the polyelectrolyte in the wet end of a paper machine, there may be insufficient time in which to attain a high degree of surface coverage. Because of its industrial relevance, the initial rapid rate of adsorption will be the primary focus of this investigation.

Factors Affecting Adsorption Rates

While there is not an abundance of information regarding the effect of different variables on the rate of polymer adsorption, there is some experimental and theoretical evidence that certain variables should have an effect. Some of the specific variables to be discussed in this review are: initial polymer concentration; number concentration of substrate or adsorbent particles; degree of mixing; polymer molecular weight; polymer charge density; ionic strength; and pH. The charge density, ionic strength, and pH may have an effect on the hydrodynamic size of the

polymer as well as on the magnitude of the attractive force between the polymer and the adsorbent.

Polymer Concentration

A qualitative understanding of the impact of initial polymer concentration on adsorption kinetics is well established. For systems using polyelectrolytes[18,19,21] or uncharged polymers,[22] under turbulent[32,33] or quiescent conditions,[34] it has been observed that the rate of adsorption increased as the initial concentration of polymer was increased.

Several studies have concluded that the initial rate of polymer adsorption was first-order with respect to polymer concentration.[19,23,35] This dependence on polymer concentration may actually be "pseudo" first-order because other factors which may affect the rate of adsorption (such as adsorbent surface area), were in sufficient excess that their concentration was essentially constant throughout the adsorption process.

Adsorbent Concentration

Indirect evidence of enhanced adsorption rate due to increased particle concentration was derived from a flocculation kinetic study.[36] In this flocculation study, which was performed under turbulent mixing conditions, polymer adsorption was assumed to be the rate-limiting step in the flocculation process. When the particle concentration was increased, an increased rate of flocculation was observed,

and was attributed to an increase in the rate of polymer adsorption. However, other factors may have been responsible for the increased flocculation rate.

Lindstrom and Soremark have presented data showing that varying the adsorbent concentration by a factor of 10 did not influence the rate of polymer adsorption.[37] It is not clear in this study whether the initial ratio of adsorbent to adsorbate was held constant. The reaction vessel was stirred in this study, but it is not clear whether the mixing conditions were turbulent.

Based on collision frequency calculations, Gregory[33] has proposed a first-order dependence on the adsorbent particle concentration. There were no experimental data to verify this dependence. From the above evidence, it is apparent that the relationship between adsorbent particle concentration and the adsorption rate has not been conclusively elucidated.

Mixing Conditions

When the intensity of mixing is increased, there is a corresponding increase in the rate of adsorption. Nearly all studies in the literature which investigated the effect of mixing on the adsorption rate have concluded that increasing the shear rate will increase the adsorption rate.[23,32,33,38,39,40,41,42]

However, one case is cited where increasing the stirring rate of a suspension did not significantly increase the adsorption rate.[20] The explanation offered by the authors was based on collision frequency calculations which showed

that mixing conditions under the slower stirring rate were already sufficient to produce the maximum adsorption rate; therefore, under these specific conditions, the increased mixing did not enhance the rate of adsorption.

Molecular Weight

The molecular weight of the polymer directly influences polymer radius of gyration, but it does not significantly alter other characteristics of the system. The dependence of adsorption rate on polymer molecular weight is not well established. As the polymer molecular weight is increased, the influence of factors such as shear rate, adsorbent properties and polymer charge density have produced results showing the rate of adsorption to increase, decrease, or remain unchanged.

It has been indirectly demonstrated by Gregory[32,33] that the rate of adsorption increases as the molecular weight increases under high shear conditions. The "lag time" in a flocculation response curve was used as the dependent variable.[32,33] The lag time was defined as the time delay between the addition of a cationic polymer to a dispersion and the onset of flocculation. The time delay was assumed to be due to the time required for adsorption of the critical amount of polymer which was needed to induce flocculation. As the molecular weight of the flocculant was increased, the lag time diminished; this result was given as evidence that the increase in molecular weight produced faster adsorption.

To fortify the above conclusion, it would be essential to know whether

the critical amount of polymer required to produce flocculation differed for the polymers of different molecular weight. The higher molecular weight polymer may be a more efficient flocculant, and therefore, less polymer would be required to cause flocculation.

Results from the work of Wigsten[42] provide information on the effect of polymer molecular weight, and they also provide insight to the validity of the above conclusion which was based on flocculation lag time. Under turbulent conditions, the adsorption rate of a high charge density polymer was not significantly affected by molecular weight, but flocculation was about 25% faster for the high molecular weight polymer. In the same study, the rate of adsorption of a low charge density polymer was found to increase with an increase in the molecular weight.

The relationship between rate of adsorption and polymer molecular weight under low shear conditions has been directly verified by Kindler and Swanson.[18] Under the conditions of their study, the rate of adsorption was shown to decrease as the molecular weight of the polymer increased. However, it should be noted that cellulose fiber was used as the adsorbent, and adsorption on the internal surfaces of the porous structure was determined to be extensive.

When a porous substance, such as papermaking fiber, is used as the adsorbent, there may be an adsorption rate dependence on the polymer molecular weight for reasons other than a change in the diffusion coefficient. If adsorption onto the internal surfaces is significant, the rate of penetration of the polymer may

also be affected by the size of the polymer.[37,39,43] The smaller molecules will pass more rapidly and easily into the porous structure, and the rate of diffusion into the substrate may be unaffected by the external shear conditions.

Complex Variables

There are several variables which affect more than one characteristic of the system. Among these variables, polymer charge density, solution ionic strength, and solution pH have been investigated in terms of their impact on polymer adsorption kinetics. The different ways in which these variables may affect the hydrodynamic dimensions of polyelectrolytes were summarized previously.

The impact of polyelectrolyte charge density on the rate of adsorption may be influenced by two factors: the change in hydrodynamic radius, and the change in the electrostatic forces. As the charge density is increased, the resulting increase in radius of gyration will increase the collision radius of the polymer with the adsorbent,[38] but will decrease the diffusion coefficient. As discussed by Gregory,[33] the relative importance of these two factors may be influenced by the shear conditions of the system (pp. 25-27).

If electrostatic attraction between the substrate and the polyelectrolyte contributes to the driving force for adsorption, increasing the charge density of the polymer may increase the magnitude of the driving force for adsorption. Changing the magnitude of the driving force may affect the rate of adsorption.

It has been shown experimentally that under turbulent conditions, the adsorption rate of a high charge density polyelectrolyte was faster than a lower charge density polyelectrolyte of the same molecular weight.[42] This evidence suggests that either the magnitude of the attractive force between the polyelectrolyte and the adsorbent increased the rate, or that under turbulent conditions, the process was not diffusion limited.

The effect of ionic strength on the rate of polyelectrolyte adsorption onto an oppositely charged surface is not a simple relationship. Changing the ionic strength will affect the characteristics of the electric double layer near the surface, as well as the hydrodynamic size of the polyelectrolyte. As previously mentioned, increasing the ionic strength will produce shielding of the electrostatic charges on the polymer and should lead to a less extended conformation of the polymer in solution; hence, a smaller radius of gyration. The ionic strength may also alter the morphology of a porous substrate having charged functional groups on its surface. Experimental data from the literature are not consistent regarding the dependence of adsorption rate on ionic strength.

Increasing the ionic strength has been shown to decrease the adsorption rate of a polyelectrolyte onto porous cellulose fiber under diffusion controlled conditions.[18] This evidence suggests that any increase in diffusion coefficient produced by increasing the ionic strength is less critical than the shielding of electrostatic charges (*i.e.* decreasing attractive force) of the oppositely charged

adsorbent and adsorbate. Changes in the morphology of the substrate cannot be ruled out in this case.

Increasing the ionic strength has also been shown to increase the rate of adsorption.[44] These data were collected on a system where a cationic polymer was adsorbed to the surface of a negatively charged, nonporous, dispersed adsorbent. This evidence is clearly contrary to the results of the other study mentioned above.

Changing the pH of the adsorption system may not have any direct effect on the adsorption rate, but the influence of pH on the properties of the materials involved can produce distinct changes. Changes in the pH can alter the charge density of polyelectrolytes (and consequently the R_g), the charge density of adsorbent surfaces; and can also modify the swelling properties (and resulting pore sizes) of cellulosic fibers. Depending on the type of charged functional group, an increase in the pH of the polymer solution may cause the polyelectrolyte charge density to increase (*e.g.*, deprotonation of carboxyl groups), decrease (*e.g.*, deprotonation of primary amine groups), or remain unchanged.

Studies using cationic polyelectrolytes and cellulosic fibers have shown that the adsorption rate increased as the pH of the system was increased.[18,19] In these cases, the increase in pH enhanced the surface charge density of the adsorbent by promoting deprotonation of carboxyl functional groups. In one case, the charge density of the polymer (PEI) decreased with increasing pH.[18] In the other case, the impact of pH on the polymer charge density could not be determined from the

information given.[19]

Modeling Literature

In addition to experimental investigations, a limited amount of theoretical work has been published regarding polymer adsorption kinetics. Rate equations have been developed which propose dependence on bulk polymer concentration, degree of surface coverage, and adsorbent particle concentration. When investigating the rate of adsorption of polyvinyl acetate onto chrome from benzene, Peterson and Kwei[22] proposed the following model:

$$\frac{d\theta}{dt} = k_1(1-\theta)c - k_{-1}\theta \qquad (12)$$

where:
θ = fractional surface coverage, range = 0 to 1
k_1 = adsorption rate constant
c = concentration of polymer in bulk
k_{-1} = desorption rate constant

Therefore, they predicted a first-order dependence on bulk concentration and a first-order dependence on the quantity (1-θ) for the forward adsorption reaction. Since irreversible adsorption was not assumed, they also predicted a first-order dependence on θ for the desorption reaction. They were able to demonstrate good agreement between the model and the experimental data.

Rate expressions for polymer adsorption kinetics have been derived by treating polymer adsorption as a collision process using Smoluchowski's theory of

rapid coagulation. Gregory has used these expressions to show that the impact of polymer hydrodynamic radius on adsorption rate will be different depending on the conditions of shear.[23,32,38]

Gregory presents the following rationale for development of a method to estimate the adsorption rate constant (k_{12}). Assuming the polymer molecules and the particles to behave as equivalent spheres, estimates of the adsorption rate constant were made using Smoluchowski's equations for perikinetic (diffusion dominated transport) and orthokinetic (uniformly sheared suspensions) collision of unequal spheres. For the perikinetic case:

$$k_{12} = \frac{2kT(a_1 + a_2)^2}{3\eta a_1 a_2} \tag{13}$$

where:
k = Boltzmann's constant
T = absolute temperature
a_1 = adsorbent particle radius
a_2 = hydrodynamic radius of polymer in solution
η = viscosity of liquid medium

For the case of orthokinetic conditions, Gregory proposes:

$$k_{12} = \frac{4G(a_1 + a_2)^3}{3} \tag{14}$$

where:
G = uniform shear rate of system

Therefore, according to the above equations, under diffusion-controlled conditions (perikinetic), if $a_1 > a_2$, increasing the polymer R_g will decrease the diffusion coefficient of the polymer, and therefore decrease the adsorption rate.

Under uniform shear conditions (orthokinetic conditions), increasing the polymer radius of gyration should increase the adsorption rate.

The effect of changing the polymer radius, according to the above equations, is demonstrated graphically in figure 2. The values for the various solvent properties correspond to those of water at 25° C, and the adsorbent particle radius (a_1) used is 225 nm. The value used for G (420 s^{-1}), corresponds to the volume averaged shear rate under laminar pipe flow at a Reynold's number of 800.[45,46]

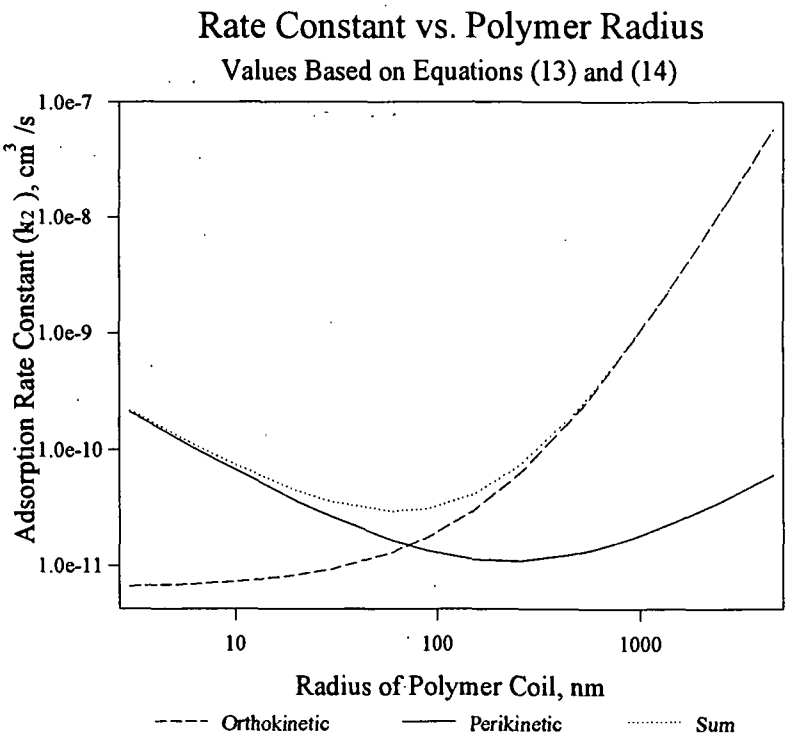

Figure 2 - k_{12} vs. polymer radius as predicted by Gregory, G= 420 s^{-1}.

DEVELOPMENT OF THEORETICAL MODEL

On a simplified level, adsorption of a dissolved polymer to the surface of a dispersed particle is similar to several fundamental systems which have been given theoretical attention. In the section that follows, a theoretical model for the rate of polymer adsorption will be developed in some detail. During this development, simplification of the system will be required. The ultimate objective is to compare the predictions of the model with experimentally obtained data.

In its simplest form, the adsorption of a dissolved polymer onto the surface of a dispersed solid particle can be viewed as a collision between two spherical particles, resulting in permanent contact. Under perikinetic conditions, the transport of polymer to the surface of the adsorbent is the result of Brownian diffusion. If we assume that the rate of diffusion is independent of concentration, the collision frequency between the species should be proportional to the concentration of each.[33]

$$\text{Collision frequency} \propto C_A C_B$$

where:
C_A = concentration of polymer
C_B = concentration of the dispersed adsorbent

If a successful collision is one which results in adsorption of the polymer, we can define the collision efficiency (ϕ) as the fraction of collisions which are successful. If the collision efficiency is constant, the rate of adsorption should be

proportional to the concentrations of each species.

$$\text{Adsorption Rate} = -\frac{dC_A}{dt} = \phi\, k\, C_A C_B \qquad (15)$$

where:
ϕ = collision efficiency
k = rate constant

However, if the polymer adsorption is limited to monolayer coverage, the collision efficiency should decrease as the amount of available surface area decreases. If we assume that the collision efficiency is proportional to the amount of available surface area, and that every collision between a polymer molecule and open surface area will result in adsorption, we can combine the ϕ and C_B terms to represent the concentration of available surface area, $C_{B\phi}$,[22]

$$-\frac{dC_A}{dt} = k\, C_A C_{B\phi} \qquad (16)$$

This type of rate equation is the same as that of a second-order bimolecular reaction. Equation (16) is similar to that of Peterson and Kwei,[22] but since polyelectrolyte adsorption is essentially irreversible, there is no desorption term. The quantity C_A is expressed in terms of mass per unit volume, while $C_{B\phi}$ is expressed in terms of area per unit volume. If we assume that a given molecule will cover the same amount of surface area regardless of the degree of surface coverage, we can express $C_{B\phi}$ in terms of the amount of polymer which can adsorb to the remaining surface area, C_S. Therefore, where Γ_{max}= maximum amount of polymer which can adsorb to the surface in units of mg/m^2;

$$C_S = C_{B\phi} \times \Gamma_{max} \qquad (17)$$

Using equation (17), both polymer and surface area can be expressed in terms of mass concentration of unadsorbed polymer per unit volume.

In order to express the progress of the adsorption as a function of time, we must integrate the above rate equation. Since we have assumed that the stoichiometry between the polymer and surface is constant throughout the adsorption process, the following two statements are true: $C_A = C_{Ao} - x$, and $C_S = C_{So} - x$. The quantities C_{Ao} and C_{So} are the initial concentrations of polymer and surface respectively, and x is the amount of polymer adsorbed at time t. Since $dC_A = dC_S = -dx$, we can substitute into equation (16) to get the following expression:

$$\frac{dC_A}{dt} = -\frac{dx}{dt} = -k\,(C_{Ao} - x)(C_{So} - x). \tag{18}$$

After rearrangement, we obtain the following integral:

$$\int \frac{dx}{(C_{Ao} - x)(C_{So} - x)} = \int k dt \tag{19}$$

Integration between the limits of time zero to t yields:

$$\frac{1}{(C_{Ao} - C_{So})} \ln\left(\frac{C_{Ao} - x}{C_{So} - x}\right) = k\,t + c. \tag{20}$$

After rearranging and substituting, we end up with the following expression:

$$\ln\left(\frac{C_A}{C_A - (C_{Ao} - C_{So})}\right) = k\,t\,(C_{Ao} - C_{So}) + \ln\left(\frac{C_{Ao}}{C_{So}}\right) \tag{21}$$

where $C_A - (C_{Ao} - C_{So})$ is equal to C_S. By plotting $\ln (C_A/C_S)$ vs. time, we will obtain a straight line with a slope of $k(C_{Ao} - C_{So})$ and an intercept of $\ln(C_{Ao}/C_{So})$. If the quantity $(C_{Ao} - C_{So})$ is known, the rate constant, k, can be determined.

In order to plot C_A vs. time, we must obtain the above rate equation in terms of C_A. By rearranging equation (21), we get the following rate equation:

$$C_A = \frac{C_{So} - C_{Ao}}{\left[\frac{C_{So}}{C_{Ao}} e^{kt(C_{So}-C_{Ao})}\right] - 1} \tag{22}$$

Pseudo First-Order Kinetics

If one of the reactants in a second-order reaction exists in sufficient excess, the rate of reaction may appear to be first-order with respect to the limiting reactant. The rate of reaction in this case is defined as pseudo first-order. In many processes where a polyelectrolyte is used for flocculation, there is likely to be a significant excess of adsorbent surface area in the system. Therefore, this type of rate behavior must be considered.

If the polyelectrolyte is the limiting reagent in an adsorption related process, the rate of reaction may be governed by the following equation:

$$-\frac{dC_A}{dt} = k\,C_A \tag{23}$$

After rearranging, and integrating, we can obtain C_A as a function of time:

$$\ln \frac{C_A}{C_{Ao}} = -k\,t \tag{24}$$

or

$$C_A = C_{Ao}\,e^{-kt} \tag{25}$$

PRESENTATION OF THE PROBLEM AND THESIS OBJECTIVES

PRESENTATION OF THE PROBLEM

Efficient use of polyelectrolytes in industrial applications can have a dramatic beneficial effect on product quality, productivity, and environmental impact. A fundamental understanding of the rate of polyelectrolyte adsorption would ultimately lead to more efficient use of these expensive chemicals. According to the currently available information, there are several unresolved issues regarding the factors which control the rate of polyelectrolyte adsorption. Several variables may influence the rate of polymer adsorption, and some of these variables are more clearly understood than others.

It is well established that increasing the initial polymer concentration will increase the rate of polymer adsorption in most cases. This is expected from the pseudo first-order rate dependence on polymer concentration. With the exception of cases where mixing is already extreme, increases in the mixing intensity have been shown to increase the rate of polymer adsorption.

For many system variables, there is either a lack of experimental evidence, or there are contradictory results regarding their impact on adsorption rate. It has been proposed that the adsorbent particle concentration has an influence on the adsorption rate, but this has not been experimentally verified.

The variables which affect the hydrodynamic radius of the polymer are

not well understood with regard to their impact on the rate of polymer adsorption. Evidence on whether the effects of these variables are different under perikinetic and orthokinetic conditions is not conclusive.

Results of experiments which vary polyelectrolyte charge density, ionic strength, and pH are difficult to interpret in terms of the effects of polymer hydrodynamic radius and strength of attraction between the polyelectrolyte and the adsorbent. More meaningful results would be obtained if the variables of hydrodynamic radius and attractive force could be studied independently. The hydrodynamic radius could be altered by changing the polyelectrolyte molecular weight; and changing the surface charge density of the adsorbent should alter the force of attraction between the polyelectrolyte and the adsorbent.

There is clearly a need for further study of the rate polyelectrolyte adsorption. Because of the industrial importance of polyelectrolyte applications, this area of research must be expanded to achieve a better fundamental understanding of the factors which affect the rate of polyelectrolyte adsorption.

THESIS OBJECTIVES

The main goals of this thesis were to measure the rate of polyelectrolyte adsorption in a model colloidal system, and to study the impact of several variables on the rate of adsorption. After developing the equipment and methods to measure the rate of polyelectrolyte adsorption, the main objective was to determine the validity of the theoretical model for predicting the rate of polyelectrolyte adsorption. The model was tested by determining the effects of the following variables on the rate of polyelectrolyte adsorption:

1) Polyelectrolyte concentration;

2) Concentration of dispersed adsorbent.

The influence of variables not accounted for in the theoretical model were also investigated. These variables included:

3) Polyelectrolyte molecular weight;

4) Polyelectrolyte charge density;

5) Adsorbent surface charge density;

6) Ionic strength;

7) Perikinetic, orthokinetic (laminar and turbulent) flow.

EXPERIMENTAL

APPROACH

In order to achieve the thesis objectives, an experimental plan using a model system was undertaken. After a general description of the model system, and a brief discussion on the method of data collection, the experimental plan will be summarized.

Model System

The results of many previous polymer adsorption studies have been clouded by the use of a poorly characterized adsorbent. To avoid these problems, polystyrene latex was used as the model colloid in all experiments. The surface of the latex was relatively nonporous and, the latex surface charge density could be independently altered. In contrast to many other adsorbents, the latex was readily characterized with respect to surface charge density, concentration, and surface area.

Polyallylamine (PAAm) was used as the polyelectrolyte in all of the experimental work conducted. Polydispersity effects were largely avoided by fractionating the polyelectrolyte into narrowly distributed molecular weight fractions. The charge density of the PAAm was controlled by pH adjustment, and concentration of the polyelectrolyte in solution could be readily determined. Further details of the latex and polyelectrolyte used in this work can be found in the materials section and the appendices.

The majority of the adsorption rate data was collected under perikinetic conditions, where transport of the materials was due to Brownian motion. Some experiments were also conducted at orthokinetic conditions under laminar and turbulent flow. The concentrations of the systems studied were such that the surface area of the adsorbent ranged from 0.03 to 0.16 m^2/liter. The solvent used throughout this work was 10^{-3} M NaCl adjusted to pH 4.0 or 10.0.

Method of Data Collection

To determine the rate of adsorption of the cationic polymer onto the negatively charged surface of the polystyrene latex, the electrophoretic mobility (E.M.) of the latex was measured continuously as the polyelectrolyte adsorbed. The amount of PAAm adsorbed was determined from correlations between the latex E.M. and the amount of PAAm adsorbed to the surface under each set of system conditions. The successive E.M. evaluations were made using a Malvern Zetasizer IIc. Under perikinetic conditions, the E.M. measurements were made continuously; therefore, the effects of the electric field had to be accounted for.

During the perikinetic experiments, equal volumes of latex dispersion and PAAm solution were simultaneously injected through a mixing unit into the sample cell of the Zetasizer. Once in the sample cell, the flow from the injection was allowed to cease, and consecutive E.M. measurements were conducted at a frequency of one measurement every 1 to 5 seconds. The orthokinetic flow experiments also relied on the E.M. of the latex to determine the amount of PAAm as a function of

time. After being thoroughly mixed, polyelectrolyte adsorption took place while the latex and polymer traveled through a variable, predetermined length of 1/8" diameter Teflon tubing. The Zetasizer was positioned at the end of the tubing, with the flow directed through the sample cell of the instrument. Once steady state conditions were achieved, the flow was stopped suddenly, and the E.M. data were collected vs. time. The data were then extrapolated to the time at which the flow was stopped.

Experimental Plan

As stated in the thesis objectives, the goal of the experimental plan was to determine the effect of several variables on the rate of polyelectrolyte adsorption. Therefore, the experiments were broken down into sets so that the number of variables in each set could be minimized. A schematic representation of the experimental plan is given in figure 3.

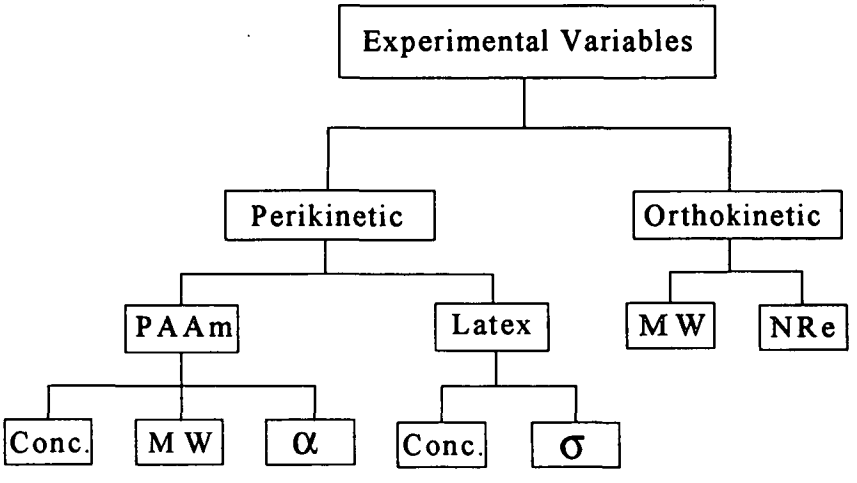

Figure 3. Schematic of experimental plan.

Perikinetic Experiments

In order to account for the effect of the electric field during data collection, each of the conditions used in the perikinetic work was replicated at three different field strengths. The methods used to determine the effect of field strength are discussed in detail in the data analysis section of this document. The following is a description of the experiment sets conducted under perikinetic conditions. The majority of the experiments were conducted in a solvent of 0.001 M NaCl at pH 4, using M_w=82,400 PAAm and latex having a charge density of 12.2 $\mu C/cm^2$. Variations from these conditions are noted below.

Polyelectrolyte Concentration

Because the bulk polyelectrolyte concentration was continually changing as it adsorbed, the effect of polyelectrolyte concentration could be determined from any of the perikinetic experiments. In this set of experiments, two different initial PAAm concentrations were used while the latex concentration was held constant.

Latex Concentration

Like the PAAm concentration, the available surface area of the latex continually decreased as the PAAm adsorbed. In these experiments, the initial PAAm concentration was held constant while four different latex concentrations were used. The intent was to isolate the effect of remaining surface area on the adsorption rate.

System Concentration

While the two above experiment sets were designed to determine the effects of changing the initial ratio of PAAm to latex surface area, this set of experiments was aimed at determining the effect of the overall system concentration. The ratio of PAAm to latex was held constant, but five different overall concentrations were used. The concentrations of PAAm and latex, at which data of high quality could be collected, were lower than those encountered in many applications. By determining the effect of system concentration on the adsorption rate, estimates may be made for other concentrations as well.

Polyelectrolyte Molecular Weight and Charge Density

In this set of experiments, three different molecular weight fractions were used at each of two polyelectrolyte charge densities. The weight average molecular weights were 18,200, 82,400, and 154,000 g/mole, and the charge densities (α) were 0.15 at pH 10, and 0.80 at pH 4.[47] The initial concentrations of latex were the same for all experiments, but two initial PAAm concentrations were used, one at each pH. The starting PAAm concentrations were chosen such that at equilibrium, the same fractional surface coverage would be achieved for both PAAm charge densities. The combination of three M_w and two polyelectrolyte charge densities produced six different polyelectrolyte hydrodynamic radii, and hence, six different diffusion coefficients.

Ionic Strength

In order to determine the effect of raising the ionic strength of the system, these experiments were conducted using a background electrolyte concentration of 0.050 M NaCl. The medium molecular weight PAAm fraction (M_w=82,400 g/mole) was adsorbed to the high charge density latex at a pH of 4.0.

Surface Charge Density

The objective in this set of experiments was to determine the effect of changing the latex surface charge density on the rate of adsorption. Latex samples having charge densities (σ) of 12.2, 6.5, and 1.6 $\mu C/cm^2$ were used. Changing the surface charge density also had an impact on the amount of adsorbed polymer required to reach surface saturation. In these experiments the initial PAAm concentration, and latex concentration were held constant.

Orthokinetic Experiments

Many applications of polyelectrolytes involve adsorption onto dispersed surfaces while the entire system is being forced through piping or reactors. These experiments were designed to investigate the effects of different flow conditions and polyelectrolyte molecular weights on the rate of polyelectrolyte adsorption. .

Two different molecular weight fractions of PAAm (M_w= 18,200 and 154,000 g/mole) were used at the same initial concentrations, and the same

concentrations of latex. For each of the molecular weight fractions, the rate of adsorption was measured at two different rates of flow corresponding to Reynolds numbers (N_{Re}) of 800 (laminar flow) and 4,000 (turbulent flow).

MATERIALS

Polyallylamine

The polyelectrolyte used throughout this work was polyallylamine hydrochloride (PAAm). This cationic polyelectrolyte was commercially available (Aldrich Chemical Co.) in a polydisperse form with molecular weights ranging between 8,000 to 150,000 grams per mole. The structural formula for polyallylamine is presented in figure 4.

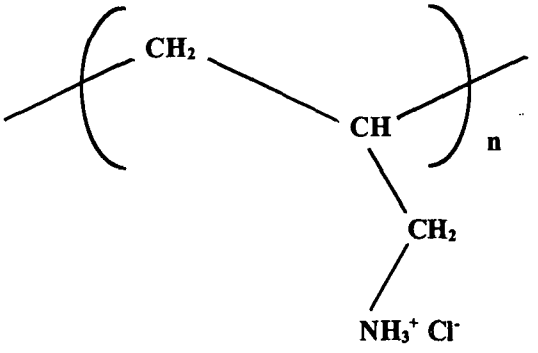

Figure 4. Structural formula for polyallylamine hydrochloride monomer unit.

Because of the primary amine functional group on the side chain of each monomer unit, the charge density (α) of PAAm was dependent upon the pH of the aqueous solvent. The concentration of polyallylamine in aqueous solution was readily determined through several methods, including the colloid titration technique.

Fractionation of Polyallylamine

Since polyelectrolyte molecular weight was one of the key experimental variables in this work, and since the commercial samples of PAAm had broad molecular weight distributions, it was necessary to fractionate the PAAm using size exclusion chromatography (SEC). Details of the procedures and equipment used in the fractionation work can be found in Appendix I.

SEC for Molecular Weight Determination

SEC can be used for molecular weight determinations, but it is not an absolute technique; it must be calibrated. For a given polymer/solvent system, and an appropriate size exclusion column, a linear relationship exists between the logarithm of the molecular weight and the peak elution volume of the polymer sample. Therefore, with a set of polymer standards of known molecular weight, a linear calibration can be established relating molecular weight to elution volume. This type of calibration is useful only if the unknown sample and the calibration standards have exactly the same chemical composition. Therefore, this method is not helpful if calibration standards of the unknown polymer are not available.

SEC separates molecules based on the size of the polymer molecule in solution. According to the Fox-Flory theory of solution viscosity, the size of a polymer coil in solution is directly proportional to the product of its molecular

weight (M) and intrinsic viscosity ([η]).[48] On this basis, the column can be calibrated with a series of samples of one polymer, having known M and [η]. Because this curve can be used for several other polymers, it is called the universal calibration curve. Once the universal calibration curve has been established, the molecular weight of the unknown samples can be calculated after measuring [η] and determining the elution volume. If the volumetric flow of eluent through the system is constant, the elution volume is equivalent to the elution time, *t*.

A series of samples of poly(2-vinyl pyridine) (Polysciences Inc. and Scientific Polymer Products Inc.), having narrow molecular weight distributions, was used to develop a universal calibration curve. After recording the detector output using CODAS® data acquisition software, the peak elution times were determined using the automatic peak picking function in the software package LabCalc®. The intrinsic viscosities of these standards were derived from the data of Nagy and Terwilliger, who worked with poly(2-vinyl pyridine) in the same solvent (0.20 M $NaNO_3$ in 0.1% aqueous trifluoroacetic acid) used here.[49] The universal calibration curve is presented in figure 5. Linear regression on these data yields the slope and intercept corresponding to the universal calibration curve as given in equation (26) below.

$$\ln(M[\eta]) = -2.77\,t + 31.6 \qquad (26)$$

When a series of fractions of a given polymer is to be characterized, it is not necessary to measure the intrinsic viscosity of every sample. According to the

Mark-Houwink-Sakurada equation, $[\eta] = K' M^a$, there is a linear relationship between ln[η] and lnM with an intercept of lnK' and a slope of a (see eqn.(27)).[50]

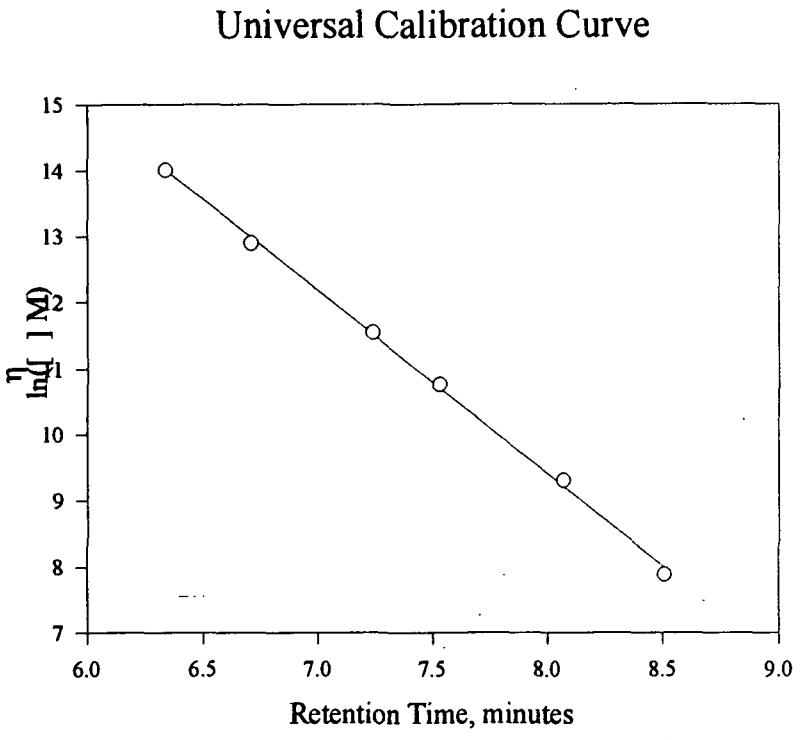

Figure 5. Universal calibration calibration curve for SEC system.

$$\ln[\eta] = \ln K' + a \ln M \tag{27}$$

Accordingly, the constants K' and a can be determined for a given polymer/solvent system by performing linear least squares regression analysis on a plot of ln[η] vs. lnM. The peak elution times and the intrinsic viscosities of six of the PAAm fractions were measured, and their molecular weights were determined from equation (26). The M-H-S plot of these data is shown in figure 6. Linear regression of these

data gave $\ln K'$=-7.97 and a=0.672 with R^2=0.974. The experimental procedures involved in intrinsic viscosity determinations are presented in Appendix II along with the viscosity data.

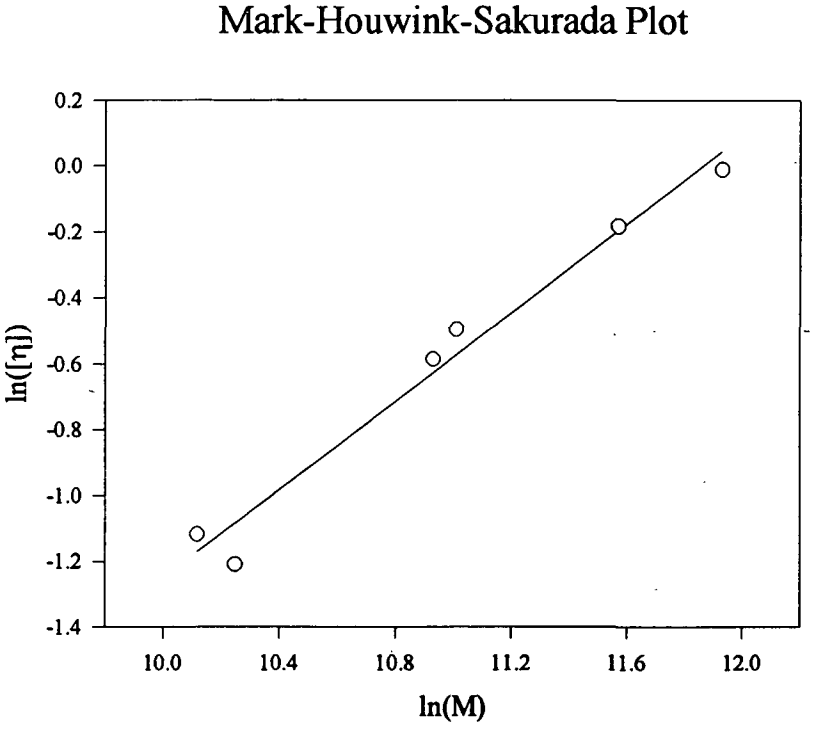

Figure 6. Mark-Houwink-Sakurada plot of ln[η] vs. ln(MW).

By substituting equation (26) into equation (27) for ln[η], and solving for M, we arrive at an expression (28) which allows us to calculate the molecular weight of the remaining fractions knowing only the elution time.

$$M = \exp\left[\frac{-2.77\,t + 31.6 - \ln(K')}{1 + a}\right] = e^{-1.66\,t + 23.7} \qquad (28)$$

Fraction Polydispersity

As stated earlier, it is desirable to have narrow molecular weight distributions for the polymer samples to be used in the experiments. One way of describing the breadth of the molecular weight distribution is to determine the polydispersity, which is the ratio of the weight average molecular weight, M_W, to the number average molecular weight, M_N. In the ideal case, where each molecule in the sample has exactly the same molecular weight, the polydispersity is equal to one.

Once the fractionation was completed, LabCalc® was used to evaluate the polydispersity of the fractions of PAAm using the following procedure. The digitized chromatogram for each fraction was divided into 50 equally spaced bins. The fractional area under the curve within each bin was taken as the relative mass of PAAm in each bin. The molecular weight of the each bin was taken as the average molecular weights corresponding to the boundaries of the bin according to the universal calibration curve. The equations used for calculating the number average and weight average molecular weights are as follows.

$$M_W = \frac{\sum_{i=1}^{50} A_i M_i}{\sum_{i=1}^{50} A_i} \tag{29}$$

$$M_N = \frac{\sum_{i=1}^{50} A_i}{\sum_{i=1}^{50} \frac{A_i}{M_i}} \tag{30}$$

where:
A_i = area under curve in bin "i"
M_i = viscosity average molecular weight of bin "i"

The results of the characterization of the three main PAAm fractions used in this work can be found in table 1 below. A complete summary of the results from all fractions can be found in Appendix II.

Table 1. Characterisitics of PAAm fractions used in experiments.

Fraction ID	M_W	M_N	M_W/M_N
L11	18,200	12,600	1.45
H7	82,400	50,400	1.64
H4	154,000	109,000	1.40

Concentration Analysis

One of the reasons for choosing PAAm as the polyelectrolyte to be used in this work was the fact that its concentration in solution can be readily determined over a broad range. During the course of this work, three different techniques were used to determine the concentration of PAAm in solution: differential refractive index; colloid titration; and a spectrophotometric technique based on the colloid titration technique.

During the SEC fractionation work, a differential refractive index detector was used to detect the peaks of PAAm during elution. This detector was also used to determine PAAm concentration during the intrinsic viscosity work. After calibration with standards of known concentration, small quantities of PAAm were manually injected into the detector for analysis. This technique worked well in

the concentration range of 0.01% to 0.20 % PAAm and should be amenable to lower concentrations as well.

The colloid titration technique was used to determine moderate to high concentrations of PAAm throughout most of the work. Using a spectrophotometric probe to detect the titration endpoint, *o*-toluidine blue (TB) was added to the unknown PAAm solution, and the mixture was titrated continuously with potassium polyvinylsulfate (PVSK) using an automated titrator. Benzethonuim chloride was used as the primary standard to determine the PVSK concentration, and the error associated with the determinations was normally less than 1.0%. A thorough investigation of PAAm analysis via this technique was conducted by Friese.[47]

The most sensitive method of PAAm concentration analysis involved the use of a visible spectrophotometer. This technique used the same reagents as the colloid titration technique, but relied on the absorbance of the toluidine blue dye as the dependent variable. Whereas the detection method in the colloid titration technique measures the onset of excess PVSK, the present technique quantifies the amount of excess PVSK. In this technique, an excess amount of PVSK was added to the sample of PAAm to be analyzed, and a strong complex was formed between the PAAm and PVSK. An excess amount of the cationic dye TB was then added to the solution. The uncomplexed dye had a maximum absorbance at 627 nm, but when complexed with the PVSK, the TB did not absorb at this wavelength. Therefore, the absorbance of the sample at this wavelength was a direct function of the

concentration of PAAm in solution. This method was very reliable for concentrations of PAAm as low as 0.005 mg/l, with and error of less than 2.0%.

Diffusion Coefficient Determination

To aid in the interpretation of adsorption rate data, the diffusion coefficients of the PAAm samples were determined. Under the same solvent conditions as those used in the adsorption experiments (0.001 M NaCl, pH = 4.0 and pH = 10.0), the intrinsic viscosities of the PAAm fractions were determined through viscometry. Using equations (1) and (2), and a value of 1.2 for R_η/R_t, the diffusion coefficients of the PAAm were estimated. These results are summarized in table 2. Because of the relatively low concentrations of PAAm in the adsorption experiments, the diffusion coefficients are assumed to be equivalent to D°, the diffusion coefficient at infinite dilution.

Table 2. Diffusion coefficients for PAAm in 0.001 M NaCl.

Fraction M_W, g/mole	pH	$[\eta]$, cm^3/g	$[\eta]$, 95 % confidence, +/-	D°, cm^2/s
18,200	4.0	100	28	3.3×10^{-7}
82,400	4.0	590	9	1.1×10^{-7}
154,000	4.0	1140	24	0.72×10^{-7}
82,400	10.0	131	1	1.8×10^{-7}
154,000	10.0	443	15	0.98×10^{-7}

Polystyrene Latex

The study of polymer adsorption rate has often been clouded by the use of poorly characterized and porous adsorbents such as cellulosic fibers. To minimize the number of unknown or uncontrolled variables resulting from the substrate characteristics, a model colloid was used throughout this investigation. According to Cohen Stuart *et.al.*, as outlined by Wagberg and Odberg,[51] the substrate used for fundamental studies of polymer adsorption should meet the following requirements:[52]

1) Complete chemical characterization of the surface, including charges.
2) Roughness and porosity must be small relative to the polymer in solution.
3) Curvature of surface must be known.
4) There should be no exchange of material across the solid-liquid interface.

The model colloid used throughout this investigation consisted of spherical, monodisperse polystyrene latex particles dispersed in 0.001 M NaCl. The surface of the latex particles was populated with strong acid sulfate ($-SO_4^-$) and hydroxyl (-OH) functional groups, while the particles were relatively impermeable to water because of the hydrophobic polystyrene core. Because the latex surface charge resulted from strong acid sulfate groups, the surface charge density was independent of solution pH, over the range used throughout this work (pH= 4.0 - 10.0).

Synthesis and Preparation

As stated in the thesis objectives, one goal of this work was to

determine the effect of surface charge density on the rate of adsorption. Therefore, the substrate should have different levels of surface charge while all other properties, such as particle diameter, remain the same. Because latexes with these characteristics are not commercially available, emulsifier-free emulsion polymerization was carried out to produce such particles. In general, the diameter of latex particles produced by emulsion polymerization is closely tied to the particle surface charge density, so a novel approach to latex synthesis was required.

Using potassium persulfate initiator, and sodium bicarbonate buffer, emulsifier-free emulsion polymerization was used to produce a large batch of monodisperse latex having a surface charge density of 12.2 $\mu C/cm^2$, and a mean diameter of 450 nm. The resultant latex was then cleaned using purified ion exchange resins. A portion of the cleaned latex was placed in a 75°C stirred reactor for several hours, where hydrolysis of the sulfate groups took place. This hydrolysis procedure produced a reduction in surface charge density by converting the strong acid sulfate groups to hydroxyl groups.[53] This approach was used to produce three batches of polystyrene latex having the same mean diameter, but charge densities of 12.2, 6.5, and 1.6 $\mu C/cm^2$.

The rate of hydrolysis at 75°C decreased at longer times until a pseudo-equilibrium level of charge density was achieved. Figure 7 shows the relationship between latex charge density and time at 75°C. Further hydrolysis was achieved by dilution of the reaction vessel with distilled water.

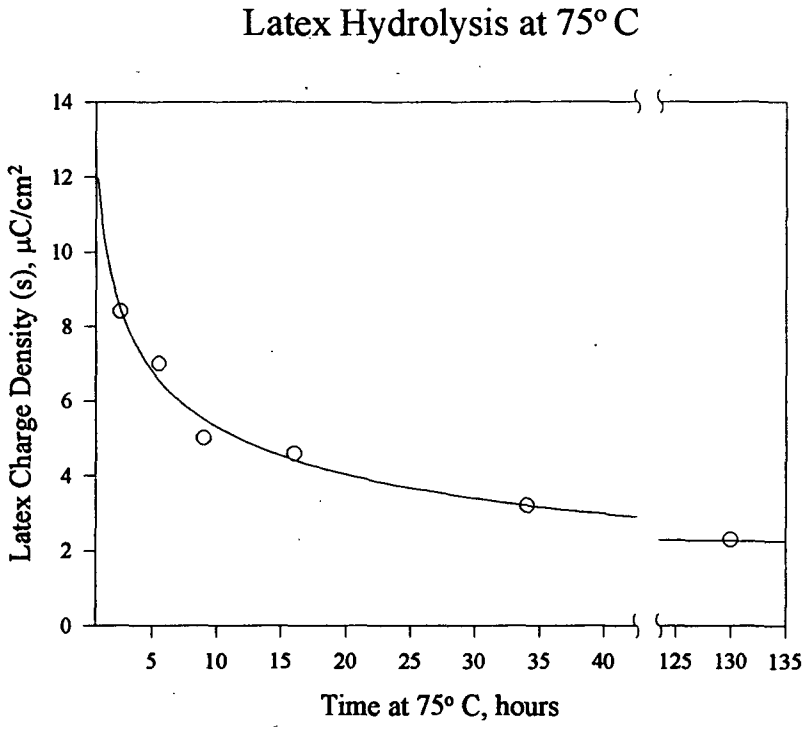

Figure 7. Latex surface charge density vs. time at 75°C.

Once the latex samples were hydrolyzed, care was taken to ensure the stability of the surface charge density. Because the hydrolysis was promoted by low pH, and elevated temperatures,[53] all latex samples were stored at 2°C, and at a pH of eleven until use. The lowest charge density latex was stored in the undiluted hydrolysis medium, under refrigeration until just prior to use. All adsorption experiments involving the hydrolyzed latexes were performed within two weeks after hydrolysis. Procedural details of the latex synthesis and hydrolysis can be found in Appendix III.

Characterization

One reason for selecting polystyrene latex as the model colloid was that it could be readily characterized with respect to surface charge density, diameter, and concentration in suspension. Conductometric titration was used to characterize the surface of the latex with respect to charge density, as well as to determine whether the charge resulted from strong or weak acid functional groups.

The conductometric titration curve of a latex sample having surface charges due solely to strong acid functional groups has a very characteristic shape.[54] There are two linear regions, beginning with a negative slope, then an abrupt change to a positive slope. The extrapolated intersection of these two linear portions gives the titration endpoint, and therefore, the number of strong acid groups.

The conductometric titration curve for latex produced in some of the initial hydrolysis work had three distinct linear regions. This type of curve was indicative of the presence of weak acid functional groups on the surface.[55] Because the surface charge of the latex used here was to be independent of pH, the presence of weak acid groups was undesirable. The latex used in this work had conductometric titration curves indicative of strong acid functional groups only. Figures 8 and 9 show the conductometric titration curves for the unhydrolyzed, high charge density latex and the lowest charge density latexes respectively. The detailed procedures for conductometric titration of the latex are contained in Appendix III. During emulsion polymerization, rapid introduction of the initiator, under high shear,

yields a very uniform latex particle size. Characterization of the latex diameter was performed using a Malvern Autosizer®. The average diameter of the latex used in these experiments was 0.450 μm with a polydispersity of 1.06.

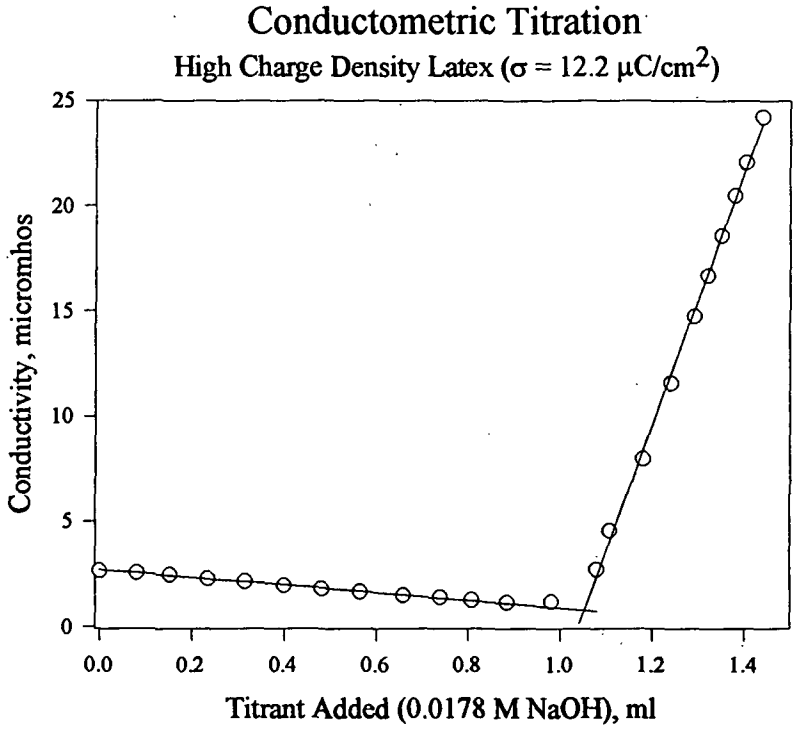

Figure 8. Conductometric titration, unhydrolyzed latex.

Once the diameter of the latex was determined, the surface area of the latex in dispersion could be calculated based on the consistency (% solids) of the dispersion. For medium to high consistency latex (>0.1%), a gravimetric technique was used to determine the latex content of a given dispersion. However, since the latex concentrations used throughout much of this work were on the order of 0.001% consistency, a more sensitive technique was needed.

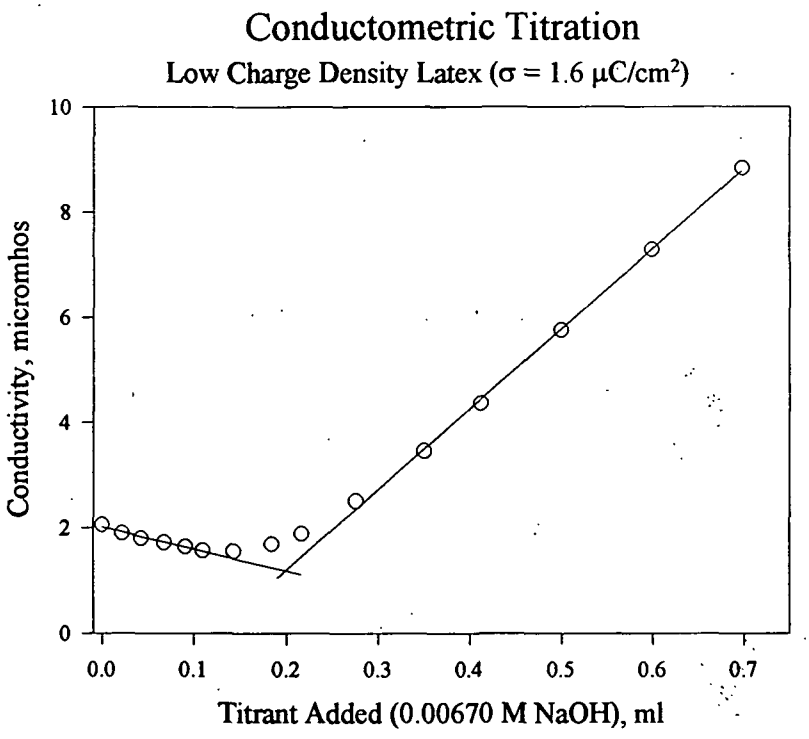

Figure 9. Conductometric Titration, lowest charge density latex.

Using the work of Miller[56] as a starting point, a technique based on UV absorbance of latex in suspension was developed. The absorbance of a latex dispersion of unknown concentration was measured at 289 nm in a quartz cuvette. Calibration curves were constructed using gravimetric determinations for the high and low charge density latexes, and are presented in figure 10. In each case, the Beer's law plot yielded the same slope.

At absorbances above 1.0, some deviation from Beer's law occurred, so the maximum concentration for this technique was about 0.002%. Dilutions of more concentrated dispersions were performed to allow analysis within the appropriate

concentration range. If cationic polymer is adsorbed to the surface of the latex, the plot of absorbance vs. time is not linear, and the above analysis is not valid.[56]

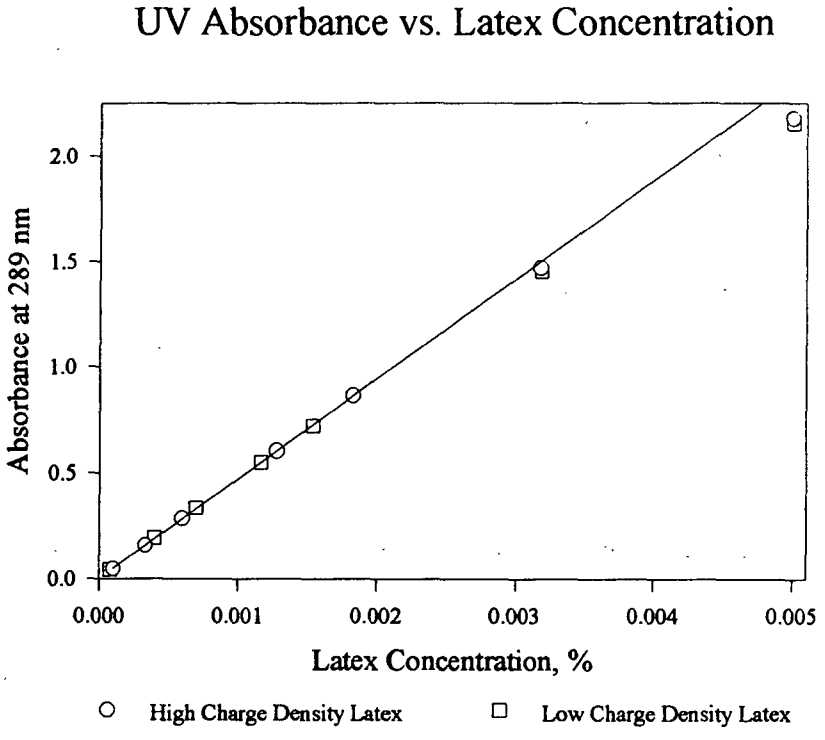

Figure 10. Absorbance of latex dispersion at 289 nm vs. concentration.

EQUIPMENT

Zetasizer IIc

The adsorption rate data throughout this work were obtained by making rapid, successive evaluations of the electrophoretic mobility of the adsorbent. The instrument used to make these measurements was the Zetasizer IIc by Malvern Instruments Inc. In the manual mode of operation, this instrument was capable of making up to twenty E.M. measurements in succession. Depending on the time scale of observation, the duration of each measurement was between one and five seconds.

The Zetasizer utilizes laser Doppler anemometry to measure the velocity of suspended particles as they migrate toward an electrode of opposite charge in an electric field. The sample was contained in a 4 mm i.d. quartz capillary with an electrode at each end, 5 cm apart. In the instrument, light from a laser was split into two beams which were focused to intersect within the capillary containing the sample. The intersection of the two beams represented the "probe volume" which was about 50 μm wide. Within the probe volume, a pattern of alternating light and dark fringes was established as a result of the constructive and destructive interference of the two beams of laser light. The spacing of the fringes was determined by the wavelength of the light and the angle of intersection of the beams. The fringe pattern was oriented perpendicularly to the direction of particle migration.

As particles passed through the probe volume, they experienced a

periodic illumination with a frequency proportional to the relative particle velocity and inversely proportional to the fringe spacing. By quantifying the illumination frequency spectrum and simultaneously measuring the electric field strength, the electrophoretic mobility was calculated.

In order to determine the direction of migration, a modulation was applied to one of the beams which caused the fringe pattern to move in a direction parallel to the particle migration. Therefore, a stationary particle had a frequency equal to the modulation frequency; a particle moving in the direction of the fringe movement had a frequency lower than the modulation frequency, and conversely, a particle moving opposite to the fringe movement had a higher frequency.

Electroosmotic Flow

One complication of particle electrophoresis results from the migration of hydrated cations which are concentrated at the negatively charged surface of the quartz capillary. This phenomena is called electroosmotic flow. To compensate for this flow, a counterflow is spontaneously established through the center of the capillary. There is a theoretical stationary layer which separates the electroosmotic flow and the counterflow. The stationary layer is located at a distance of $r(1 - 0.5^{1/2})$ from the inner capillary wall, where r is the radius of the capillary cross section.

During E.M. measurements the capillary was adjusted so the probe volume was focused on the stationary layer. Since the stationary layer is infinitely thin, and the probe volume has a finite size, some error is always present in the

measurement. The error associated with focusing the instrument and the overlap of the probe volume can be minimized by reducing the electroosmotic flow.

To minimize the electroosmotic flow, the capillary can be coated with various substances which reduce or shield the negative charge on the capillary surface. The severity of the flow was evaluated by measuring the E.M. of a sample at several points across the capillary diameter. The resulting graph of E.M. vs. position is called the cell profile. The purpose of the coating was to flatten the profile, and thereby reduce the error in the E.M. measurements.

Coating the capillary with hydroxypropyl methylcellulose is one common treatment. The procedure used here is a modification of a procedure used by Miller[56] involving a pretreatment of the capillary with γ-glycidoxypropyltrimethoxysilane, then coating with hydroxypropyl methylcellulose. Figure 11 demonstrates the dramatic improvements in the cell profile as a result of the different coatings.

This coating was effective for a period of up to two weeks under heavy use, but the profile curvature gradually returns as a result of the deterioration of the coating, or adsorption of charged species to the coating. A detailed procedure for coating the capillary is presented in Appendix IV.

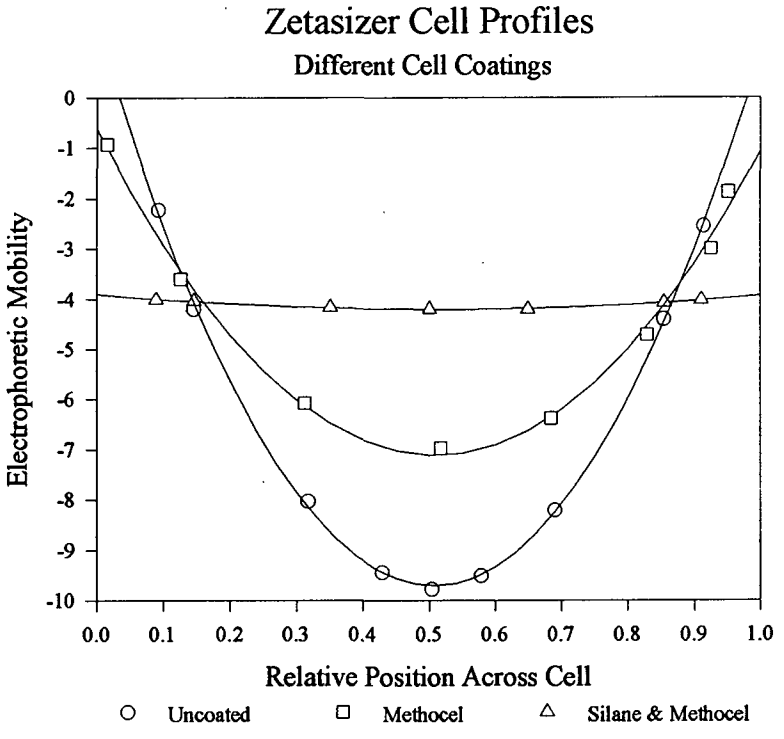

Figure 11. Profiles of Zetasizer sample cell with different coatings.

Automated Injection Apparatus (AIA)

The open-tube geometry of the Zetasizer sample cell allows the straight-through injection of a sample into the cell. Since the adsorption rate data were to be collected in the sample cell, careful consideration was given to how the samples were introduced. The automated injection apparatus was designed to rapidly mix separate streams of polymer solution and latex dispersion in equal quantities; deliver the mixture to the sample cell of the Zetasizer at a constant rate; and activate the start of data collection at the appropriate time. A picture of this apparatus is

shown in figure 12.

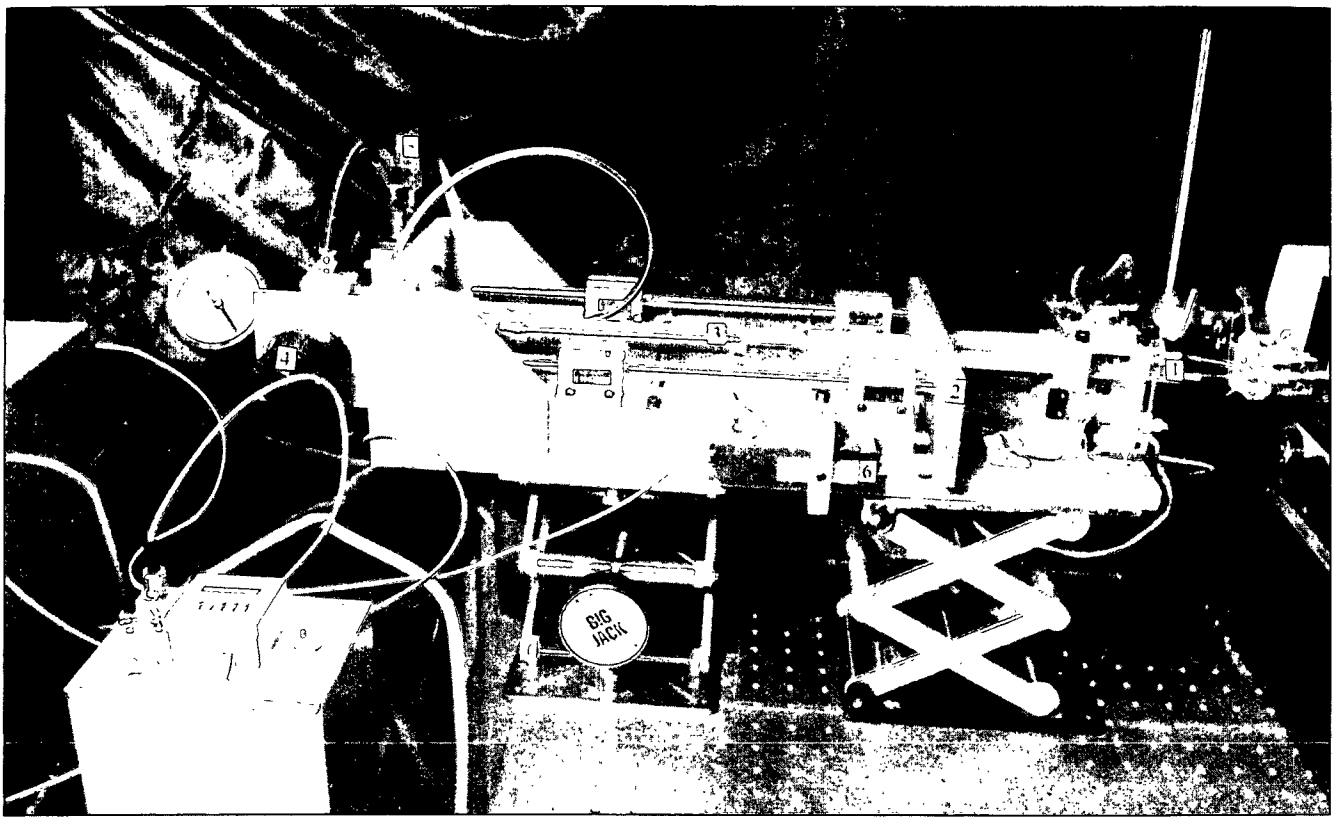

Figure 12. Automated Injection Apparatus (AIA) for perikinetic experiments.

The reagents to be combined, mixed, and injected into the Zetasizer were contained in the two polyethylene syringes (1). In contact with the ends of the syringe plungers was a ram (2) which was mounted to two sets of linear bearings, allowing it to slide parallel to the long axis of the syringes. On the backside of the ram was an air piston (3) which, when pressurized, provided the force necessary to move the ram forward at a steady rate, thus expelling the contents of the syringes at an equal rate. Controlling the supply of 20 psi nitrogen to the piston were a pressure regulator (4) and solenoid valve (5). A linear potentiometer (6) was mounted

parallel to the piston to monitor the position of the ram with respect to time during an injection. The AIA operation and subsequent data collection were controlled by a series of switches, and a switchbox (7) containing a delay timer.

Mixing of the Reactant Streams

The separate streams of PAAm and latex were brought together and mixed in a mixing unit consisting of a y-shaped flow converger and a static mixer. A schematic of the mixing unit can be found in figure 13. The Reynolds number during a typical injection was 800, based on the 1/8" diameter tube. This mixing unit was designed to produce optimum mixing, while minimizing turbulence. From the inlet ports of the flow converger to the exit port, the cross-sectional area of the reactant streams were reduced to just less than one half. Prior to reaching the first element of the static mixer, the two streams were separated by a thin partition.

The static mixer in this system consisted of a series of twelve fixed, helical elements enclosed by a tubular housing. The flow through the mixer was split at the leading edge of each element and followed the channels created by the element shape. At each succeeding element the two channels were further divided, resulting in a geometric increase in stratification.[57] The number of striations produced in this mixer was 2^{12} or 4096, all within the 1/8" i.d. tube. Neglecting any radial mixing, the width of the striations were of the same order of magnitude as the latex particle diameter. This flow converger and mixer combination provided thorough mixing of the reactants while minimizing turbulence.

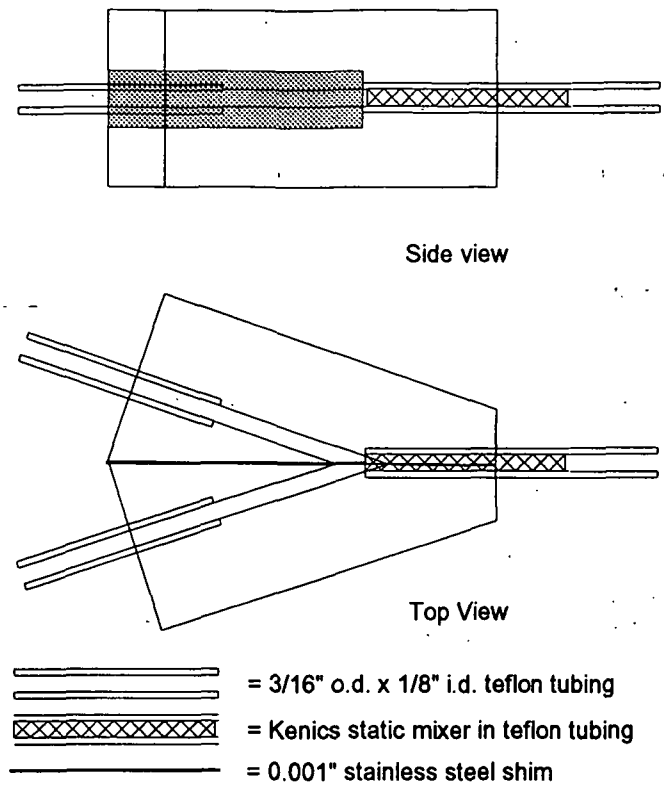

Figure 13. Diagram of the in-line mixing unit.

In a typical experiment the latex and polymer samples were drawn into separate 10 ml polyethylene syringes which were then loaded into the apparatus. Once secured, the tips of the syringes were connected to the mixing unit, which was directly connected to the sample cell of the Zetasizer. After entering the proper series of commands to the microcomputer controlling the Zetasizer, and turning the laser, photomultiplier and cell current on, the start switch on the control box was flipped to the "on" position. Immediately, the solenoid controlling the air flow to the piston was automatically opened allowing N_2 at 20 psi to fill the piston, which produced the force necessary to inject the contents of the syringes through the mixing unit and into the Zetasizer.

During the injection, approximately 20 ml of the mixture would flow through the 1 ml sample cell, and exit through the back of the instrument. When the ram reached full extension, it closed a microswitch which indicated the end of the injection. The switch closure activated the countdown timer which was set for at least one second to allow the liquid flows resulting from the injection to cease. At the end of the countdown, the microcomputer was activated to begin collection of electrophoretic mobility data. After the data were collected and saved, the system could be reset, the syringes refilled, and another run could be made.

Orthokinetic Adsorption Apparatus

The collection of adsorption rate data under laminar and turbulent conditions was accomplished by mixing the reactants in the in-line mixing unit, and allowing them to flow through a variable length of tubing, and through the sample cell of the Zetasizer. After the system reached steady state, the flow was stopped and electrophoretic mobility data were collected on the contents of the sample cell. The data collected were extrapolated back to the time at which the flow in the system was stopped.

The main components of this equipment were a control box (1) peristaltic pump (2) with flow integrators (3), reservoirs (4) for the reactants, three-way pinch valves (5), the mixing unit (6), and the Teflon tubing used to carry the mixed reactants. A picture of this apparatus is shown in figure 14.

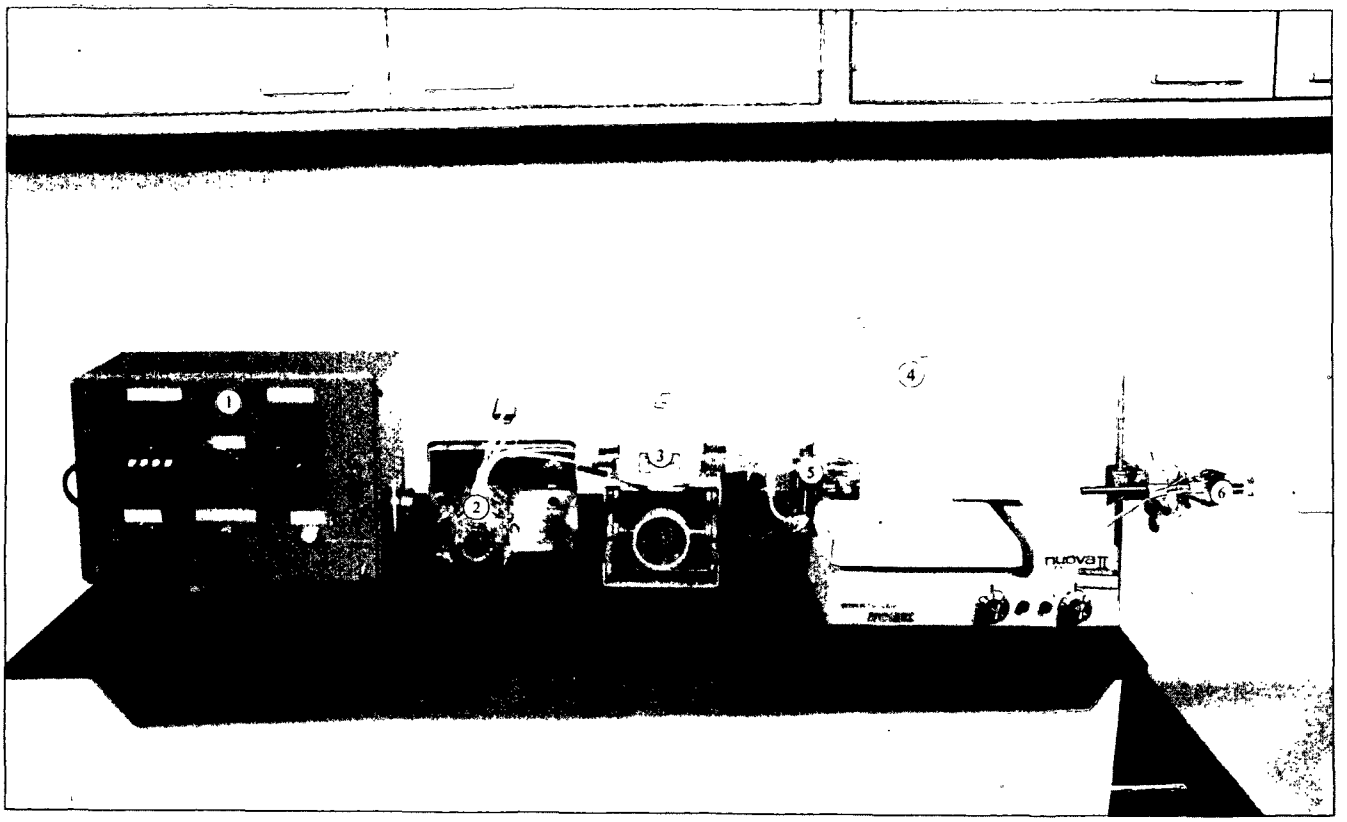

Figure 14. The reactant delivery system for orthokinetic flow experiments.

The pump used in this system consisted of two peristaltic pump heads mounted on a single variable-speed drive motor. Because peristaltic pumps are notorious for producing pulsation in the outflow, flow integrators were used immediately downstream from the pumps to eliminate the pulsation. An example of the effect of the flow integrators is given in figure 15.

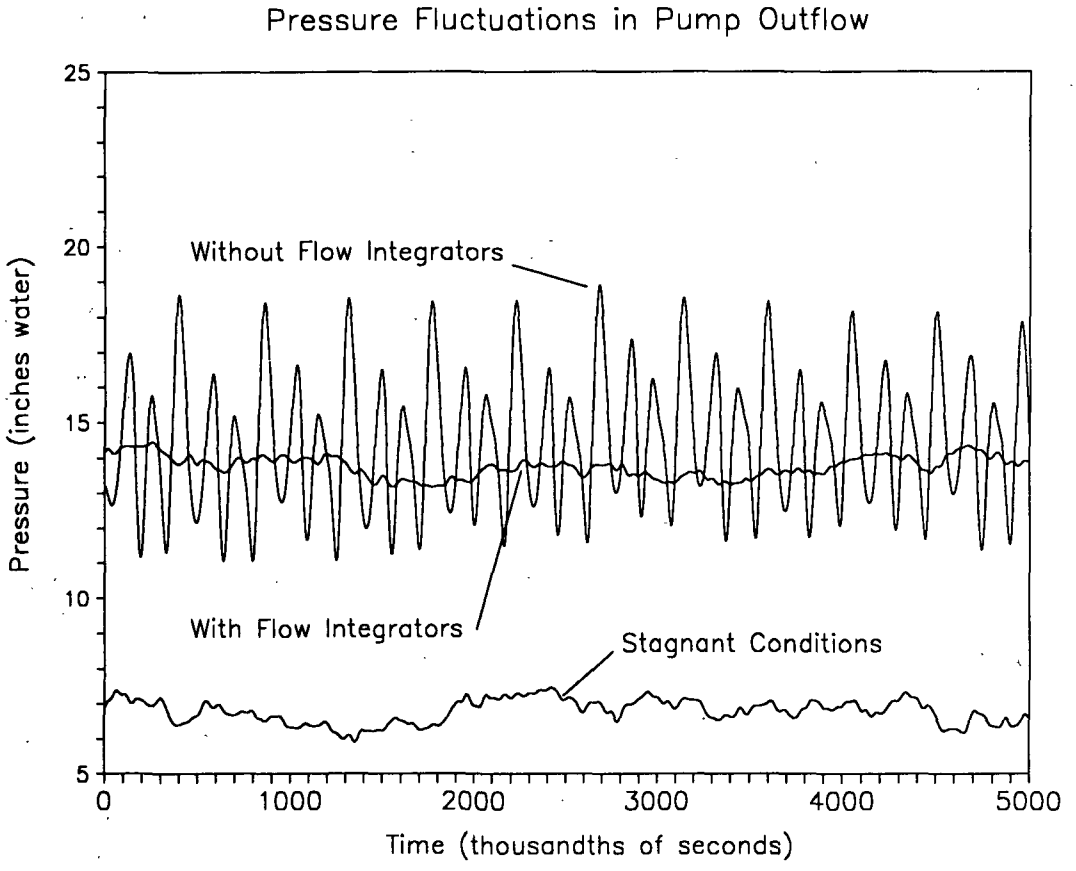

Figure 15. Pulsation dampening effect of the flow integrators.

Downstream from the pumps and integrators were two solenoid-actuated, three-way pinch valves which were used to direct the flow of reactant streams in the apparatus. Like other electronic valves, these had a very rapid response time, but their main advantage was that they did not cause undue flow perturbations as the fluid passed through the valve. The two positions of the valves directed the reactant either flow back to the reservoirs ("off" or recirculation mode) or to the mixing unit and the rest of the apparatus ("on"). A third three-way pinch valve was located near the end of the tube, just before the Zetasizer to isolate the instrument from the rest of the apparatus during data collection.

A control box coordinated the opening and closing of the valves, and also signaled the start of data collection according to the times specified by two timers. The flush timer was set to the amount of time required for the system to reach steady state, which was typically equivalent to the time required to flush the system completely at least two times. The data collection timer was set for the same time as the flush timer, plus the delay time required between the stop of flow and the beginning of data collection.

The sequence of a typical run follows. With the reservoirs filled with the appropriate latex and polymer reactants, the pump was turned on. Since the valves were initially in the "off" position, the reagents would simply recirculate. While the pump was warming up and the flow integrators were equilibrating, the appropriate data collection commands were entered into the microcomputer which controlled the Zetasizer. After about 1 minute, the start button on the controller was pressed, which immediately opened all three of the valves, and directed flow through the mixing unit, tubing and Zetasizer.

At the end of the flush time all three valves closed, thereby stopping the flow through the system, while the pump continued to recirculate the reagents to the reservoirs. Once the time on the delay timer had elapsed, the E.M. data were collected and stored on the microcomputer. Replicates could be performed by reentering the commands on the microcomputer and pressing "start".

ANALYSIS OF DATA

CORRELATION OF E.M. TO SURFACE COVERAGE

The effectiveness of polyelectrolytes in many applications depends upon the ability of the adsorbed molecules to reduce the electrokinetic potential of the adsorbent. The reduction in potential associated with polymer adsorption can be due to charge neutralization, screening, and in some cases shifting of the position of the slip plane relative to the surface. As the oppositely charged polyelectrolyte adsorbs, the electrokinetic potential of the surface decreases in magnitude, and if a sufficient amount of polyelectrolyte adsorbs, the sign of the potential can be reversed.

The method used to determine the rate of polyelectrolyte adsorption relied on measuring the electrophoretic mobility of the adsorbent throughout the adsorption process. In order to obtain useful kinetic data from the electrophoretic mobility data, it was necessary to correlate the adsorbent mobility with the amount of adsorbed PAAm.

In order to establish the correlations, the equilibrium electrophoretic mobilities of latex having different amounts of adsorbed PAAm were measured. These samples were prepared in the following manner. After preparing a stock latex dispersion of known concentration, and PAAm solutions of different concentrations, equal volumes of latex dispersion and polyelectrolyte solution were combined. The mixtures were shaken for at least one hour, allowing the PAAm to adsorb to the latex. A portion of each mixture was used to determine the electrophoretic mobility

of the latex, while the remainder of each sample was used to determine the residual concentration of the PAAm in the bulk. After conducting a mass balance on each sample, the average surface coverage (Γ) was calculated in terms of milligrams of PAAm per square meter of latex surface area.

Factors which had a dramatic effect on the correlation of E.M. to surface coverage included the surface charge density of the adsorbent, and the charge density of the polyelectrolyte. Changes in the ionic strength of the system had a subtle, but significant effect. Therefore, different correlations were developed for each combination of polyelectrolyte charge density, latex surface charge density, and ionic strength. Other factors, such as polyelectrolyte molecular weight may also have an effect on the correlation under certain conditions, but the effects observed here were small compared to the effects of polyelectrolyte charge density, surface charge density, and ionic strength.

To allow interpolation of these data, nonlinear regression analysis was performed to produce an empirical equation relating E.M. to surface coverage. After developing equations for each set of conditions, the equations were used to determine the amount of adsorbed PAAm from the latex electrophoretic mobility. Figure 16 presents an example of the correlation for one set of conditions. The PAAm sample used in figure 16 was not fractionated and had a M_w of 18,400 g/mole with a polydispersity of 1.6. The raw data can be found in Appendix V.

Other workers have recently used a similar approach by fitting an

empirical equation to equilibrium data which correlated the amount of adsorbed polymer with the thickness of the adsorbed layer.[58] The equilibrium correlation was then used to determine the amount of adsorbed polymer throughout the adsorption.

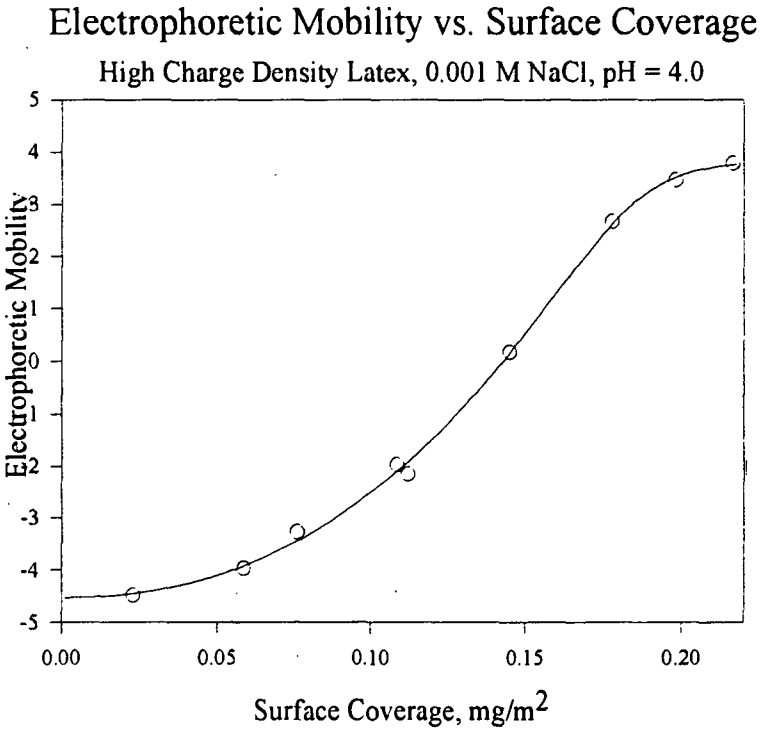

Figure 16. Correlation between E.M. and surface coverage.

An inherent assumption made in using the above correlations to monitor a changing system is that rate of reconformation of the polymer molecule on the surface is faster than the time scale of the kinetic observations. In the adsorption rate experiments conducted here, the kinetic observations were made at intervals on the order of one to five seconds. Since the reconformation of polyelectrolytes is relatively fast, especially on latex at low surface coverages, this assumption should be valid, at least at lower surface coverages. The correlations were only used at

surface coverages below 70% of the maximum surface coverage (Γ_{max}).

An attempt to measure the rate of reconformation of polyallylamine on the surface of polystyrene latex was made in preliminary experiments. The approach used was based on the assumptions that 1) high and low charge density polyelectrolytes of the same molecular weight have different equilibrium conformations and 2) the conformation of the adsorbed polyelectrolyte has an impact on the electrophoretic mobility (E.M.) of the latex.

For the same surface coverage (mg/m^2), equilibrium values of latex E.M. were established for pH 4 and pH 8, corresponding to high and moderate polyelectrolyte charge densities respectively. A sample of the pH 8 latex/polymer sample was rapidly adjusted to pH 4, and the E.M. of the latex was evaluated three seconds after the pH adjustment occurred. The E.M. just after the pH adjustment was equal to the equilibrium value established for pH 4. An analogous experiment was conducted by adjusting the pH from 4 to 8, and similar results were found.

From these results, we can conclude that any reconformation which took place as a result of changing the charge density of the polyelectrolyte either happened in less than three seconds, or simply had no effect on the electrophoretic mobility of the latex.

PERIKINETIC ADSORPTION

Correcting for Effect of Field Strength

To evaluate the rate of polyelectrolyte adsorption under a given set of conditions, a series of injections was performed. During each injection, equal volumes of latex dispersion and polyelectrolyte solution were combined in-line, passed through the mixing unit, and delivered to the sample cell of the Zetasizer IIc. Once the injection was complete, the electrophoretic mobility (E.M.) of the latex was measured as a function of time through sequential measurements.

In order to measure the E.M. of any suspended particle, there must be an electric field present. The electric field causes the charged species to migrate toward the oppositely charged electrode at a velocity proportional to the field strength.

$$\text{Velocity } (\mu m/s) = \text{E.M.} \times \text{Field Strength (V/cm)} \qquad (31)$$

In addition to enabling the measurement of E.M., the electrophoretic migration also increased the observed rate of polyelectrolyte adsorption under perikinetic conditions. This observation was also made by Luettgen when measuring the homogeneity of adsorption.[59] Since most applications of polyelectrolytes do not involve an electric field, it was worthwhile to determine the rate of adsorption without the effects of the electric field. To determine whether the electrophoretic effect could be readily accounted for, perikinetic adsorption data were collected at

five different field strengths ranging from 7.4 to 28.3 volts/cm. These experiments were conducted in 0.001 M NaCl at pH 4 using 0.0005% high charge density latex and an initial PAAm concentration (M_W=18,200, unfractionated) of about 0.02 mg/L. The data from these experiments are presented in figure 17.

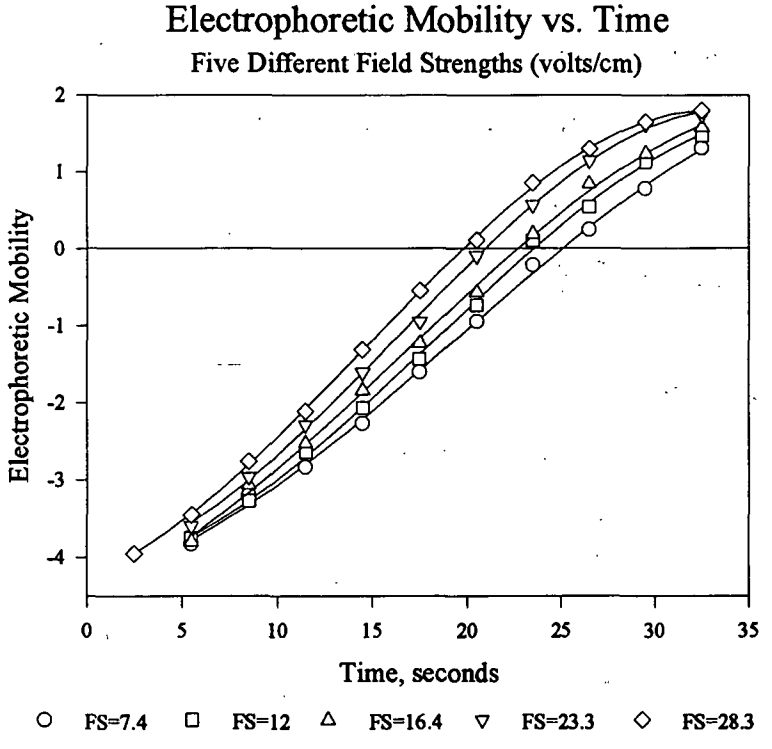

Figure 17. Electrophoretic Mobility vs. Time, 5 different field strengths.

Four injections were made at each field strength. Each symbol in figure 17 represents the average value for the four replicates. Since correlations between electrophoretic mobility and surface coverage had been developed, it was possible to convert the mobility data to surface coverage. The total amount of polymer in the system was known, and therefore, a mass balance was performed to express the

surface coverage data as the amount of unadsorbed polymer in the system vs. time.

The kinetic model developed in the theory section predicts that the adsorption should proceed according to second-order kinetics. The only time-dependent variables in the rate equation are the concentration of PAAm (C_A) and available latex surface area (C_S). Therefore, any differences in the rate due to factors other than C_A and C_S should be accounted for in the rate constant k. From data giving C_A as a function of time, we can test whether the data collected at each of the five different field strengths is consistent with the model predictions.

If adsorption were viewed as a collision process, the incremental increase in the rate of transport of the polymer and/or latex, due to an increase in the electric field, should produce a greater collision frequency. Increasing the collision frequency by a given amount should result in a proportionate increase in the rate of adsorption. Since the electrophoretic transport is proportional to the field strength, the incremental increase in the rate of adsorption due to the electric field should also be proportional to the field strength. Accordingly, the effect of field strength on the rate of adsorption should be reflected in the rate constant.

The data collected at each field strength were treated according to equation (21) by plotting $\ln(C_A/(C_A-(C_{Ao}- C_{So}))$ vs. time, where C_{Ao} and C_{So} are the initial concentrations of PAAm and latex surface area respectively. Following from equation (21), the plot should be linear, with a slope of $k(C_{Ao}-C_{So})$.

These plots were constructed for the data at each field strength, and linear least squares regression analysis was performed to determine the slope and intercept of the best straight line through the data. Figure 18 shows the data and regression lines determined through this method. A summary of the regression results are given in table 3.

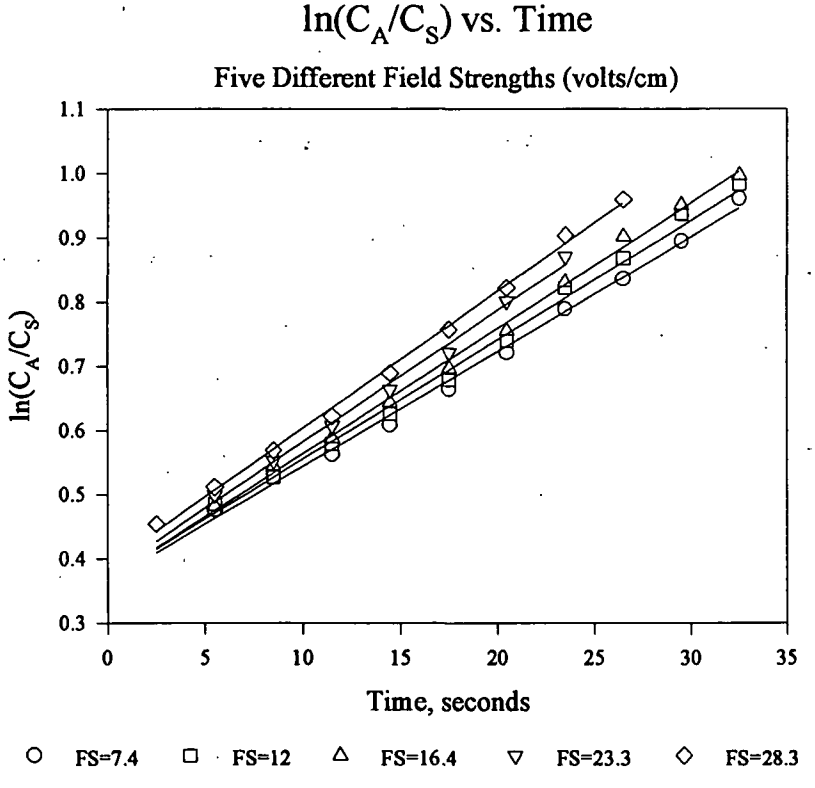

Figure 18. $\ln(C_A/C_S)$ vs. Time, 5 different field strengths.

Table 3. Summary of regression results.

Field Strength, volt/cm	Rate Constant, k, liter/mg·s	R^2
7.4	2.94	0.996
12.0	3.05	0.994
16.4	3.20	0.997
23.3	3.37	0.994
28.3	3.50	0.997

To view the data in the form of C_A vs. time with the overlay of the fitted model, equation (22) was used. The results are presented in figure 19.

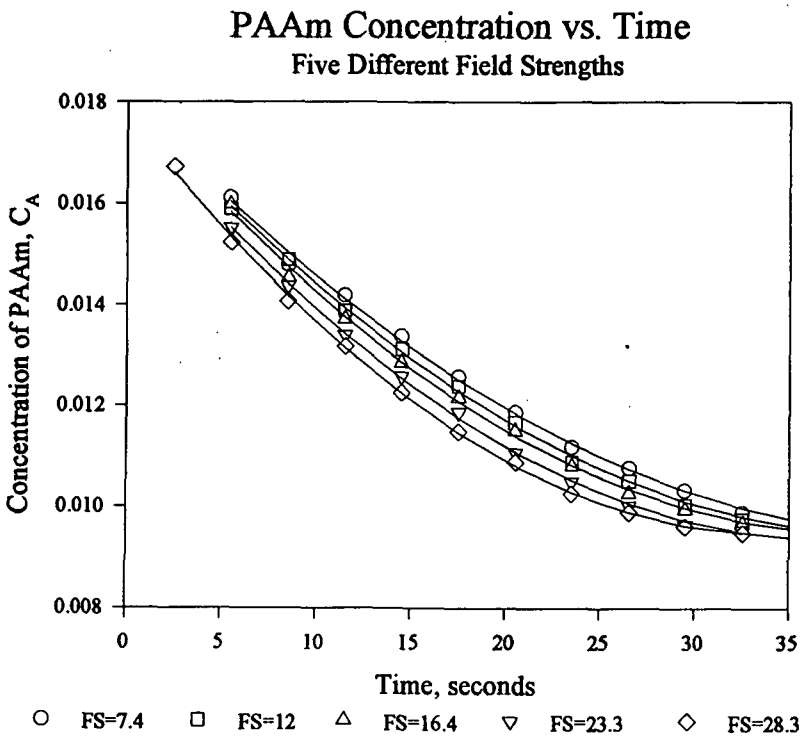

Figure 19 - C_A vs. Time, data with model equations overlaid.

If we are correct in assuming that the incremental rate increase due to the field strength is proportional to the field strength, a plot of the rate constant vs. field strength will be a straight-line. The rate constant for the case where the field strength is equal to zero, k_o, should be given by the intercept of this plot. The rate constants from the above data are plotted vs. field strength in figure 20 and the linear regression line is also included.

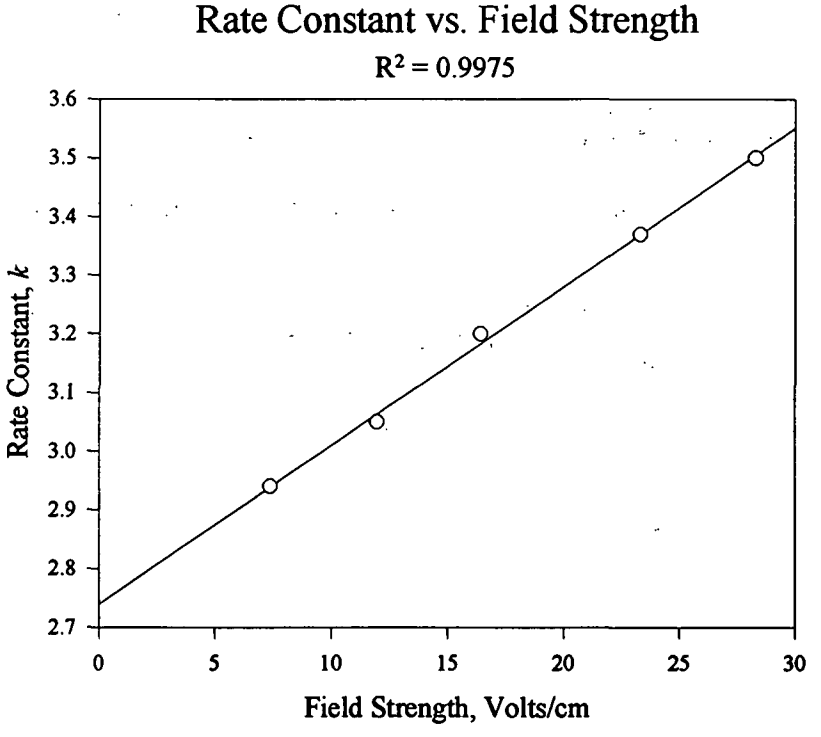

Figure 20 - Rate constant, k, vs. field strength.

The fit of these data to a straight line ($R^2 = 0.9975$) supports the conclusion that the incremental increase in the rate of adsorption is proportional to the field strength. If perikinetic rate data are collected at several different field strengths, this simple relationship will permit the rate enhancements due to the

electric field to be accounted for.

Determination of k_o

As we have demonstrated above, the adsorption rate constant for a given set of conditions is related to the field strength by the general equation;

$$k = m\,(\text{F.S.}) + k_o \tag{32}$$

where m is the slope, F.S. is the field strength, and k_o is the rate constant at zero field strength. Substituting this equation into the linear form of the rate equation, then rearranging, we get the following expression:

$$\ln\left(\frac{C_A}{C_S}\right) = m\,(C_{Ao} - C_{So})\,(\text{F.S.})\,t + k_o\,(C_{Ao} - C_{So})\,t + \ln\left(\frac{C_{Ao}}{C_{So}}\right) \tag{33}$$

Perikinetic data collected under a given set of conditions at several field strengths can be expressed according to equation (33). The coefficients for the equation can be obtained through multiple linear regression using (F.S.)x t and t as the independent variables. The value of k_o can be determined from the coefficient for the t variable, knowing the quantity (C_{Ao}-C_{So}). Likewise, the dependence on field strength, m, can be evaluated from the coefficient for the (F.S.)(t) variable. The regression results gave the best-fit coefficients for the independent variables as well as the standard error associated with each coefficient.

Values for the rate constant at zero field strength were determined using the above method of analysis. Adsorption rate differences due to factors other than C_A and C_S will be seen as differences in k_o. Calculation of individual values of

k_o for each replicate permitted statistical analysis of the results. One-way analysis of variance was performed on the data when more than two levels of the variable of interest were used. For cases where only two levels of the variable of interest were used, t-tests were used to determine whether significant differences in the rate of adsorption existed.

ORTHOKINETIC ADSORPTION

Determination of Rate Constant

As in the perikinetic investigations, the E.M. of the latex was used to determine the PAAm concentration as a function of time during the orthokinetic experiments. However, in the present experiments, there was no superimposed electric field throughout the adsorption process, and therefore, there was no need to correct for the effect of field strength.

A stopped-flow technique, described earlier, was used to determine the rate of adsorption. The E.M. vs. time data were collected once the flow was stopped. These data were converted to give the amount of adsorbed PAAm as a function of time since the flow was stopped. The intercept determined from regression was used to determine the PAAm concentration at the time when the flow was stopped. For a given set of conditions, and a given length of tubing, at least three replicates were performed. For each set of conditions, four to six different lengths of tubing were used, giving four to six different residence times.

According to equation (21), a plot of $\ln(C_A/C_S)$ vs. time should give a straight line with a slope of $k(C_{Ao}-C_{So})$. The linear regression results of this type of plot were used to calculate the rate constant for each set of conditions. An example of data treated in this manner is presented in figure 21 below.

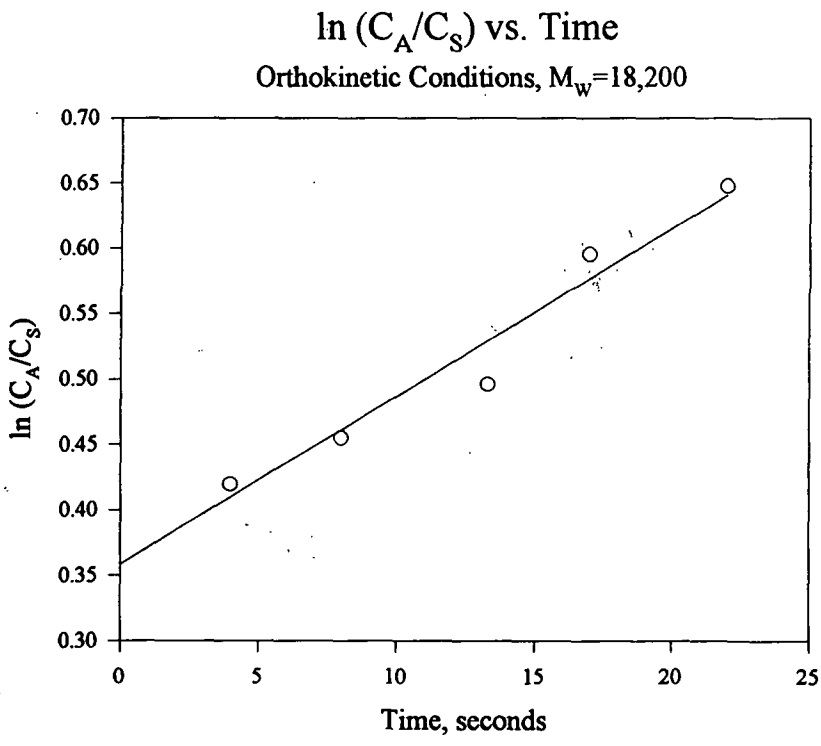

Figure 21. Example of data analysis for orthokinetic experiments, N_{Re}= 800.

EXPERIMENTAL RESULTS

The results of the adsorption rate experiments are contained in this section. The majority of the considerations and implications of the results are addressed in the *DISCUSSION* section which begins on page 98.

PERIKINETIC EXPERIMENTS

Polyelectrolyte Concentration

It is widely accepted that the rate of polymer adsorption is strongly dependent upon the concentration of polymer in the bulk. A first-order adsorption rate dependence on polymer concentration has been proposed by other workers.[19,23,35] In many of these studies, the dependence on fractional surface coverage was neglected. The model proposed here predicts a first-order dependence on PAAm concentration and on the amount of available adsorbent surface area. Therefore, the rate of adsorption should be proportional to the concentration of unadsorbed PAAm. Since the bulk concentration of PAAm decreases throughout the adsorption process, the fact that there is good agreement with the model throughout a single experiment gives support to the proposed first-order rate dependence on polyelectrolyte concentration. An example of data from a single experiment and the corresponding model fit is given in figure 22.

Another approach to test the dependence on PAAm concentration was also taken. Two similar sets of experiments were performed where the only

difference was the initial concentration of PAAm. If the rate of adsorption were first-order with respect PAAm concentration, the adsorption rate constant should be the same for each initial concentration of PAAm.

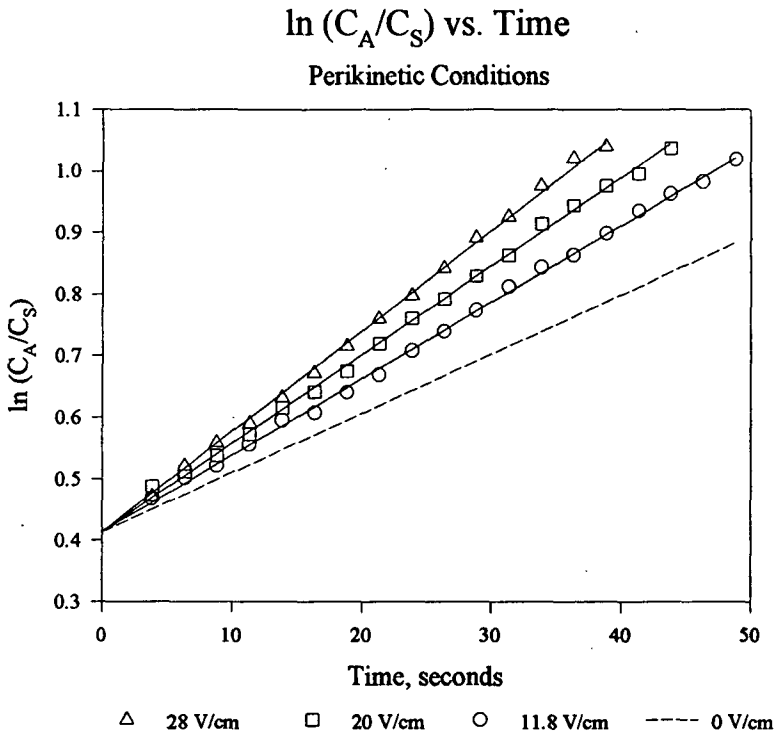

Figure 22. Example of model fit to data.

Adsorption experiments were conducted using the M_W=82,400 PAAm fraction and the high charge density latex in 0.001 M NaCl at a pH of 4.0. The latex concentration in each case was held constant while the initial PAAm concentrations were 0.020, and 0.030 mg/L. Four replicates were performed at each of three different field strengths for each initial PAAm concentration. The linear form of the model rate equation was used to determine the rate constant at zero field strength for

each of the experiments. The results from the analyses are summarized in table 4.

Table 4. Polyelectrolyte concentration results summary.

	Adsorption Rate Constant, k_o, liter/mg·s	
Replicate	C_{Ao}= 0.02 mg/L	C_{Ao}= 0.03 mg/L
1	1.60	1.55
2	1.69	1.56
3	1.52	1.56
4	1.56	1.57
Mean	1.59	1.56
Std. Dev.	0.07	0.01

A t-test performed on the above data showed that at the 95% confidence level, there was no significant difference between the average adsorption rate constants for the two different initial concentrations of PAAm. Therefore, any difference in the rate of adsorption between the two cases was accounted for by the C_A term in the model equation, without affecting the rate constant.

Latex Concentration

The results of studies conducted by other workers reveal that there is not a clear consensus regarding the effect of dispersed adsorbent concentration on the rate of polyelectrolyte adsorption. The kinetic model developed here, and the collision frequency arguments of Gregory[23,32,38] propose that there should be a

first-order dependence on the adsorbent particle concentration. The following experiments were designed to test this dependence.

Several experiments were conducted using the high charge density latex and the 82,400 M_w PAAm fraction in 0.001 M NaCl at pH 4.0. The initial PAAm concentration was 0.02 mg/L and the latex concentrations were 0.00025%, 0.00050%, 0.00075% and 0.00100%. Therefore, the only variable changed was the latex concentration. If the rate of adsorption is directly proportional to the latex concentration, any change in rate as a result of the latex concentration should not affect the calculated rate constant at zero field strength, k_o.

The adsorption rate data for each latex concentration were collected at three different field strengths, and four replicates were performed at each field strength. The rate constant at zero field strength was calculated from the data using the method outlined in the preceding section. The results of the analysis are summarized in table 5.

Table 5. Latex concentration results summary.

	Adsorption Rate Constant, k_o, liter/mg·s			
Replicate #	[latex] = 0.00025%	[latex] = 0.00050%	[latex] = 0.00075%	[latex] = 0.00100%
1	1.56	1.60	1.39	1.52
2	1.60	1.69	1.61	1.44
3	1.57	1.52	1.55	1.50
4	1.49	1.56	1.47	1.71
Mean	1.56	1.59	1.51	1.54
St. Dev.	0.05	0.07	0.10	0.12

One-way analysis of variance was performed on these data to determine the significance of the differences between the mean values of k_o for each condition. According to the analysis there were no significant differences among the values for k_o at the 95% confidence level. Therefore, since changing the latex concentration does not affect the rate constant, the proposed model correctly predicts that the rate of polyelectrolyte adsorption shows a first-order dependence on the concentration of the dispersed adsorbent.

System Concentration Experiments

According to the proposed rate equation, if the concentrations of PAAm and latex are changed simultaneously, the calculated rate constant should not change significantly. To test this hypothesis, adsorption experiments were conducted such

that the ratio of PAAm concentration to latex concentration was held constant, but the overall concentration of the system was adjusted to five different levels.

Using the medium molecular weight PAAm (M_w=82,400) and the high charge density latex (12.2 $\mu C/cm^2$), perikinetic adsorption experiments were carried out in 0.001 M NaCl at pH 4.0. The concentrations of the reagents at each condition are summarized in table 6.

Table 6. System concentration, experimental conditions.

Condition	Initial PAAm Concentration	Latex Concentration
1	0.010 mg/L	0.00025%
2	0.020 mg/L	0.00050%
3	0.030 mg/L	0.00075%
4	0.040 mg/L	0.00100%
5	0.050 mg/L	0.00125%

For each condition, adsorption rate data were collected at three different field strengths, and four replicates were run at each field strength. Each replicate was analyzed according to the previously outlined method, and the results are summarized in table 7.

Table 7. System concentration results summary.

	Adsorption Rate Constant, k_o, liter/mg·s				
Replicate	Condition 1	Condition 2	Condition 3	Condition 4	Condition 5
1	1.53	1.60	1.42	1.54	1.49
2	1.35	1.69	1.43	1.58	1.55
3	1.37	1.52	1.51	1.54	1.46
4	1.24	1.56	1.46	--	1.61
Mean	1.37	1.59	1.46	1.55	1.53
Std. Dev.	0.12	0.07	0.04	0.02	0.07

One-way analysis of variance was performed on these data, and the results showed that there was a statistically significant difference between at least one pair of means. In order to determine which means were significantly different, the least significant difference at 95% confidence ($L.S.D._{Q,0.95}$) was determined from statistical tables.[60] Out of the ten paired comparisons of k_o, the only case where there was a statistically significant difference in rate constant was between conditions 1 and 2. However, in all other comparisons, there was no difference between the rate constants. It is seems likely that the difference between cases one and two was a result of uncontrolled experimental error.

To minimize variation within a condition, all replicates were performed from master batches of reagents. An implicit assumption made in the above statistical analysis was that any error associated with the concentrations of these

master batches was negligible. Even very small errors in the PAAm concentration can have a significant effect on the calculated rate constant.

Since the rate constant did not change as the overall system concentration was increased by 250%, the model should be appropriate for accounting for changes in the rate of polyelectrolyte adsorption as the overall concentration of the system is changed. Experimental error may have contributed to finding a significant difference in one out of the ten comparisons made.

Polyelectrolyte Molecular Weight and Charge Density

The experimental results of other workers have shown that as the polyelectrolyte M_w increases, the rate of adsorption may increase, decrease or remain unchanged. The polyelectrolyte charge density has also been shown to affect the relationship between M_w and the rate of adsorption. The effects of polyelectrolyte M_w and charge density were investigated here using three different molecular weight fractions (M_w=18,200; 82,400; and 154,000 g/mole) and two polyelectrolyte charge densities (α=0.80 and α=0.15).

For all M_w experiments, the high charge density latex was used in a solvent of 0.001 M NaCl adjusted to either pH 4.0 (α=0.80) or pH 10.0 (α=0.15) using HCl and NaOH respectively. The concentration of latex in all experiments was 0.0005%. The initial PAAm concentrations were 0.02 mg/L for all pH 4.0 experiments, and 0.10 mg/L for all experiments conducted at pH 10.0. In order to

collect adsorption rate data of sufficient quality for analysis, it was necessary to be able to measure a significant change in the electrophoretic mobility of the latex. At pH 10 the PAAm charge density was 0.15 compared to 0.80 at pH 4. Because of this large difference in charge density, the amount of adsorbed PAAm required to cause a significant change in E.M. at pH 10 was greater than at pH 4. Therefore, the initial PAAm concentration at pH 10 was increased by a factor equal to the ratio of Γ_{max}(pH 10):Γ_{max}(pH 4). Since differences in initial PAAm concentrations are accounted for in the model, adsorption rate differences among these experiments due to factors other than PAAm concentration should be reflected in the calculated rate constants.

For each condition of M_W and charge density, four replicates were performed at each of three field strengths. The data were analyzed according to the previously described method of regression of the linear rate equation to determine k_o. The results of these analyses are summarized in table 8.

Analysis of variance was performed on the data, and all of the mean rate constants from each condition were significantly different at the 95% confidence level. Therefore, we can conclude that the rate of adsorption under perikinetic conditions increases as the M_W of the polyelectrolyte decreases. This trend holds for both the high and low charge density polyelectrolytes. It is also noted that the rate constants for the adsorption at pH 10 are significantly less than any of the corresponding rate constants for the pH 4 conditions.

Table 8. PAAm molecular weight and charge density, results summary.

	Adsorption Rate Constant, k_o, liter/mg·s					
	pH 4.0, α=0.80			pH 10.0, α=0.15		
Replicate	M_w = 154,000	M_w = 82,400	M_w = 18,200	M_w = 154,000	M_w = 82,400	M_w = 18,200
1	1.03	1.60	3.35	0.196	0.246	0.421
2	0.96	1.69	3.34	0.200	0.266	0.439
3	1.05	1.52	3.12	0.183	0.241	0.459
4	1.01	1.56	3.35	0.188	0.246	0.432
Mean	1.01	1.59	3.29	0.192	0.250	0.438
Std. Dev.	0.04	0.07	0.11	0.008	0.011	0.016

Ionic Strength

The majority of experiments conducted here have been performed at an ionic strength of 0.0011. In many industrial applications of polyelectrolytes, salt concentrations in the system are much higher, producing a higher ionic strength. In order to determine the effect of increasing the ionic strength, adsorption experiments were conducted at an ionic strength of 0.050, corresponding to a specific conductance of approximately 5000 μmho/cm. The medium molecular weight fraction (M_w=82,400) was adsorbed to the high charge density latex at pH 4.0 with a background NaCl concentration of 0.050 M.

As in other experiments, the electrophoretic mobility of the latex was measured as a function of time throughout the adsorption process. However, this method of data collection was not as useful at higher ionic strengths. As the ionic strength increased, the magnitude of the E.M. was diminished, giving a narrower range within which to differentiate between mobility readings. Another problem encountered when using the higher ionic strength was that the electric field strength could not be varied over as broad a range. These limitations invariably led to greater uncertainty when calculating the rate of adsorption at zero field strength. Despite these disadvantages, useful adsorption rate data were collected under the higher ionic strength conditions.

Four replicates were performed at each of three field strengths. The resulting data were analyzed according to the previously outlined procedures. Since the latex and PAAm concentrations were the same, any differences in the rate of adsorption should be accounted for by the rate constant. The results of the analysis are summarized in table 9.

Table 9. Ionic strength results summary.

	Adsorption Rate Constant, k_o, liter/mg·s	
Replicate	I = 0.0501	I = 0.0011
1	0.90	1.60
2	0.91	1.69
3	1.41	1.52
4	1.43	1.56
Mean	1.16	1.59
Std. Dev.	0.30	0.07

Though there appears to be a relatively large difference between the rate constants calculated at the high and low ionic strengths, this difference was not statistically significant. Since we cannot assume that the variances of the two sets of data are the same, an approximate t-test was used. If there were some real effect of ionic strength between these two cases, the variance of the data was too large to observe the effect. Regardless, any difference in the rate of adsorption due to ionic strength was small compared to other factors such as PAAm concentration, latex concentration, PAAm molecular weight and PAAm charge density.

Effect of Latex Surface Charge Density

If the electrostatic attraction between the anionic latex surface and the cationic polyelectrolyte contributes to the driving force for adsorption, decreasing the surface charge density of the latex may decrease the rate of polyelectrolyte

adsorption. Very little is known about the effect of surface charge density on the rate of adsorption. The following set of experiments was designed to investigate the effect of latex surface charge density on the rate of polyelectrolyte adsorption.

These experiments were conducted in 0.001 M NaCl at pH 4.0 using the same molecular weight PAAm sample (M_W= 82,400 g/mole). In all other experiments, the latex used had a surface charge density of 12.2 $\mu C/cm^2$. To study the effect of the latex surface charge density, adsorption experiments were conducted using latex having medium (6.5 $\mu C/cm^2$) and low (1.6 $\mu C/cm^2$) surface charge densities. In each experiment, the same latex (0.00025%) and initial PAAm (0.01 mg/L) concentrations were used.

As demonstrated by the correlations between latex E.M. and surface coverage, the amount of adsorbed PAAm required to reach saturation (Γ_{max}) was a function of the latex surface charge density. From the correlations between E.M. and surface coverage, the amounts required to reach Γ_{max} for the high (σ_H), medium (σ_M), and low (σ_L) charge density latexes were 0.22, 0.143 and 0.093 mg/m^2 respectively. The concentrations of latex surface area, C_s, for each of the different latexes were determined by using the respective Γ_{max} for each latex according to equation (17). Therefore, the surface concentration per mass of latex was different for each latex.

The data from these experiments were analyzed according to the procedures used in other cases by determining the rate constant at zero field strength using the linear model equation. The results from the analysis are summarized in

table 10. The results from the experiments using the high charge density latex are also included.

Table 10. Latex surface charge density, results summary.

	Adsorption Rate Constant, k_o, liter/mg·s		
Replicate	σ_L	σ_M	σ_H
1	1.71	1.60	1.60
2	1.65	1.69	1.69
3	1.61	1.59	1.52
4	1.48	--	1.56
Mean	1.61	1.63	1.59
Std. Dev.	0.10	0.06	0.07

One-way analysis of variance was performed on the data in table 10, and there were no statistically significant differences among the average rate constants for the three different latex surface charge densities. Therefore, we can conclude that the latex surface charge density does not directly affect the rate of polyelectrolyte adsorption.

ORTHOKINETIC FLOW EXPERIMENTS

Since many applications of polyelectrolytes involve systems under flow, it was of interest to investigate the rate of polyelectrolyte adsorption at orthokinetic conditions under laminar and turbulent flow. Compared to the perikinetic investigations, relatively few experiments were performed under these flow conditions. However, some conclusions were drawn from the limited data. All of the experiments conducted under these flow conditions used the same initial concentrations of PAAm (0.02 mg/L) and latex (0.0005%). Therefore, according to the model, any differences in the rate of adsorption should be reflected in the adsorption rate constant, k_o.

In these experiments, the rate of polyelectrolyte adsorption to the high charge density latex was measured using PAAm at two molecular weights (M_w=18,200 and 154,000) and two Reynolds numbers (800 and 4000) corresponding to laminar and turbulent flow. Because of the limited amount of data collected for each experiment, it was not possible to perform a rigorous statistical analysis of the results. However, the standard error of the coefficients from the regression analysis gave some indication regarding the error associated with the estimates of k_o. The results of the rate constant determinations are summarized in table 11.

Table 11. Laminar and turbulent flow, results summary.

Molecular Weight, g/mole	Reynolds Number	Adsorption Rate Constant, liter/mg·s	Standard Error	R^2
18,200	4000	3.39	0.36	0.956
18,200	800	2.16	0.27	0.957
154,000	4000	1.73	0.22	0.969
154,000	800	0.81	0.10	0.955

According to the results in table 11, there are two general conclusions which can be drawn. For both the high and low molecular weight fractions, the rate of adsorption was greater under turbulent flow than under laminar flow conditions. These results are consistent with previous studies which have shown that increasing the amount of mixing in the system increased the rate of adsorption.[38-42] The second general conclusion is that under both laminar and turbulent conditions, the rate of adsorption was faster for the lower molecular weight fraction.

Some orthokinetic experiments were performed without using the in-line mixing unit. In these experiments it was found that after a residence time of 22 seconds under laminar flow, the amount of PAAm which had adsorbed was less than 50% of the amount adsorbed when the static mixer was used. This evidence suggests that the initial mixing of the reactants is very important in determining the rate of polyelectrolyte adsorption.

DISCUSSION

Several interesting results from the experimental investigation of the rate of polyelectrolyte adsorption have been found. A discussion of the implications of these results with respect to previous work, theoretical predictions, and practical applications is presented below.

PERIKINETIC CONDITIONS

Concentration Dependence

In the three sets of experiments which dealt with the effects of PAAm concentration, latex concentration, and overall system concentrations, the results supported the model assumptions that there was a first-order rate dependence on both PAAm concentration and the amount of latex surface area available for adsorption. Since within a given system, the initial surface area was proportional to the adsorbent concentration, the adsorption rate was shown to be first-order with respect to adsorbent concentration. Other workers have concluded that the adsorption rate was first-order with respect to polymer concentration only.[19,23,35] In these other systems, it is likely that the adsorbent concentration was high enough that changes in the concentration of available surface area were insignificant compared to changes in polymer concentration.

The results indicating the first-order dependence on both PAAm and latex concentrations are consistent with the predictions based on collision rate; as the

concentrations increased, there was a proportionate increase in the rate of adsorption.

One of the assumptions of the theoretical model was that the collision efficiency was proportional to the amount of surface area available for adsorption. By assuming that the surface area covered by an adsorbed molecule was the same regardless of the amount already adsorbed, the quantity Γ/Γ_{max} was used to determine the relative collision efficiency. Because of the success of the model predictions, this assumption was adequate for these conditions over the range of fractional surface coverage within which the data were collected (Γ/Γ_{max} from 0.25 to 0.70).

Polyelectrolyte Molecular Weight and Charge Density

It was established that as the molecular weight of the polyelectrolyte increased, the rate of adsorption decreased. This trend was found under all experimental conditions investigated. Since the diffusion coefficient of the polyelectrolyte decreased as the molecular weight increased, this trend in adsorption rate was consistent with a diffusion dominated process. The trends observed were likely due to the diffusion coefficients of the respective polyelectrolytes. If we apply the concepts developed in von Smoluchowski's theoretical treatment of rapid coagulation to polyelectrolyte adsorption, the rate constant of the adsorption process should be linearly related to the sum of diffusion coefficients of the polyelectrolyte and the latex (see equations (8)-(11)) . The assumption here is that the polyelectrolyte in solution may be approximated as a spherical random coil.

To test the applicability of Smoluchowski's treatment to this case, it was necessary to determine diffusion coefficients, and radii of the polyelectrolytes and latex, and to make appropriate conversion of units. The diffusion coefficients of the PAAm fractions at pH 4.0 and pH 10 in 0.001 M NaCl were calculated from intrinsic viscosity results using the methods discussed on page 51. For the latex particles having an average radius of 225 nm, the diffusion coefficient was calculated to be 9.7 x 10^{-9} cm^2/s using the Stokes-Einstein equation (2).

For second order rate equations, the rate constants are expressed in terms of reciprocal concentration per unit time. In Smoluchowski's treatment, the concentration of particles is given in terms of number of particles, n, per unit volume. The units used to express the Smoluchowski rate constant (k_s) are $cm^3/n \cdot s$, while the units on the experimentally determined adsorption rate constants are $L/mg \cdot s$. Therefore, the measured rate constants were converted into the Smoluchowski units using equation (34).

$$k_o\left(\frac{L}{mg \cdot s}\right) \times \Gamma_{max}\left(\frac{mg}{m^2}\right) \times A(m^2) \times \left(\frac{10^3 cm^3}{L}\right) = k_o\left(\frac{cm^3}{n \cdot s}\right) \qquad (34)$$

where:
Γ_{max} = maximum surface coverage of latex by PAAm
A = surface area of a single latex particle

The values of Γ_{max} for each condition were obtained from the correlation curves (*e.g.*, figure 16), and the results are summarized in table 12. The theoretical rate constant for colliding spheres of different size predicted by Smoluchowski (k_s) was calculated using equation (35).

$$k_s = 4\pi \times (r_{Latex} + r_{PAAm}) \times (D_{Latex} + D_{PAAm}) \qquad (35)$$

The results of these calculations are summarized in table 13.

Table 12. Summary of Γ_{max} for different latexes and pH.

Latex	pH	Γ_{max}, mg/m^2
σ_H	4.0	0.220
σ_M	4.0	0.143
σ_L	4.0	0.093
σ_H	10	0.870

Table 13. Summary of calculations for Smoluchowski predictions.

M_W	pH	PAAm Radius, cm	PAAm D°, cm^2/s	k_S, cm^3/n·s	k_o, cm^3/n·s
18,200	4	6.6×10^{-7}	3.3×10^{-7}	0.99×10^{-10}	4.6×10^{-10}
82,400	4	20×10^{-7}	1.1×10^{-7}	0.37×10^{-10}	2.2×10^{-10}
154,000	4	30×10^{-7}	0.72×10^{-7}	0.26×10^{-10}	1.4×10^{-10}
82,400	10	12×10^{-7}	1.8×10^{-7}	0.57×10^{-10}	0.35×10^{-10}
154,000	10	22×10^{-7}	0.98×10^{-7}	0.36×10^{-10}	0.27×10^{-10}

In figure 23 a plot of k_o vs. D° was constructed including the theoretical and observed values of k in units of cm^3/n·s. Linear regression was used to fit the best straight line through the data. According to the theoretical development, the rate constant should be zero when the diffusion coefficient is zero; therefore, the intercept was forced to the origin in the linear regression.

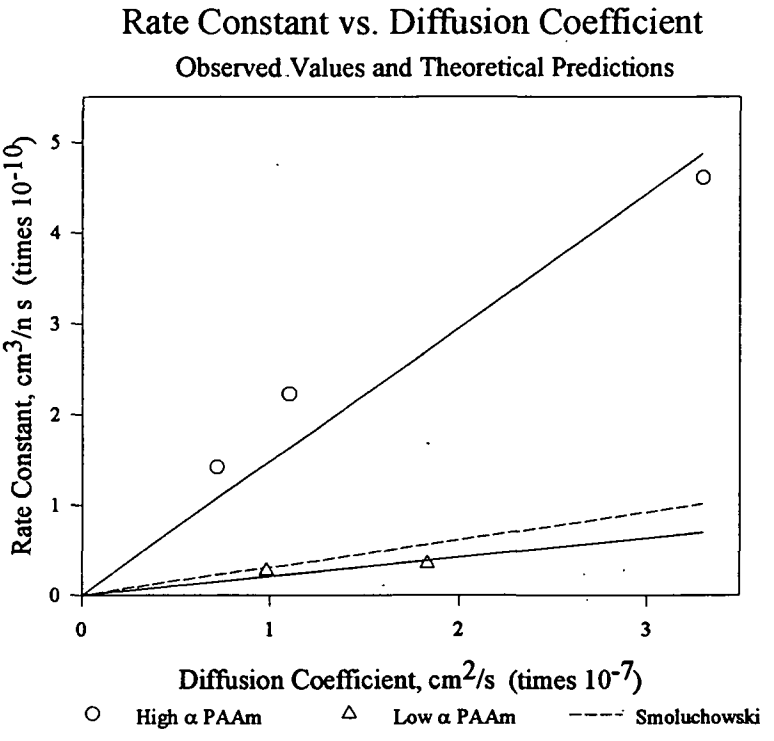

Figure 23. Adsorption rate constant vs. diffusion coefficient.

For the high charge density polyelectrolyte, the observed rate constants are significantly higher than those predicted by the Smoluchowski treatment. If diffusion of the polyelectrolyte is the rate limiting step in the adsorption process, the linear relationship between the rate constant and diffusion coefficient should exist.

The observed rate constants for the high α PAAm are approximately five times greater than those calculated using Smoluchowski's equation. Some of the difference between the observed and expected values may be accounted for by error in the estimates of polyelectrolyte diffusion coefficients. The equations used to calculate these values have been shown to be valid for uncharged polymers.

However, the actual diffusion coefficients of polyelectrolytes may be higher due to the close association between the polyelectrolyte and the very mobile counter-ions. The diffusion coefficient of these counter-ions is much higher than that of the polyelectrolyte. As the counter-ions diffuse more rapidly, they resist separation from the polyelectrolyte due to the electrostatic attraction between them. The net effect of this phenomenon is that the diffusion of the counter-ions is decreased, but the diffusion of the polyelectrolyte is enhanced.[1]

The importance of this effect is related to the polyelectrolyte concentration, solution ionic strength, and polyelectrolyte charge density.[61] This acceleration of the polyelectrolyte due to the counter-ions is more important as the polyelectrolyte concentration decreases,[62] as the ionic strength is decreased,[3] and should be more pronounced as the charge density of the polyelectrolyte is increased. If the acceleration of the polyelectrolyte decreases as the charge density of the polyelectrolyte decreases, this effect may also explain why the observed rate constants for the low charge density polyelectrolytes are lower than those for the high charge density polyelectrolytes. The fact that the adsorption rate for the higher charge density, less concentrated polyelectrolyte is much faster is consistent with the trends of enhanced polyelectrolyte diffusion. Since in the low α case the PAAm charge density is a factor of five less than the high α, and the concentration of PAAm in these experiments is a factor of five greater than the high α, it is not unreasonable to expect the polyelectrolyte diffusion effect to be much less important for the low α experiments.

The observed rate constants for the low α PAAm were lower than those predicted by the Smoluchowski treatment. It was demonstrated that a relatively strong relationship exists between the adsorption rate constant and the calculated diffusion coefficient for the high α experiments. By comparing the relative slopes of the high and low α plots in figure 23, this relationship is not as strong for the low α experiments. This suggests that some factor other than diffusion of the PAAm to the surface of the latex may be limiting the rate of polyelectrolyte adsorption.

In the Smoluchowski treatment, the collision efficiency is assumed to be unity, so that if appropriate diffusion coefficients were used, k_s should give the upper limit for k_o. The efficiency of the PAAm-latex collisions at pH 10 may be overestimated by the adsorption model due to reconformation of the polyelectrolyte on the surface of the latex.

The amount of reconformation which occurs for the two α's may be different. From the respective values of Γ_{max} for the high and low α PAAm, we can calculate the average surface area required for a single polyelectrolyte molecule at saturation. From the radii of gyration of the high and low α molecules, we can calculate the projected area of the respective random coils. These values for the highest M_W fraction (154,000 g/mole) are given in table 14.

Table 14. Comparison of adsorbed and unadsorbed molecular dimensions.

pH	Projected Area of PAAm in solution	Area occupied at saturation	Projected Area / Area at Saturation
4.0	$2.8 \times 10^3\ nm^2$	$1.2 \times 10^3\ nm^2$	2.4
10	$1.5 \times 10^3\ nm^2$	$2.8 \times 10^2\ nm^2$	5.2

According to the results in table 14, if only steric factors are considered, the low α PAAm may undergo more reconformation during the adsorption process. If the reconformation of the polyelectrolyte takes a finite amount of time, the rate of adsorption should be diminished. Prior to reconformation, the adsorbed polymer would cover a larger amount of surface area which decreases the amount of area available for adsorption, hence, decreasing the collision efficiency.

Latex Surface Charge Density

The investigation of the effect of latex surface charge density revealed that despite a nearly eight fold difference between the surface charge density of the high and low latexes, there was no significant effect on the rate of adsorption. At the very least, these effects are small compared to other effects such as PAAm concentration, latex concentration, PAAm molecular weight and PAAm charge density.

This result was at first surprising. Previous workers have suggested

that since the polymer and adsorbent are oppositely charged, the rate of polymer adsorption should be faster than if no charges were present. The experimental outcome observed here can be readily explained by comparing the relative thickness of the electric double layer with the average distance traveled by an adsorbing PAAm molecule. Since the electric double layer is electrically neutral, the electrostatic attraction between the negatively charged latex surface and the positively charged PAAm molecule would only affect the rate of approach of the molecule when it is within the electric double layer.

From equation (3), the thickness of the electric double layer (κ^{-1}) was approximately 10 nm in 0.001 M NaCl at pH 4.0. We can approximate the average distance traveled by an adsorbing molecule by first determining that the average distance of separation between latex particles (0.45μm diameter) at 0.0005% solids is approximately 30 μm. If we assume that a given latex particle will adsorb polymer from within a sphere of 30 μm in diameter, the median distance between the surface of the latex and the molecules within this sphere is about 12μm. Therefore, the average distance traveled by an adsorbing molecule would be about 10μm. This distance is three orders of magnitude greater than the thickness of the electric double layer. Therefore, the average distance over which the adsorbing molecule was influenced by the electrostatic attraction of the negatively charged latex surface was on the order of 0.1 % of the total path.

Based on these calculations, there is little likelihood that the magnitude

of the attractive force would have a significant effect on the rate of polyelectrolyte adsorption. According to this argument, it is possible that the effect of adsorbent surface charge density may become more important as the adsorbent concentration is increased such that the average distance traveled by an adsorbing molecule is orders of magnitude less.

ORTHOKINETIC CONDITIONS

From the results of the adsorption rate experiments conducted at orthokinetic conditions under laminar and turbulent flow, we concluded that the rate of adsorption was faster under turbulent flow than under laminar flow. This result can readily be explained by the enhanced rate of transport due to convection under turbulent conditions. Numerous other workers have concluded that increasing the intensity of mixing will increase the rate of polymer adsorption.

It was also found that under both laminar and turbulent flow conditions, the rate of polyelectrolyte adsorption increased as the molecular weight of the polyelectrolyte decreased. These results indicate that the diffusion of the PAAm molecules to the surface of the latex is still a significant mode of transport.

Figure 24 shows the adsorption rate constants predicted by Gregory's application of collision theory to orthokinetic conditions under laminar flow. The values of laminar shear rate (G=420s^{-1}) and adsorbent radius used in figure 24 correspond to the experimental values used here. At pH 4.0, the hydrodynamic radii

of the low and high M_w fractions were calculated to be 6.6 and 30 nm respectively. In this range of polymer radii, the contribution of the laminar shear to the rate of adsorption is small. Therefore, we would expect the rate of adsorption under laminar conditions to not be significantly greater than the perikinetic rate. The data collected under laminar conditions indicate that the rate of adsorption is not significantly greater than the rate under perikinetic conditions (table 15).

Table 15. Rate constants for orthokinetic and perikinetic conditions (pH 4.0).

Molecular Weight, g/mole	Reynolds Number	Adsorption Rate Constant, liter/mg·s	Standard Error
18,200	4000	3.39	0.36
18,200	800	2.16	0.27
18,200	0	3.29	0.06
154,000	4000	1.73	0.22
154,000	800	0.81	0.10
154,000	0	1.01	0.02

As demonstrated in figure 24, equation (14) predicts that as the polymer radius increases, the effect of shear on the rate of adsorption becomes more important. While the resolution of the data collected under turbulent flow may not be appropriate for involved numerical comparisons, the prediction that shear becomes more important as the polymer radius increases is consistent with the experimental results seen here.

It has been suggested that for turbulent conditions, equation (14) may be used to predict the relative rate constant of the adsorption by using the effective shear rate for the system.[32] The effective shear rate in turbulent flow is given by equation (36).

$$G = \left(\frac{\varepsilon}{\nu}\right)^{\frac{1}{2}} \tag{36}$$

where:
ε = energy dissipation
ν = kinematic viscosity

Other workers have used several methods of calculating ε for turbulent pipe flow by considering various portions of the flow cross-section. An upper bound for the effective shear rate is given by using the total pressure drop to calculate ε, while the lower limit is given by calculating the effective shear at the center of the tube. Using these two methods, the effective shear rates for tube flow at a Reynolds number of 4000 were calculated to be $3550s^{-1}$, and $940s^{-1}$ respectively. Equation (14) was used to calculate the theoretical rate constants for these levels of effective shear rate, and the results are represented graphically in figure 24. The perikinetic and laminar (G=$420s^{-1}$) curves are also plotted for comparison.

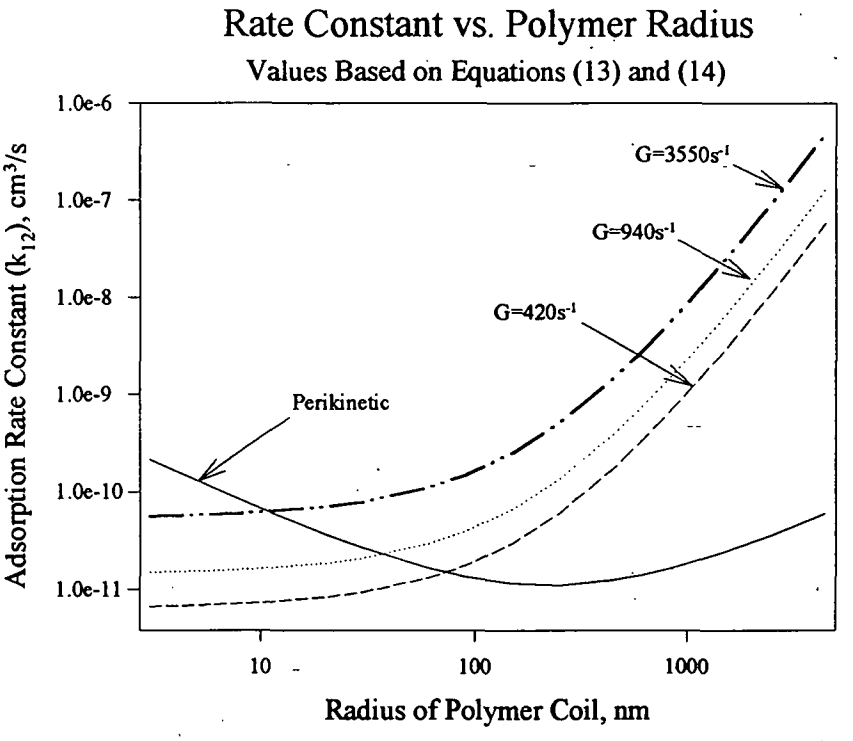

Figure 24. The effect of G on the relationship between k and polymer radius.

Even at the highest shear rate of $3550s^{-1}$, the rate of adsorption of the low molecular weight polyelectrolyte (6.6 nm radius) is not predicted to be significantly affected by the turbulence since, at this radius, the perikinetic rate is significantly larger. For the high molecular weight polyelectrolyte (30 nm radius), the predicted rate constant for the sheared conditions is beginning to become more significant relative to the perikinetic conditions. Therefore, the theoretical predictions based on equation (14) are consistent with the experimental results.

IMPLICATIONS FOR PAPER MANUFACTURE

Cationic polyelectrolytes are commonly used as retention aids at the wet end of the paper machine. The adsorption of these retention aids to the stock suspension is essential for their efficient use. Since the time frame within which polyelectrolyte adsorption must take place is on the order of seconds, the rate of adsorption is critical. Although there are some limitations involved in direct application of the results of this study to industrial situations, there are several meaningful implications. This discussion will first identify some of the probable differences between the wet end of the paper machine and the system studied here. With these differences in mind, the results of these experiments will be applied to the industrial use of polyelectrolytes in papermaking.

When cationic polyelectrolytes are added to the dilute stock just prior the headbox, the dosage of polymer with respect to Γ_{max} is relatively small compared to the dosage used in this work. In this industrial application, the fractional change in available adsorbent surface area will be small. Therefore, there is likely to be a pseudo first-order dependence on polyelectrolyte concentration.

It was shown here that the rate of polyelectrolyte adsorption under perikinetic, laminar, and turbulent conditions was inversely related to the molecular weight of the polyelectrolyte. The molecular weight of the polyelectrolytes used here were very low compared to polyelectrolytes typically used as retention aids. Based on this information, one might anticipate that the rate of adsorption in

papermaking may be diminished. Theoretical predictions made by Gregory[23,32,38] imply that the rate of adsorption under high shear conditions, such as those found in paper making, would increase as the molecular weight of the polyelectrolyte is increased. Because of the order of magnitude difference between the molecular weights of the polyelectrolytes used here and those used in papermaking, Gregory's theoretical prediction could not be tested.

Relatively low concentrations of polyelectrolyte and adsorbent concentration were used in these experiments in order to achieve better resolution of the adsorption rate data. In the system concentration experiments, it was shown that as the concentration of the system was increased, the rate of adsorption increased geometrically. For example, when the system concentration was changed by a factor of n, the rate of adsorption increased by a factor of n^2. The furnish concentrations found in a typical papermaking system are approximately three orders of magnitude greater than those used in these experiments. Based on this information, the rate of polyelectrolyte adsorption in a papermaking system should be much faster than the rates seen here.

Thus far, the discussion has been limited to variables where significant differences existed between this experimental system and a typical papermaking system. Direct comparisons can be made with regard to the effect of salt concentrations and adsorbent surface charge density. The rate of polyelectrolyte adsorption was not significantly affected by the ionic strength of the system. The high end of the range of ionic strength used in these experiments was comparable to

those found in the wet end of a paper machine. Therefore, it is not likely that the ionic strength of a papermaking system will have a significant effect on the rate of polyelectrolyte adsorption.

One of the most significant factors affecting the rate of polyelectrolyte adsorption in papermaking was not part of the main objectives of this work. In all of the thesis experiments, the system was assumed to be homogeneous. This assumption was reasonable because the reagents were thoroughly mixed by passing them through the in-line mixing unit. However, the methods of polymer introduction and subsequent mixing appear to be very important. Under orthokinetic conditions, the observed rate of adsorption was more than 50% slower when the streams of PAAm and latex were not passed through the mixing unit. If thorough mixing is not achieved, when the retention aid is introduced to the furnish, a similar decrease in the rate of adsorption may be observed.

CONCLUSIONS

Throughout the course of this thesis, several conclusions have been made regarding the rate of polyelectrolyte adsorption onto the surface of a dispersed adsorbent of opposite charge. Strictly speaking, these conclusions are limited to the specific system studied here, but the concepts can readily be applied to other systems. A kinetic model of polyelectrolyte adsorption was developed to account for changes in the rate of adsorption due to the concentration of polyelctrolyte and adsorbent surface area. This model was verified by performing several individual sets of experiments. The specific conclusions from these experiments are:

1) The rate of polyelectrolyte adsorption is directly proportional to the concentration of unadsorbed polyelectrolyte.

2) a) The rate of polyelectrolyte adsorption is directly proportional to the relative amount of available surface area on the dispersed adsorbent.

b) Since the initial surface area is directly proportional to the adsorbent concentration, the initial rate of polyelectrolyte adsorption is directly proportional to the number concentration of the dispersed adsorbent.

3) The collision efficiency between the PAAm molecules and the dispersed adsorbent is proportional to $1-\Gamma/\Gamma_{max}$.

4) Under perikinetic conditions, there is a linear relationship between the adsorption rate constant, and the strength of the superimposed electric field.

In addition to the effects of concentration of various components, several other factors were investigated with regard to their effect on polyelectrolyte adsorption rate. These factors include polyelectrolyte molecular weight, polyelectrolyte charge density, adsorbent surface charge density, and mixing.

5) As the molecular weight of the polyelectrolyte increases, the rate of polyelectrolyte adsorption decreases. This trend was observed under perikinetic conditions, and at orthokinetic conditions under both laminar and turbulent flow. This effect was stronger for the high charge density PAAm than for the low charge density polyelectrolyte.

6) The rate of adsorption is higher for the high charge density polyelectrolyte. This phenomenon was attributed to an enhanced diffusion rate due to the effect of counter-ions, and lower collision efficiency for the lower charge density PAAm as a result of slow reconformation of the molecule on the surface.

7) The surface charge density of the adsorbent does not affect the rate of polyelectrolyte adsorption. However, according to the argument given in support of this phenomenon, the adsorbent surface charge density is more likely to have an effect at much higher adsorbent concentrations.

8) Changes in ionic strength of the system do not have a significant effect on the rate of polyelectrolyte adsorption in this system.

9) Inadequate mixing at the point of polyelctrolyte introduction will result in a much slower rate of polyelectrolyte adsorption.

SUGGESTIONS FOR FUTURE WORK

The results obtained in this work apply very well to the system at hand. Several trends have been shown with regard to the effects of polyelectrolyte molecular weight, and the flow conditions which exist in the system. Most industrial applications of polyelectrolytes involve much larger molecules, and turbulent flow conditions. The equipment and methods developed in this thesis can be readily extended to polyelectrolyte molecular weights on the order of several million. An investigation of the factors governing the adsorption rate of these higher molecular weight polyelectrolytes would add to the practical application of these conclusions.

ACKNOWLEDGMENTS

The successful completion of this work would not have been possible without the support provided by many individuals and organizations. I would like to thank my thesis advisory committee: Dr. Barry W. Crouse, Dr. H. L."Jeff" Empie, and my primary advisor, Dr. Robert A. Stratton. Special appreciation goes to Dr. Stratton who was a constant source of technical information, as well as advice and friendship. I am grateful to the Institute of Paper Science and Technology, and its supporting member companies for the opportunity to advance my education, and for the financial support to conduct this work.

Mr. Pei-Hua Yang, Dr. Gary Poehlein, and Dr. F. Joseph Schork of the Emulsion Polymers Group at the Georgia Institute of Technology are gratefully acknowledged for their technical and laboratory support during the latex synthesis. I would also like to thank Mike Friese for his role in the PAAm preparation and characterization; and Dr. Thomas J. McDonough for suggesting the approach to the statistical analysis used in this work. I am also grateful to Warren Davis, who was responsible for the design and troubleshooting of the electronic equipment; and Joe Nadeau, who constructed the flow converger and the automated injection apparatus.

I would like to thank my fellow students for their assistance on numerous occasions, and for their friendship which will not soon be forgotten.

Finally, I am most grateful to my wife, Kerry, for her unrelenting support of my endeavors, and for her constant encouragement and love.

LIST OF SYMBOLS AND ABBREVIATIONS

A	latex surface area, cm^2
a	particle radius of curvature, nm
a	slope of Mark-Houwink-Sakurada plot
a_1	adsorbent particle radius, nm
a_2	radius of polymer in solution, nm
AIA	automated injection apparatus
C_B	concentration of dispersed adsorbent, %
c	concentration of polymer in bulk
c_i	concentration of ion i, moles/L
C_A	bulk polyelectrolyte concentration, mg/L
$C_{B\phi}$	concentration of adsorbent surface area, m^2/L
C_S	concentration of adsorbent surface area, mg/L
cm	centimeter
C_{So}	initial concentration of adsorbent surface area, mg/L
C_{Ao}	initial concentration of polyelectrolyte, mg/L
D	diffusion coefficient, cm^2/s
D^o	diffusion coefficient at infinite dilution, cm^2/s
DP	degree of polymerization
e	electron charge
E.M.	electrophoretic mobility, (μm·cm)/(V·s)
F.S.	electric field strength, V/cm

G	uniform shear rate, s^{-1}
i.d.	inside diameter
J	collision frequency, s^{-1}
k_1	adsorption rate constant, Peterson and Kwei
k_{-1}	desorption rate constant, Peterson and Kwei
k_{12}	adsorption rate constant, Gregory
k	adsorption rate constant, L/mg·s
k_o	adsorption rate constant at zero field strength, L/mg·s
k_S	Smoluchowski rate constant, $cm^3/n·s$
k	Boltzmann's constant
K'	exp(intercept), Mark-Houwink-Sakurada plot
L	liter
M	molecular weight, g/mole
M_W	weight average molecular weight, g/mole
M_N	number average molecular weight, g/mole
M_i	viscosity average molecular weight of bin i, g/mole
M	moles per liter
m	meter
m	slope of rate constant vs. field strength
M-H-S	Mark-Houwink-Sakurada
mg	milligrams
ml	milliliter
mm	millimeter
N_A	Avogadro's number

n	number concentration
N_{Re}	Reynold's number
nm	nanometer
°C	temperature, degrees celcius
PAAm	polyallylamime hydrochloride
PEI	polyethylenimine
psi	pressure, pound per square inch
PVSK	potassium polyvinylsulfate
R	collision radius, sum of radii of two colliding species, cm
R_g	polymer radius of gyration, cm
R^2	coefficient of determination from regression
R_t	polymer radius determined from diffusion measurement
R_η	polymer radius determined by viscometry
r	inside diameter of capillary or tube
r	radius of particle in suspension, cm
s	seconds
SEC	size exclusion chromatography
Std. Dev.	sample standard deviation
T	absolute temperature, K
t	time
TB	*o*-toluidine blue indicator
V	volts
x	amount of adsorbed polyelectrolyte at time *t*, mg/L
z_i	valence of ion i

α	polyelectrolyte charge density, %/100
ε	dielectric constant
ε_o	permittivity of vacuum
Φ	Flory Constant
ϕ	collision efficiency
Γ	surface coverage, g/m^2
Γ_{max}	maximum surface coverage at saturation, g/m^2
$[\eta]$	intrinsic viscosity, cm^3/g
η_o	solvent viscosity
κ^{-1}	Debye-Huckel screening length, nm
μm	micrometer or micron
μC	microcoulomb
ν_o	initial number concentration of singlet particles
ν	number concentration of singlet particles
π	pi = 3.1416.
θ	fractional surface coverage
σ_H	high charge density latex, 12.2 $\mu C/cm^2$
σ_L	low charge density latex, 1.6 $\mu C/cm^2$
σ_M	medium charge density latex, 6.5 $\mu C/cm^2$
Ψ_o	surface potential, mV
ζ	zeta potential, mV

LITERATURE CITED

1. Richards, E. G. An Introduction to Physical Properties of Large Molecules in Solution. Cambridge, Cambridge University Press, 1980:1.

2. Tanford, C. Physical Chemistry of Macromolecules. New York, John Wiley & Sons, 1961:150-70.

3. Morawetz, H. Macromolecules in solution. 2nd Ed., High Polymers. Vol. XXI. New York, Wiley-Interscience, 1975. 549 p.

4. Flory, P. J.; Fox, T. G. Treatment of intrinsic viscosities. Journal of the American Chemical Society 73:1904-8(1951).

5. Shaw, D. J. Introduction to Colloid and Surface Chemistry, 3rd ed. London, Butterworth & Company Limited, 1980 273 p.

6. Tsvetkov, V. N.; Klenin, S. I. A study of diffusion in polymer solutions by the use of polarization interferometer. Journal of Polymer Science 30:187-200(1958).

7. Kruyt, H. R. (Editor) Colloid Science. Vol. 1. New York, Elsevier Publishing, 1952:115-243.

8. Matijevic, E. (Editor) Surface and Colloid Science. Vol. 7. New York, John Wiley and Sons, 1974, 356p.

9. Hunter, R. J. Zeta Potential in Colloid Sceince: Principles and Applications. New York, Academic Press, 1981, 386p.

10. Hiemenz, P. C. Principles of Colloid and Surface Chemistry. New York, NY, Marcel Dekker, Inc., 1977:457-63.

11. Smoluchowski, M. Von Physik. Z.17:557-85(1916).

12. Smoluchowski, M. Von Z. physik. Chem. 92:129(1917).

13. Overbeek, J. Th. G. Kinetics of Flocculation, In Kruyt's Colloid Science, Vol. 1, New York, Elsevier Publishing Company, 1952:278-301.

14. Levich, V. G. Physicochemical Hydrodynamics. Englewood Cliffs, N.J., Prentice Hall, Inc. 1962:207-21.

15. Probstein, R.F. Physicochemical Hydrodynamics. Boston, Butterworth-Heineman, 1989:236-42.

16. Aptel, H. D.; Carroy, P. D.; Dejardin, P.; Pefferkorn, E.; Schaaf, P.; Schmitt, A.; Varoqui, R.; Voegel, J. C. ACS Symposium Series No. 343, Washington, DC, American Chemical Society, 1987:222-38.

17. Lindstrom, T.; Soremark, C. Adsorption of cationic polyacrylamides on cellulose. Journal of Colloid and Interface Sceince 55(2):305-12(1976).

18. Kindler, W. A.; Swanson, J. W. Adsorption kinetics in the polyethylenimine-cellulose fiber system. Journal of Polymer Science 9(A-2):853-65(1971).

19. Abril Gonzalez, A.; Hernandez Castro, C. Adsorption of cationic polyelectrolyte by bleached bagasse chemical pulp; Adsorption kinetics. Investigacion Y Tecnica del Papel 23(89):521-31(1986).

20. Falk, M.; Odberg, L.; Wagberg, L.; Risinger, G. Adsorption kinetics for cationic polyelectrolytes onto pulp fibers in turbulent flow. Colloids and Surfaces 40:115-124(1989).

21. Khlebstov, N. G.; Sirota, A. I.; Fomina, V. I.; Vypov, M. G. Use of an electrooptic method to study polymer-bearing disperse systems. Kolloidnyi Zhurnal 52(1):178-82(Jan.-Feb. 1990).

22. Peterson, C.; Kwei, T. K. The kinetics of polymer adsorption onto solid surfaces. Journal of Physical Chemistry 65(8):1330-3(1961).

23. Dijt, H. C.; Cohen Stuart, M. A.; Hofman, J. E.; Fleer, G. J. Kinetics of polymer adsorption in stagnation point flow. Colloids and Surfaces 51:141-58(1990).

24. Baran, A. A.; Kocherga, I. I. Kinetics of polyethylene oxide adsorption by particles of coal and clay suspensions. Kolloidnyi Zhurnal 52(3):419-23(May-June 1990).

25. Johnson, H. E.; Granick, S. Penetration kinetics into a previously adsorbed polymer layer. Polymer Preprints 31(2):523-4(1990).

26. Cohen Stuart, M. A.; Tamai, H. Dynamics of adsorbed polymers. 1. Thickness relaxation of poly(vinylpyrrolidone) on glass. Macromolecules 21:1863-6(1988).

27. Wagberg, L.; Odberg, L. Polymer adsorption on cellulosic fibers. Nordic Pulp and Paper Research Journal 2:135-40(1989).

28. Einarson, M.; Aksberg, R.; Odberg, L.; Berg, J. C. Adsorption and reconformation of a series of cationic polyacrylamides on charged surfaces. Colloids and Surfaces 53:183-91(1991).

29. Wagberg, L.; Odberg, L.; Lindstrom, T.; Aksberg, R. Journal of Colloid and Interface Science 123:287(1988).

30. Pefferkorn, E.; Carroy, A.; Varoqui, R. Journal of Polymer Science, Polymer Physics Edition 23:1997(1985).

31. Singer, J. M.; Vekemans, F. C. A.; Lichtenbelt, H. W. Th.; Hesselink, F. Th.; Wiersema, P. H. Journal of Colloid and Interface Science 45:608(1973).

32. Gregory, J. Polymer adsorption and flocculation in sheared suspensions. Colloids and Surfaces 31:231-53(1988).

33. Gregory, J.; Lee, S. Y.; The effect of charge density and molecular mass of cationic polymers on flocculation kinetics in aqueous solution. Journal of Water SRT-Aqua 39(4):265-74(1990).

34. Somasundaran, P; Sivakumar, A. Short term kinetics of polymer adsorption on glass substrate. Colloids and Surfaces 30:401-3(1988).

35. Mahanta, D.; Chaliha, B. C.; Baruah, J. N. Adsorption kinetics of cationic polyacrylamide onto cellulose fibers. Colloids and Surfaces 25:101-9(1987).

36. Wagberg, L.; Lindstrom, T. Flocculation of cellulosic fibers by cationic polyacrylamides with different charge densities. Nordic Pulp and Paper Research Journal 2(4):152-60(1987).

37. Lindstrom, T.; Soremark, C. Adsorption of cationic polyacrylamides on cellulose. Journal of Colloid and Interface Science 55(2):305-12(1976).

38. Gregory, J. Kinetic aspects of polymer adsorption and flocculation. In Flocculation in Biotechnology and Separation Systems, Attia, Y. A., Editor. Amsterdam, Elsevier Science Publishers, 1987:31-44.

39. Abson, D.; Brooks, D. F. Wet-end behavior of dry strength additives. Tappi Journal 68(1):76-8(1985).

40. Jankovics, L. Effect of agitation and molecular weight on polymer adsorption and deflocculation. Journal of Applied Polymer Science 9:545-52(1965).

41. Wagberg, L.; Lindstrom, T. Kinetics of polymer-induced flocculation of cellulosic fibers in turbulent flow. Colloids and Surfaces 27:29-42(1987).

42. Wigsten, A. L.; Stratton, R. A. Polymer adsorption and particle flocculation in turbulent flow. In Polymer adsorption and dispersion stability, Goddard, E. D. and Vincent, B., Editors. ACS Symposium Series No. 240:429-44(1984).

43. Wagberg, L.; Odberg, L.; Lindstrom, L.; Aksberg, R. Kinetics of adsorption and ion-exchange reactions during adsorption of cationic polyelectrolytes onto cellulosic fibers. Journal of Colloid and Interface Science 123(1):287-95(1988); Colloids and Surfaces 31:119-24(1988).

44. Sukhishvili, S. A.: Polinskii, A. S.; Yaroslavov, A. A.: Kabanov, V. A. Extreme temperature dependence of the rate of adsorption of a polycation on the surface of negatively charged latex. Doklady Akademii Nauk SSSR 302(3):640-3(Sept. 1988).

45. White, F. M. Viscous Fluid Flow. 2nd Ed. New York, McGraw-Hill, Inc. 1991:116.

46. Gregory, J. Flocculation in laminar tube flow. Chemical Engineering Science 36(11):1789-94(1981).

47. Friese, M. A. Equilibrium Adsorption of Polyallylamine from Aqueous Media. Doctoral Dissertation. Atlanta, GA, The Insitiute of Paper Science and Technology, 1993. 190p.

48. Young, R. J. Introduction to Polymers. New York, NY, Chapman and Hall, 1983, 368p.

49. Nagy, D. H.; Terwilliger, D. A. Size exclusion chromatography/differential viscometry of cationic polymers. Journal of Liquid Chromatigraphy 12(8):1431-49(1989).

50. Hiemenz, P. C. Polymer Chemistry. New York, NY, Marcel Dekker, Inc., 1984. 738p.

51. Wagberg, L.; Odberg, L. Polymer adsorption on cellulosic fibers. Nordic Pulp and Paper Research Journal 2(2):135-40(1989).

52. Cohen Stuart, M. A.; Cosgrove, T.; Vincent, B. Experimental aspects of polymer adsorption at solid/solution interfaces. Advances in Colloid and Interface Science 24:143-239(1986).

53. Kamel, A. A.; El-Aasser, M. S.; Vanderhoff, J. W. The preparation and surface characterization of an ideal model colloid. Journal of Dispersion Science and Technology 2(2&3):183-214(1981).

54. Vanderhoff, J. W. Characterization of latexes by ion exchange and conductometric titration. In Characterization Methods of Polymer Surfaces. New York, NY, Academic Press, 1977:365-95.

55. Stone-Masui, J.; Watillon, A. Characterization of surface charge on polystyrene latices. Journal of Colloid and Interface Science 52(3):479-503(Sept. 1975).

56. Miller, C. E. An Investigation of the Effects of Polymer Partitioning on Fines Retention. Doctoral Dissertation. Atlanta, GA, The Institute of Paper Science and Technology, 1989. 169 p.

57. Kenics® Mixer Module Design Bulletin. Kenics Corporation, 1978.

58. Dijt, J. C.; Cohen Stuart, M. A.; Fleer, G. J. Kinetics of polymer adsorption and desorption in capillary flow. Macromolecules 25:5416-23(1992).

59. Luettgen, C. O. An Investigation of the Role of Mixing Conditions During Polymeric Retention Aid Addition on the Adsorption Homogeneity. Doctoral Dissertation. Atlanta, GA, The Institute of Paper Science and Technology, 1992.

60. Pearson, E. S.; Hartley, H. O. Biometrika Tables for Statisticians. New York, Cambridge University Press, 1954.

61. Schmitz, K. S. Dynamic Light Scattering by Macromolecules. San Diego, CA, Academic Press, Inc. 1990:239-44.

62. Schmitz, K. S. Macroions in Solution and Colloidal Suspension. New York, NY, VCH Publishers Inc. 1993:163-4.

63. van den Hul, H. J.; Vanderhoff, J. W. Well characterized monodisperse latexes. Journal of Colloid and Interface Science 28(2):336-7(Oct. 1968).

64. Vanderhoff, J. W.; van den Hul, H. J.; Tausk, R. H. M.; Overbeek, J. Th. G. In Clean Surfaces: Their Preparation and Characterization for Interfacial Studies, Goldfinger, G. Editor. New York, Marcel Dekker, Inc., 1970, p. 15.

APPENDIX I

FRACTIONATION OF POLYALLYLAMINE

The following section will describe the GPC system and the operating parameters which were used to fractionate the polyallylamine into narrowly distributed molecular weight fractions.

Eluent

The eluent used throughout this work consisted of 0.1% trifluoroacetic acid (TFA) in 0.2 molar sodium nitrate ($NaNO_3$). Once made, the eluent was filtered through a Millipore® Type HV 0.45μm filter to remove solid contaminants, or undissolved $NaNO_3$.

Polymer Solution

High and low molecular weight samples of polyallylamine were obtained from Aldrich Chemical Co. in dry form. Because this form is very hygroscopic, the dry samples were stored in a desiccator over $CaSO_4$. Concentrated solutions of the PAAm were made using the eluent as the solvent. The concentration of the polymer solutions used in the bulk injections was 100mg/ml or approximately 10 percent.

Equipment Description

The GPC system consisted of the following components: Varian 5020

liquid chromatograph; size exclusion columns (SynChropak CATSEC 1000 by SynChrom, Inc., Lafayette, IN; guard column measuring 65 x 21.2 mm ID NO. 166502, and the bulk column measuring 250 x 21.2 mm ID No. 166503); column heater; Hewlett Packard HP1047A refractive index detector; an A/D converter to convert the analog signal from the detector to a digital output; a microcomputer to collect the raw chromatograph data; and a Gilson FC-100K fractionator to collect the fractions. The application software CODAS® was used to acquire the raw data on the PC, and to store the data in ASCII format. Lab Calc® was used to reduce the noise in the data, and to produce presentation graphics of the work.

Operating Parameters

The liquid chromatograph was set at the following operating parameters: Flow rate = 10.0 ml/min; Temperature = 35° C; Sample loop volume = 250 µl; maximum pressure= 200 ATM; minimum pressure = 2 ATM. The chromatograph was programmed according to the following scheme:

Program Settings	**Explanation**
0.0 FLOW 10.0	Sets eluent flow at 10.0 ml/min
0.0 % 100.0	All eluent is pumped from same reservoir
0.0 RSVR A	The eluent is pumped from reservoir A
0.0 EVNT 0	All external events are off at start
6.0 EVNT 8	Supplies power to fractionator at 6 min
9.9 EVNT 0	Cuts off power to fractionator

Fractionation Procedures

Once the system was turned on and the eluent flow was started, the system required about an hour to come to temperature, and stabilize. Once the system was stable, the unfractionated polymer solution was injected into the sample loop, and the fractionation was begun. Twelve fractions were collected between six and ten minutes after the initial injection, and the total elution time for a single injection was sixteen minutes. Fractions were collected for 402 injections of the low molecular weight polyallylamine sample and 402 injections of the high molecular weight fractions.

Table I-1. Summary of polyallylamine fraction characterization, HMW sample.

High Molecular Weight Sample				
Sample	Elution Time	M_W	M_N	M_W/M_N
Bulk	8.17	38,600	13,400	2.87
H4	7.09	154,000	109,000	1.40
H5	7.28	124,000	82,800	1.49
H6	7.48	100,000	64,600	1.55
H7	7.60	82,400	50,400	1.64
H8	7.74	65,300	38,900	1.68
H9	7.90	58,600	30,300	1.93
H10	8.02	51,400	24,400	2.10
H11	8.08	44,200	22,000	2.01
H12	8.07	43,100	22,500	2.05
H13	8.10	41,500	20,300	2.05
H14	8.14	54,000	22,400	2.41
H15	8.17	48,800	20,200	2.42

Table I-2. Summary of polyallylamine fraction characterization, LMW sample.

Low Molecular Weight Sample				
Sample	Elution Time	M_W	M_N	M_W/M_N
Bulk	8.41	18,400	11,500	1.59
L5	7.49	72,300	58,000	1.25
L6	7.66	56,500	42,600	1.33
L7	7.82	43,600	34,400	1.27
L8	7.97	33,600	25,800	1.30
L9	8.12	25,300	19,300	1.31
L10	8.27	20,300	14,900	1.36
L11	8.37	18,200	12,600	1.45
L12	8.42	16,100	10,900	1.48
L13	8.50	14,200	9,620	1.48
L14	8.58	15,800	8,940	1.77
L15	8.51	15,900	9,150	1.74
L16	8.40	15,600	8,990	1.74

APPENDIX II

INTRINSIC VISCOSITY MEASUREMENT

For characterization of the PAAm fractions with respect to molecular weight, it was necessary to measure the intrinsic viscosity of several of the fractions. The measurements were performed at the same solvent conditions used in the GPC work: 0.1% TFA in 0.2M $NaNO_3$ at 35°C. The experimental details of the viscosity measurements, and the experimental data can be found below.

Equipment

The viscosity of the solvent and the PAAm fractions was measured using a Cannon 75 M150 suspended-level (Ubbelohde) capillary viscometer. The temperature of the viscometer and the samples was maintained at 35°C by immersion in a constant-temperature water bath. The temperature of the bath was maintained by a Braun Thermomix 1460 heater/pump. A digital stopwatch, which read to 0.01 seconds, was used to measure the flow times.

It was necessary to concentrate some of the PAAm fractions in order to obtain reproducible viscosity measurements. A 400ml Amicon ultrafiltration cell with a Diaflo® YM3 ultrafiltration membrane was used to concentrate the solutions. The pore size of the membrane was appropriate for allowing solvent to pass through, but not the polymer. A Hewlett Packard HP 1047A differential refractive index detector was used to determine the concentrations of the polymer solutions.

Viscosity Measurement

Determination of the intrinsic viscosity of the PAAm fractions required measurement of the viscosity of the solvent (0.1% TFA in 0.2M $NaNO_3$) and a series of concentrations of several of the fractions. The intrinsic viscosity of each fraction was obtained by determining the intercept of a plot of reduced specific viscosity vs. concentration. The reduced specific viscosity was defined as: $\frac{(t-t_o)/t_o}{C}$ where t_o and t are the flow times of solvent and polymer sample respectively, and C is the concentration of the polymer sample. The units of intrinsic viscosity are reciprocal concentration.

Viscosity Data

Table II-1. Measurement of t_0 for the PAAm fraction solvent.

Flow Time, sec	Average
99.04	
99.03	
99.13	
99.13	
99.01	99.07

Table II-2. Data for the intrinsic viscosity determination of PAAm fraction H4.

Fraction H4	concentration (% w/w)	time (seconds)	average time	η_r	η_{sp}	η_{sp}/c
Sample 1	0.234	122.35				
		122.45				
		122.35				
		122.45				
		122.26	122.37	1.235	0.235	1.004
Sample 2	0.188	117.58				
		117.49				
		117.59				
		117.63				
		117.61	117.58	1.187	0.187	0.997
Sample 3	0.156	114.47				
		114.45				
		114.41				
		114.46				
		114.51	114.46	1.155	0.155	0.995
Sample 4	0.134	112.48				
		111.85				
		112.16				
		112.19				
		112.16	112.17	1.132	0.132	0.988
Sample 5	0.117	111.34				
		110.56				
		110.80				
		110.44				
		110.51				
		110.49	110.69	1.117	0.117	1.001
Sample 6	0.104	109.25				
		109.27				
		109.59				
		109.15				
		109.59				
		109.27	109.35	1.104	0.104	0.997

Linear Regression Analysis, H4: $\eta_{sp}/c = 0.9891 + 0.04903c$

$R^2 = 0.177$ (intrinsic viscosity, [η] = y-intercept)

Table II-3. Data for the intrinsic viscosity determination of PAAm fraction H5.

Fraction H5	concentration (% w/w)	time (seconds)	average time	η_r	η_{sp}	η_{sp}/c
Sample 1	0.423	136.46				
		136.75				
		136.59				
		136.52				
		136.55	136.57	1.379	0.379	0.895
Sample 2	0.339	129.07				
		128.59				
		129.19				
		128.81				
		128.72	128.88	1.301	0.301	0.889
Sample 3	0.282	123.51				
		123.55				
		123.55				
		123.74				
		123.48	123.57	1.247	0.247	0.877
Sample 4	0.242	119.95				
		119.94				
		119.99				
		119.87				
		120.15	119.98	1.211	0.211	0.873
Sample 5	0.212	117.19				
		117.17				
		117.02				
		117.34				
		117.18	117.18	1.183	0.183	0.864
Sample 6	0.188	115.26				
		114.95				
		115.09				
		114.93				
		115.13	115.07	1.162	0.162	0.859

Linear Regression Analysis, H5: $\eta_{sp}/c = 0.8328 + 0.1537c$

$R^2 = 0.954$ (intrinsic viscosity, $[\eta]$ = y-intercept)

Table II-4. Data for the intrinsic viscosity determination of PAAm fraction H7.

Fraction H7	concentration (% w/w)	time (seconds)	average time	η_r	η_{sp}	η_{sp}/c
Sample 1	0.448	128.68				
		129.08				
		128.79				
		128.93				
		128.91	128.88	1.301	0.301	0.672
Sample 2	0.358	122.54				
		122.70				
		123.03				
		122.70				
		122.62	122.72	1.239	0.239	0.666
Sample 3	0.299	118.34				
		118.44				
		118.47				
		118.74				
		118.34	118.47	1.196	0.196	0.656
Sample 4	0.256	115.47				
		115.53				
		115.30				
		116.04				
		115.60	115.59	1.167	0.167	0.652
Sample 5	0.224	113.31				
		113.39				
		113.34				
		113.17				
		113.25	113.29	1.144	0.144	0.641
Sample 6	0.199	111.59				
		111.61				
		111.45				
		111.57				
		111.63	111.57	1.126	0.126	0.634

Linear Regression Analysis, H7: $\eta_{sp}/c = 0.6090 + 0.1495c$

$R^2 = 0.925$ (intrinsic viscosity, $[\eta]$ = y-intercept)

Table II-5. Data for the intrinsic viscosity determination of PAAm fraction L6.

Fraction L6	concentration (% w/w)	time (seconds)	average time	η_r	η_{sp}	η_{sp}/c
Sample 1	0.133	107.20				
		107.17				
		107.14				
		107.13				
		107.20	107.17	1.082	0.082	0.617
Sample 2	0.106	105.49				
		105.57				
		105.66				
		105.39				
		105.48	105.52	1.065	0.065	0.614
Sample 3	0.088	104.27				
		104.44				
		104.31				
		104.16				
		104.21	104.28	1.053	0.053	0.595
Sample 4	0.076	103.65				
		103.55				
		103.48				
		103.59				
		103.42	103.54	1.045	0.045	0.596
Sample 5	0.066	102.99				
		103.02				
		102.96				
		102.81				
		102.87	102.93	1.039	0.039	0.588
Sample 6	0.059	102.47				
		102.49				
		102.50				
		102.52				
		102.37	102.47	1.034	0.034	0.583

Linear Regression Analysis, L6: $\eta_{sp}/c = 0.5565 + 0.4777c$

$R^2 = 0.915$ (intrinsic viscosity, $[\eta]$ = y-intercept)

Table II-6. Data for the intrinsic viscosity determination of PAAm fraction L9.

Fraction L9	concentration (% w/w)	time (seconds)	average time	η_r	η_{sp}	η_{sp}/c
Sample 1	0.816	123.78				
		123.73				
		123.70				
		123.74				
		123.56	123.70	1.249	0.249	0.305
Sample 2	0.653	118.99				
		118.59				
		119.16				
		118.77				
		118.70	118.84	1.200	0.200	0.306
Sample 3	0.544	115.59				
		115.28				
		115.37				
		115.29				
		115.34	115.37	1.165	0.165	0.303
Sample 4	0.466	113.10				
		113.07				
		112.99				
		113.15				
		113.09	113.08	1.141	0.141	0.303
Sample 5	0.408	111.13				
		111.06				
		111.06				
		111.27				
		111.20	111.14	1.122	0.122	0.299
Sample 6	0.363	109.66				
		109.83				
		109.92				
		110.58				
		109.79	109.96	1.110	0.110	0.303

Linear Regression Analysis, L9: $\eta_{sp}/c = 0.2980 + 0.009160c$

$R^2 = 0.417$ (intrinsic viscosity, $[\eta]$ = y-intercept)

Table II-7. Data for the intrinsic viscosity determination of PAAm fraction H14.

Fraction H14	concentration (% w/w)	time (seconds)	average time	η_r	η_{sp}	η_{sp}/c
Sample 1	0.438	113.03				
		113.86				
		114.45				
		113.03				
		113.19				
		113.22				
		113.06	113.41	1.145	0.145	0.330
Sample 2	0.351	110.33				
		110.32				
		110.24				
		110.45				
		110.98	110.46	1.115	0.115	0.328
Sample 3	0.292	108.50				
		108.56				
		108.62				
		108.52				
		108.56	108.55	1.096	0.096	0.328
Sample 4	0.250	107.39				
		107.02				
		107.34				
		107.11				
		107.34				
		107.10	107.22	1.082	0.082	0.329
Sample 5	0.219	106.06				
		106.08				
		106.08				
		106.26				
		106.61	106.22	1.072	0.072	0.330
Sample 6	0.195	105.55				
		105.40				
		105.64				
		105.27				
		105.25				
		105.27	105.40	1.064	0.064	0.328

Linear Regression Analysis, H14: $\eta_{sp}/c = 0.3272 + 0.00536c$

$R^2 = 0.247$ (intrinsic viscosity, $[\eta]$ = y-intercept)

APPENDIX III

SYNTHESIS OF POLYSTYRENE LATEX

One of the main independent variables in this study of polyelectrolyte adsorption rate was the surface charge density of the adsorbate. It was desired to have several samples of latex, each having the same diameter particle, but different surface charge densities. Because the pH of the system was used to modify other properties, the latex charge density had to be independent of system pH. Latexes meeting these criteria were not commercially available. Therefore, emulsifier-free emulsion polymerization was carried out to produce the desired latex.

Using different strategies, numerous attempts were made to synthesize these model colloids. Early strategies included seeded growth using different initiator concentration during the swelling stage, and shot-growth using polystyrene sulfonate as a co-monomer. The strategy eventually used here consisted of synthesizing a very high charge density, sulfated polystyrene latex, then hydrolyzing the sulfate surface groups to different extents.

It has been shown by several workers that under the proper conditions, the surface sulfate groups will undergo hydrolysis to form hydroxyl groups.[53] To achieve different surface charge densities, a large batch of latex having a very high charge density, and a narrow particle size distribution, was divided into several batches. Hydrolysis was then carried out to different extents on each batch, yielding

latex having the same size and the same number of functional groups, but different ratios of sulfate to hydroxyl functional groups. Since sulfate is a strong acid group, it retains a negative charge through the entire pH range used in the adsorption experiments. Since the hydroxyl group has a very high pKa, it should remain protonated and therefore, uncharged.

The surface charge of sulfated polystyrene latex is typically very stable. However, after proper preparation, hydrolysis is spontaneous at room temperature. The conditions which promote hydrolysis of the sulfate groups are heat and low pH.[53] By allowing different subsets to remain under hydrolytic conditions for different lengths of time, different degrees of hydrolysis were achieved.

Synthesis of Polystyrene

Chemicals

- Styrene, 99%, with 10-15 ppm 4-tert-butyl catechol, Aldrich Chemical Co.
- Sodium bicarbonate, Fisher Scientific.
- Potassium persulfate, Fisher Scientific.
- Sodium hydroxide, Fisher Scientific.

Polymerization Reactor

The laboratory setup for carrying out the polymerizations had several features. The basic reaction vessel was a three liter, three neck, round bottom flask. The flask was equipped with the following items: nitrogen inlet; reflux condenser;

sampling-injection port; and a variable speed stirrer. To maintain a stable temperature during the polymerization, the flask was immersed in a constant temperature bath. The various ports and inlets were air-tight at low pressures, and a slow flow of nitrogen was maintained throughout a polymerization. This apparatus allowed for isothermal, emulsifier-free emulsion polymerizations to be carried out in an oxygen-free environment.

Emulsion Polymerization Procedure

1. 2000 ml of N_2-sparged deionized water were added to the polymerization flask, and the temperature was set to 80°C. The flow of nitrogen was turned on, and the stirring was started at a moderate speed.

2. 1.70g of sodium bicarbonate ($NaHCO_3$) were dissolved in 275 ml of deionized water and added to the flask.

3. The inhibitor was removed from approximately 200 ml of styrene monomer by washing twice with 200 ml of 1.0 M NaOH in a separatory funnel.

4. 163 grams (approximately 180ml) of washed styrene were added to the reaction flask.

5. 2.10 g of potassium persulfate initiator ($K_2S_2O_8$) were added to 60 ml of N_2-sparged water. The dissolution of the initiator was assisted by gentle heating (45°C) under an N_2 environment.

6. When the temperature of the reaction flask contents stabilized at 80°C, the stirring rate was drastically increased to about 500 rpm. The initiator solution was loaded into a 60 ml syringe, and quickly (less than 2 seconds) injected into the bulk of the flask contents via the sampling-injection port.

7. The reaction was carried out for 3.5 hours, at which time the reactor was cooled in an ice bath for about 25 minutes with gentle mixing. The temperature of the contents was decreased to 30°C.

8. The contents of the cooled reaction flask were poured into a large polypropylene bottle through a funnel packed with glass wool. The latex was then stored under refrigeration (3° C) until further use or characterization.

The final consistency of the emulsifier-free latex was 5.6 % solids.

Purification of Ion Exchange Resins

The use of ion exchange resins for cleaning of latex was once discouraged because of the impurities present in the exchange resins themselves. It has been shown that if the resins are thoroughly purified, they can be readily used without contamination.[63] The purification procedure here was adapted from the work of Kamel *et.al.*[53] as suggested by Vanderhoff *et.al.*[64] In this procedure the following resins were purified: Bio-Rad Analytical Grade Anion Exchange Resin AG® 1-X4, 20-50 mesh, chloride form; and Bio-Rad Analytical Grade Cation Exchange Resin AG® 50W-X4, 20-50 mesh, hydrogen form.

The purification procedure involved washing the exchange resins using a fritted glass filter funnel. The cation and anion exchange resins were treated separately according to the following steps. The resin was placed into the funnel, and alternately rinsed with several volumes of 60°C distilled water and methanol until the filtrate was clear. The resins were then washed with a fivefold excess by volume of 3.0 M NaOH, 90°C distilled water, methanol, 20°C distilled water, 3.0 M HCl, 90°C distilled water, methanol, and 20°C distilled water. This cycle was repeated two times for each resin.

Following these cycles, the exchange resins were washed with two consecutive volumes of 3.0 M HCl followed by four consecutive volumes of 20°C distilled water. The cation exchange resin was stored in this form until use. Just prior to use, the anion exchange resin was washed with two consecutive volumes of 3.0 M NaOH followed by four consecutive volumes of 20°C distilled water.

According to the resin supplier, the cation exchange resin had a capacity of 3.5 meq/g of dry resin and the anion exchange resin had a capacity of 5.2 meq/g of dry resin. After purification, the percent solids of each resin was determined by drying a small portion in a vacuum oven. When used to clean latex, the resins were used according to an equal exchange capacity. The typical percent solids of the cation and anion exchange resins after purification were about 48% and 32% respectively. Therefore, they could be used in equal wet weight fractions to achieve equivalent ion exchange capacities.

Reduction of Latex Surface Charge Density

It has been demonstrated by Kamel *et.al.* that latex which has been thoroughly cleaned with ion exchange resins will spontaneously lose all surface charge as a result of hydrolysis of the surface sulfate groups. Complete hydrolysis of the surface sulfate groups here was not desired. The objective here was to hydrolyze the high charge density latex to different extents resulting in lower values of surface charge which are relatively stable.

Procedure

In preparation for hydrolysis, the high charge density latex was treated with a mild cleaning step using the purified ion exchange resins. The latex resulting from the polymerization had a charge density of 12.2 $\mu C/cm^2$, an average diameter of 0.45 μm and a consistency of 5.6% solids. The cleaning step consisted of adding 0.24g (wet weight) of each purified ion exchange resin per gram of latex solids to a polypropylene container. The container was shaken with the ion exchange resins for two hours, after which time the resins were removed *via* filtration.

The reactor for the hydrolysis consisted of a round bottom flask equipped with a stirrer, and immersed in a 75°C water bath to maintain temperature. The gently cleaned latex was then placed in the 75°C reactor and the stirring was begun at a moderate rate (~200 rpm).

Samples were initially taken at intervals of 15 minutes, then hourly, and

finally every five hours. The surface charge density of the different samples was determined *via* conductometric titration. The results indicated that the rate of charge density decrease under hydrolytic conditions was initially very fast, but the rate decreased exponentially. Therefore, at very long times, the rate of surface charge reduction was so slow, a pseudo equilibrium level of surface charge was attained.

In an attempt to achieve an even lower surface charge density, the partially hydrolyzed latex was removed from the reaction flask, cleaned with ion exchange resin, and then subjected to the hydrolytic conditions. After a period of five hours, the latex was conductometrically titrated, but there was no measurable surface charge remaining on the latex.

It was discovered that the rate of surface charge reduction could again be increased, without further cleaning with ion exchange resins, by adding distilled dilution water to the reaction flask. A lower pseudo equilibrium level of surface charge density was then attained. This dilution process was repeated until the desired latex surface charge density was achieved. Based on this evidence, the attainment of a pseudo equilibrium value of surface charge density was likely due to an excessive concentration of reaction products.

The latex samples used in the adsorption experiments had charge densities of 12.2 $\mu C/cm^2$ (unhydrolyzed), 6.5 $\mu C/cm^2$ and 1.6 $\mu C/cm^2$. All samples were stored under refrigeration (3°C) until used. The shape of the conductometric

titration curves indicated the presence of strong acid functional groups only.

CONDUCTOMETRIC TITRATION

The surface charge density of the latex samples used throughout this work was determined through conductometric titration. The general procedures for this technique are summarized below.

Procedure

1. The latex sample was prepared for titration by combining a sample containing approximately 1 gram of latex solids with 1 gram of each purified ion exchange resin. The container was closed tightly, and shaken.

2. After 2 hours of shaking, the resins were removed, and were replaced by 1 gram of each purified ion exchange resin. This sample was again shaken for two hours.

3. The ion exchange resins were removed via filtration, and the filter was rinsed with a small amount of distilled water. Two samples of the cleaned latex were taken from the filtrate flask for consistency determination by drying in an oven at 105°C until a constant weight was achieved.

4. The filtrate flask containing the cleaned latex was weighed, and the latex was poured into a 100 ml, three neck, round bottom titration flask. The empty filtration flask was weighed to determine the amount of latex added to the

titration flask by difference.

5. While stirring with a magnetic stir bar, nitrogen was bubbled through the sample for 30 minutes to remove carbonate species.

6. At the end of the 30 min, the nitrogen probe was left above the level of the sample to provide a nitrogen blanket.

7. A 5 ml burette with 0.01 ml graduations was used to deliver a standardized solution of NaOH in increments of about 0.05 ml. The conductivity of the sample was measured after each addition of NaOH by plunging the conductivity probe into the sample and drawing up a sample with a small bulb. After the measurement was taken, the contents of the probe were returned to the titration flask.

8. A plot of ml NaOH solution added vs. conductivity was made from the data. The intersection of the two linear portions of the curve was used to determine the equivalence point where the equivalents of OH^- equaled the total number of charged functional groups on the latex surface.

9. The charge density of the latex was calculated by determining the total surface area of the titrated sample and the number of strong acid groups titrated at the equivalence point.

APPENDIX IV

ZETASIZER CELL COATING PROCEDURE

1. The glass capillary was cleaned by soaking overnight in a strong oxidizing / cleaning solution (NoChromix), which removed any previous coating or impurity from the glass surface.

2. After being cleaned, the cell was thoroughly rinsed with deionized water to remove residual cleaning solution.

3. The clean cell was placed in a 105°C oven for one hour to evaporate any remaining water.

4. A 0.1% Methocel® (hydroxypropyl methylcellulose) solution was made with deionized water. The pH was adjusted to 10 with dilute NaOH to dissolve the protective coating on the Methocel® granules. The pH was then adjusted to 6.5 using dilute HCl.

5. The cell was removed from the oven and allowed to cool in a desiccator.

6. After cooling, the dry cell was capped on one end with a neoprene stopper and filled with γ-glycidoxypropyltrimethoxysilane for 30 minutes.

7. The silating agent was then poured out, and the capillary was rinsed with 0.01 M acetic acid.

8. Without drying the cell, it was transferred to the 0.1% Methocel solution for at least 30 minutes. The cell was also stored in this solution until use.

9. The capillary was removed from the 0.1% Methocel solution, installed in the Zetasizer, and the cell was flushed with 5 10 ml volumes of the electrolyte solution to be used in the electrophoretic mobility measurements.

APPENDIX V

CORRELATION OF E.M. TO SURFACE COVERAGE

As discussed in the data analysis section, empirical correlations were developed to determine the relationship between the electrophoretic mobility of the latex and the amount of PAAm adsorbed to the surface. The experimental procedures were summarized in the section entitled appropriately. What follows is a summary of the data collected to determine the correlation for each condition of polyelectrolyte charge density, latex surface charge density, and ionic strength. The form of the correlation equation used to interpolate the data is given below. Because the equation is empirical, it may only be used within the range where the data were collected; extrapolations are not advised.

$$\text{E.M.} = \left[\frac{a-d}{\left(1-(x/c)^{b}\right)^{e}} \right] + d$$

where x is the surface coverage in mg/m^2; and a, b, c, d and e are the coefficients of the best fit curve through the data.

Table V-1. E.M. to Surface Coverage: σ= 12.2 $\mu C/cm^2$; pH = 4.0; I = 0.001.

Data		Empirical Fit	
Surface Coverage	E.M.	Coefficient I.D.	Value
0.0112	-2.16	a	3.825
0.0028	-4.49	b	-17.94
0.0198	3.46	c	0.187
0.0145	-0.16	d	-4.523
0.0059	-3.97	e	0.126
0.0217	3.78		
0.0076	-3.27		
0.0187	2.66		
0.0108	-1.98		

Table V-2. E.M. to Surface Coverage: σ= 6.5 $\mu C/cm^2$; pH = 4.0; I = 0.001.

Data		Empirical Fit	
Surface Coverage	E.M.	Coefficient I.D.	Value
0.1430	3.16	a	-4.68
0.0946	-0.02	b	2.635
0.0631	-2.45	c	0.477
0.0472	-3.47	d	4.27
0.0156	-4.65	e	56.4
0.1277	3.05		
0.0773	-1.45		
0.0313	-4.22		
0.1099	1.57		

Table V-3. E.M. to Surface Coverage: σ= 1.6 $\mu C/cm^2$; pH = 4.0; I = 0.001.

Data		Empirical Fit	
Surface Coverage	E.M.	Coefficient I.D.	Value
0.0469	-1.59	a	-4.99
0.0355	-2.78	b	1.98
0.0942	3.25	c	0.103
0.0118	-4.69	d	12.31
0.0717	1.11	e	1.09
0.0236	-3.81		
0.0590	-0.26		
0.0829	2.76		

Table V-4. E.M. to Surface Coverage: σ= 12.2 $\mu C/cm^2$; pH = 4.0; I = 0.050.

Data		Empirical Fit	
Surface Coverage	E.M.	Coefficient I.D.	Value
0.0951	-2.22	a	-4.10
0.0633	-3.74	b	2.98
0.1278	3.60	c	0.742
0.1590	0.67	d	3.288
0.3170	2.92	e	112.6
0.1269	-0.83		

Table V-5. E.M. to Surface Coverage: σ= 12.2 $\mu C/cm^2$; pH = 10; I = 0.001.

	Data		Empirical Fit	
M_w	Surface Coverage	E.M.	Coefficient I.D.	Value
18,200	0.263	-2.52	a	-4.85
18,200	0.346	-1.17	b	5.043
18,200	0.538	0.28	c	0.191
18,200	0.707	1.08	d	4.61
18,200	0.874	1.36	e	0.152
82,400	0.161	-4.46		
82,400	0.243	-2.94		
82,400	0.327	-1.76		
82,400	0.504	-0.39		
82,400	0.645	1.18		
82,400	0.823	1.60		
154,000	0.156	-4.41		
154,000	0.234	-2.97		
154,000	0.315	-1.92		
154,000	0.469	0.03		
154,000	0.626	1.13		
154,000	0.775	1.46		

APPENDIX VI

ADSORPTION RATE DATA

Table VI-1. M_W=84,400; σ_H latex; pH=4.0; C_{Ao}=0.02 mg/L; latex=0.0005%.

Replicate "A"	Concentration of PAAm, mg/L		
	Field Strength, volts/cm		
Time, seconds	11.8	20	28
3.85	0.0159	0.0158	0.0163
6.35	0.0154	0.0155	0.0150
8.85	0.0150	0.0146	0.0142
11.35	0.0141	0.0141	0.0138
13.85	0.0135	0.0133	0.0130
16.35	0.0136	0.0129	0.0125
18.85	0.0128	0.0124	0.0120
21.35	0.0123	0.0119	0.0114
23.85	0.0120	0.0115	0.0111
26.35	0.0115	0.0113	0.0107
28.85	0.0113	0.0108	0.0104
31.35	0.0110	0.0107	0.0101
33.85	0.0107	0.0102	0.0099
36.35	0.0104	0.0102	0.0095
38.85	0.0102	0.0099	0.0094
41.35	0.0099	0.0098	
43.85	0.0099	0.0094	
46.35	0.0097		
48.85	0.0096		

Table VI-2. M_W=84,400; σ_H latex; pH=4.0; C_{Ao}=0.02 mg/L; latex=0.0005%.

Replicate "B"	Concentration of PAAm, mg/L		
	Field Strength, volts/cm		
Time, seconds	11.8	20	28
3.85	0.0167	0.0158	0.0161
6.35	0.0160	0.0159	0.0153
8.85	0.0147	0.0147	0.0141
11.35	0.0145	0.0139	0.0137
13.85	0.0138	0.0133	0.0131
16.35	0.0132	0.0129	0.0125
18.85	0.0130	0.0124	0.0120
21.35	0.0126	0.0119	0.0115
23.85	0.0120	0.0114	0.0113
26.35	0.0119	0.0111	0.0108
28.85	0.0113	0.0109	0.0104
31.35	0.0109	0.0106	0.0102
33.85	0.0107	0.0101	0.0098
36.35	0.0106	0.0100	0.0095
38.85	0.0102	0.0097	0.0094
41.35	0.0100	0.0097	
43.85	0.0098	0.0094	
46.35	0.0097		
48.85	0.0094		

Table VI-3. M_W=84,400; σ_H latex; pH=4.0; C_{Ao}=0.02 mg/L; latex=0.0005%.			
Replicate "C"	Concentration of PAAm, mg/L		
	Field Strength, volts/cm		
Time, seconds	11.8	20	28
3.85	0.0168	0.0151	0.0152
6.35	0.0162	0.0145	0.0150
8.85	0.0149	0.0148	0.0145
11.35	0.0143	0.0138	0.0137
13.85	0.0134	0.0133	0.0130
16.35	0.0132	0.0128	0.0124
18.85	0.0128	0.0124	0.0119
21.35	0.0123	0.0119	0.0115
23.85	0.0120	0.0115	0.0111
26.35	0.0118	0.0111	0.0107
28.85	0.0112	0.0109	0.0103
31.35	0.0109	0.0104	0.0101
33.85	0.0109	0.0103	0.0098
36.35	0.0106	0.0099	0.0096
38.85	0.0103	0.0098	0.0095
41.35	0.0101	0.0095	
43.85	0.0099	0.0095	
46.35	0.0098		
48.85	0.0097		

Table VI-4. M_W=84,400; σ_H latex; pH=4.0; C_{Ao}=0.02 mg/L; latex=0.0005%.

Replicate "D"	Concentration of PAAm, mg/L		
	Field Strength, volts/cm		
Time, seconds	11.8	20	28
3.85	0.0162	0.0165	0.0173
6.35	0.0145	0.0151	0.0148
8.85	0.0150	0.0145	0.0142
11.35	0.0145	0.0142	0.0136
13.85	0.0137	0.0133	0.0129
16.35	0.0135	0.0130	0.0125
18.85	0.0127	0.0125	0.0118
21.35	0.0124	0.0118	0.0114
23.85	0.0121	0.0114	0.0110
26.35	0.0115	0.0111	0.0107
28.85	0.0113	0.0108	0.0103
31.35	0.0109	0.0105	0.0101
33.85	0.0105	0.0102	0.0096
36.35	0.0105	0.0099	0.0095
38.85	0.0103	0.0098	0.0095
41.35	0.0101	0.0097	
43.85	0.0099	0.0094	
46.35	0.0098		
48.85	0.0095		

Table VI-5. M_W=84,400; σ_H latex; pH=4.0; C_{Ao}=0.03 mg/L; latex=0.0005%.

Replicate "A"	Concentration of PAAm, mg/L		
	Field Strength, volts/cm		
Time, seconds	11.8	20	28
10.375	0.02386	0.02266	0.02208
11.625	0.02257	0.02236	0.02212
12.875	0.02256	0.02183	0.02133
14.125	0.02201	0.02165	0.02093
15.375	0.02155	0.02125	0.02063
16.625	0.02146	0.02062	0.02027
17.875	0.02098	0.02040	0.01996
19.125	0.02084	0.01999	0.01961
20.375	0.02057	0.02005	0.01947
21.625	0.02064	0.01970	0.01932
22.875	0.02016	0.01925	0.01932
24.125	0.01990	0.01942	
25.375	0.01973	0.01916	
26.625	0.01971		

Table VI-6. M_W=84,400; σ_H latex; pH=4.0; C_{Ao}=0.03 mg/L; latex=0.0005%.

Replicate "B"	Concentration of PAAm, mg/L		
	Field Strength, volts/cm		
Time, seconds	11.8	20	28
10.375	0.02286	0.02261	0.02208
11.625	0.02342	0.02239	0.02171
12.875	0.02248	0.02188	0.02139
14.125	0.02190	0.02136	0.02092
15.375	0.02187	0.02124	0.02063
16.625	0.02142	0.02085	0.02027
17.875	0.02124	0.02043	0.01995
19.125	0.02096	0.02037	0.01959
20.375	0.02072	0.02001	0.01941
21.625	0.02030	0.01972	0.01935
22.875	0.02008	0.01948	0.01933
24.125	0.01988	0.01929	
25.375	0.01970	0.01929	
26.625	0.01943		

Table VI-7. M_W=84,400; σ_H latex; pH=4.0; C_{Ao}=0.03 mg/L; latex=0.0005%.

Replicate "C"	Concentration of PAAm, mg/L		
	Field Strength, volts/cm		
Time, seconds	11.8	20	28
10.375	0.02328	0.02271	0.02208
11.625	0.02329	0.02242	0.02147
12.875	0.02251	0.02181	0.02112
14.125	0.02244	0.02137	0.02080
15.375	0.02165	0.02112	0.02043
16.625	0.02155	0.02080	0.02019
17.875	0.02119	0.02047	0.01996
19.125	0.02051	0.02023	0.01956
20.375	0.02065	0.02004	0.01934
21.625	0.02006	0.01967	0.01946
22.875	0.01989	0.01962	0.01919
24.125	0.01978	0.01948	
25.375	0.01951	0.01942	
26.625	0.01963		

Table VI-8. M_W=84,400; σ_H latex; pH=4.0; C_{Ao}=0.03 mg/L; latex=0.0005%.

Replicate "D"	Concentration of PAAm, mg/L		
	Field Strength, volts/cm		
Time, seconds	11.8	20	28
10.375	0.02318	0.02266	0.02208
11.625	0.02262	0.02239	0.02177
12.875	0.02246	0.02184	0.02128
14.125	0.02192	0.02146	0.02088
15.375	0.02192	0.02120	0.02056
16.625	0.02129	0.02076	0.02024
17.875	0.02101	0.02044	0.01996
19.125	0.02106	0.02019	0.01959
20.375	0.02028	0.02003	0.01941
21.625	0.02038	0.01970	0.01938
22.875	0.02023	0.01945	0.01928
24.125	0.01954	0.01940	
25.375	0.01965	0.01929	
26.625	0.01963		

Table VI-9. M_W=84,400; σ_H latex; pH=4.0; C_{Ao}=0.02 mg/L; latex=0.00025%.

Replicate "A"	Concentration of PAAm, mg/L		
	Field Strength, volts/cm		
Time, seconds	12.0	20.2	28.4
6.75	0.01699	0.01727	0.01743
8.25	0.01739	0.01712	0.01696
9.75	0.01735	0.01705	0.01678
11.25	0.01698	0.01676	0.01665
12.75	0.01710	0.01674	0.01641
14.25	0.01677	0.01639	0.01619
15.75	0.01644	0.01631	0.01599
17.25	0.01636	0.01612	0.01582
18.75	0.01631	0.01585	0.01562
20.25	0.01598	0.01580	0.01542
21.75	0.01613	0.01556	0.01531
23.25	0.01578	0.01546	0.01521
24.75	0.01561	0.01534	0.01504
26.25	0.01555	0.01520	0.01492
27.75	0.01537	0.01508	0.01484
29.25	0.01526	0.01498	0.01470
30.75	0.01517	0.01488	
32.25	0.01494	0.01479	
33.75	0.01503	0.01477	
35.25	0.01472	0.01465	

Table VI-10. M_W=84,400; σ_H latex; pH=4.0; C_{Ao}=0.02 mg/L; latex=0.00025%.

Replicate "B"	Concentration of PAAm, mg/L		
	Field Strength, volts/cm		
Time, seconds	12.0	20.2	28.4
6.75	0.01982	0.01790	0.01745
8.25	0.01695	0.01719	0.01687
9.75	0.01726	0.01706	0.01682
11.25	0.01731	0.01689	0.01658
12.75	0.01666	0.01670	0.01632
14.25	0.01701	0.01648	0.01625
15.75	0.01641	0.01625	0.01612
17.25	0.01638	0.01598	0.01586
18.75	0.01634	0.01592	0.01569
20.25	0.01620	0.01571	0.01547
21.75	0.01603	0.01557	0.01534
23.25	0.01579	0.01545	0.01521
24.75	0.01562	0.01537	0.01504
26.25	0.01552	0.01514	0.01495
27.75	0.01529	0.01508	0.01478
29.25	0.01536	0.01491	0.01472
30.75	0.01508	0.01488	
32.25	0.01504	0.01478	
33.75	0.01502	0.01449	
35.25	0.01492	0.01478	

Table VI-11. M_W=84,400; σ_H latex; pH=4.0; C_{Ao}=0.02 mg/L; latex=0.00025%.

Replicate "C"	Concentration of PAAm, mg/L		
	Field Strength, volts/cm		
Time, seconds	12.0	20.2	28.4
6.75	0.01739	0.01836	0.01744
8.25	0.01786	0.01732	0.01691
9.75	0.01722	0.01703	0.01680
11.25	0.01738	0.01686	0.01662
12.75	0.01711	0.01663	0.01636
14.25	0.01695	0.01657	0.01622
15.75	0.01652	0.01640	0.01605
17.25	0.01638	0.01611	0.01584
18.75	0.01632	0.01595	0.01565
20.25	0.01610	0.01585	0.01544
21.75	0.01590	0.01560	0.01533
23.25	0.01575	0.01553	0.01521
24.75	0.01562	0.01535	0.01504
26.25	0.01552	0.01526	0.01494
27.75	0.01536	0.01510	0.01481
29.25	0.01528	0.01499	0.01471
30.75	0.01518	0.01488	
32.25	0.01499	0.01482	
33.75	0.01501	0.01478	
35.25	0.01495	0.01470	

Table VI-12. M_W=84,400; σ_H latex; pH=4.0; C_{Ao}=0.02 mg/L; latex=0.00025%.

Replicate "D"	Concentration of PAAm, mg/L		
	Field Strength, volts/cm		
Time, seconds	12.0	20.2	28.4
6.75	0.01761	0.01739	0.01747
8.25	0.01712	0.01750	0.01694
9.75	0.01717	0.01687	0.01683
11.25	0.01708	0.01692	0.01665
12.75	0.01688	0.01667	0.01639
14.25	0.01673	0.01637	0.01625
15.75	0.01664	0.01630	0.01608
17.25	0.01638	0.01604	0.01587
18.75	0.01626	0.01593	0.01568
20.25	0.01606	0.01580	0.01547
21.75	0.01605	0.01565	0.01536
23.25	0.01585	0.01547	0.01524
24.75	0.01560	0.01536	0.01507
26.25	0.01552	0.01516	0.01497
27.75	0.01537	0.01502	0.01484
29.25	0.01530	0.01499	0.01474
30.75	0.01518	0.01489	
32.25	0.01509	0.01480	
33.75	0.01501	0.01464	
35.25	0.01495	0.01470	

Table VI-13. M_W=84,400; σ_H latex; pH=4.0; C_{Ao}=0.02 mg/L; latex=0.00075%.

Replicate "A"	Concentration of PAAm, mg/L		
	Field Strength, volts/cm		
Time, seconds	12.0	20.2	28.4
5.60	0.01382	0.01454	0.01300
9.60	0.01357	0.01253	0.01203
13.60	0.01192	0.01107	0.01060
17.60	0.01112	0.00992	0.00956
21.60	0.01041	0.00924	0.00879
25.60	0.00962	0.00837	0.00778
29.60	0.00858	0.00769	0.00719
33.60	0.00818	0.00724	0.00655
37.60	0.00731	0.00669	0.00620
41.60	0.00693	0.00620	0.00583
45.60	0.00647	0.00584	0.00553
49.60	0.00622	0.00573	0.00516
53.60	0.00591	0.00554	0.00474
57.60	0.00567	0.00518	0.00456
61.60	0.00546	0.00493	
65.60	0.00523	0.00454	
69.60	0.00489	0.00460	
73.60	0.00475		
77.60	0.00453		

Table VI-14. M_W=84,400; σ_H latex; pH=4.0; C_{Ao}=0.02 mg/L; latex=0.00075%.

Replicate "B"	Concentration of PAAm, mg/L		
	Field Strength, volts/cm		
Time, seconds	12.0	20.2	28.4
5.60	0.01351	0.01322	0.01368
9.60	0.01361	0.01177	0.01197
13.60	0.01190	0.01112	0.01070
17.60	0.01116	0.01023	0.00975
21.60	0.01015	0.00938	0.00837
25.60	0.00894	0.00851	0.00781
29.60	0.00869	0.00798	0.00738
33.60	0.00770	0.00754	0.00676
37.60	0.00742	0.00687	0.00645
41.60	0.00691	0.00661	0.00606
45.60	0.00628	0.00607	0.00573
49.60	0.00601	0.00575	0.00554
53.60	0.00579	0.00543	0.00519
57.60	0.00534	0.00527	0.00487
61.60	0.00506	0.00500	
65.60	0.00497	0.00496	
69.60	0.00508	0.00470	
73.60	0.00454		
77.60	0.00448		

Table VI-15. M_W=84,400; σ_H latex; pH=4.0; C_{Ao}=0.02 mg/L; latex=0.00075%.

Replicate "C"	Concentration of PAAm, mg/L		
	Field Strength, volts/cm		
Time, seconds	12.0	20.2	28.4
5.60	0.01498	0.01418	0.01334
9.60	0.01368	0.01338	0.01200
13.60	0.01210	0.01121	0.01065
17.60	0.01072	0.01003	0.00965
21.60	0.01031	0.00915	0.00858
25.60	0.00933	0.00848	0.00779
29.60	0.00827	0.00785	0.00729
33.60	0.00776	0.00729	0.00665
37.60	0.00728	0.00678	0.00633
41.60	0.00676	0.00623	0.00594
45.60	0.00663	0.00598	0.00563
49.60	0.00622	0.00564	0.00535
53.60	0.00602	0.00509	0.00497
57.60	0.00577	0.00496	0.00471
61.60	0.00528	0.00464	
65.60	0.00476	0.00473	
69.60	0.00476	0.00453	
73.60	0.00480		
77.60	0.00447		

Table VI-16. M_W=84,400; σ_H latex; pH=4.0; C_{Ao}=0.02 mg/L; latex=0.00075%.

Replicate "D"	Concentration of PAAm, mg/L		
	Field Strength, volts/cm		
Time, seconds	12.0	20.2	28.4
5.60	0.01440	0.01436	0.01317
9.60	0.01363	0.01295	0.01201
13.60	0.01201	0.01114	0.01062
17.60	0.01092	0.00998	0.00961
21.60	0.01036	0.00919	0.00869
25.60	0.00947	0.00842	0.00779
29.60	0.00842	0.00777	0.00724
33.60	0.00797	0.00727	0.00660
37.60	0.00729	0.00674	0.00627
41.60	0.00685	0.00622	0.00589
45.60	0.00655	0.00591	0.00558
49.60	0.00622	0.00568	0.00525
53.60	0.00596	0.00532	0.00485
57.60	0.00572	0.00507	0.00464
61.60	0.00537	0.00479	
65.60	0.00500	0.00464	
69.60	0.00482	0.00457	
73.60	0.00478		
77.60	0.00450		

Table VI-17. M_W=84,400; σ_H latex; pH=4.0; C_{Ao}=0.02 mg/L; latex=0.00100%.

Replicate "A"	Concentration of PAAm, mg/L		
	Field Strength, volts/cm		
Time, seconds	12.0	20.2	28.4
9.0	0.01214	0.01083	0.01087
13.5	0.01020	0.00965	0.00871
18.0	0.00900	0.00849	0.00752
22.5	0.00780	0.00738	0.00623
27.0	0.00697	0.00604	0.00519
31.5	0.00606	0.00527	0.00403
36.0	0.00551	0.00438	0.00364
40.5	0.00473	0.00413	0.00285
45.0	0.00372	0.00321	0.00237
49.5	0.00385	0.00279	0.00194
54.0	0.00293	0.00235	0.00166
58.5	0.00263	0.00213	0.00121
63.0	0.00259	0.00197	0.00119
67.5	0.00221	0.00166	0.00092
72.0	0.00192	0.00157	0.00082
76.5	0.00160	0.00146	0.00044
81.0	0.00157	0.00107	

Table VI-18. M_W=84,400; σ_H latex; pH=4.0; C_{Ao}=0.02 mg/L; latex=0.00100%.

Replicate "B"	Concentration of PAAm, mg/L		
	Field Strength, volts/cm		
Time, seconds	12.0	20.2	28.4
9.0	0.01139	0.01083	0.01047
13.5	0.01055	0.00965	0.00864
18.0	0.00884	0.00795	0.00727
22.5	0.00833	0.00700	0.00582
27.0	0.00713	0.00603	0.00492
31.5	0.00591	0.00517	0.00413
36.0	0.00535	0.00415	0.00315
40.5	0.00495	0.00370	0.00285
45.0	0.00393	0.00325	0.00219
49.5	0.00347	0.00293	0.00187
54.0	0.00276	0.00242	0.00150
58.5	0.00270	0.00174	0.00134
63.0	0.00231	0.00176	0.00095
67.5	0.00221	0.00183	0.00085
72.0	0.00222	0.00143	0.00037
76.5	0.00164	0.00100	0.00029
81.0	0.00160	0.00122	

Table VI-19. M_W=84,400; σ_H latex; pH=4.0; C_{Ao}=0.02 mg/L; latex=0.00100%.

Replicate "C"	Concentration of PAAm, mg/L		
	Field Strength, volts/cm		
Time, seconds	12.0	20.2	28.4
9.0	0.01152	0.01121	0.01067
13.5	0.01067	0.00972	0.00874
18.0	0.00937	0.00827	0.00708
22.5	0.00821	0.00721	0.00589
27.0	0.00724	0.00606	0.00501
31.5	0.00621	0.00544	0.00405
36.0	0.00556	0.00447	0.00333
40.5	0.00464	0.00397	0.00272
45.0	0.00403	0.00308	0.00213
49.5	0.00362	0.00264	0.00178
54.0	0.00300	0.00246	0.00136
58.5	0.00283	0.00213	0.00117
63.0	0.00235	0.00183	0.00092
67.5	0.00221	0.00162	0.00067
72.0	0.00199	0.00133	0.00047
76.5	0.00174	0.00136	0.00039
81.0	0.00164	0.00095	

Table VI-20. M_W=84,400; σ_H latex; pH=4.0; C_{Ao}=0.02 mg/L; latex=0.00100%.

Replicate "D"	Concentration of PAAm, mg/L		
	Field Strength, volts/cm		
Time, seconds	12.0	20.2	28.4
9.0	0.01278	0.01112	0.01047
13.5	0.01031	0.00965	0.00890
18.0	0.00877	0.00852	0.00732
22.5	0.00789	0.00724	0.00645
27.0	0.00716	0.00603	0.00526
31.5	0.00577	0.00519	0.00445
36.0	0.00526	0.00415	0.00376
40.5	0.00411	0.00383	0.00308
45.0	0.00407	0.00345	0.00257
49.5	0.00353	0.00296	0.00237
54.0	0.00323	0.00255	0.00195
58.5	0.00278	0.00226	0.00164
63.0	0.00231	0.00174	0.00134
67.5	0.00226	0.00157	0.00111
72.0	0.00187	0.00146	0.00104
76.5	0.00187	0.00128	0.00080
81.0	0.00160	0.00108	

Table VI-21. M_W=84,400; σ_H latex; pH=4.0; C_{Ao}=0.01 mg/L; latex=0.00025%.

Replicate "A"	Concentration of PAAm, mg/L		
	Field Strength, volts/cm		
Time, seconds	11.8	20.2	28.0
6.60	0.00864	0.00824	0.00828
11.60	0.00817	0.00794	0.00792
16.60	0.00766	0.00757	0.00743
21.60	0.00741	0.00716	0.00703
26.60	0.00719	0.00701	0.00689
31.60	0.00688	0.00672	0.00653
36.60	0.00682	0.00643	0.00638
41.60	0.00656	0.00623	0.00603
46.60	0.00641	0.00603	0.00587
51.60	0.00605	0.00588	0.00566
56.60	0.00577	0.00575	0.00551
61.60	0.00569	0.00556	0.00537
66.60	0.00562	0.00544	0.00519
71.60	0.00548	0.00531	0.00503
76.60	0.00536	0.00522	0.00494
81.60	0.00520	0.00509	0.00480
86.60	0.00504	0.00499	
91.60	0.00505	0.00490	
96.60	0.00492		

Table VI-22. M_W=84,400; σ_H latex; pH=4.0; C_{Ao}=0.01 mg/L; latex=0.00025%.

Replicate "B"	Concentration of PAAm, mg/L		
	Field Strength, volts/cm		
Time, seconds	11.8	20.2	28.0
6.60	0.00827	0.00774	0.00799
11.60	0.00795	0.00799	0.00784
16.60	0.00774	0.00747	0.00748
21.60	0.00742	0.00727	0.00715
26.60	0.00716	0.00699	0.00685
31.60	0.00696	0.00666	0.00659
36.60	0.00674	0.00643	0.00632
41.60	0.00655	0.00626	0.00613
46.60	0.00640	0.00603	0.00587
51.60	0.00625	0.00587	0.00563
56.60	0.00597	0.00568	0.00550
61.60	0.00586	0.00554	0.00532
66.60	0.00576	0.00531	0.00519
71.60	0.00551	0.00531	0.00504
76.60	0.00537	0.00531	0.00495
81.60	0.00533	0.00513	0.00479
86.60	0.00519	0.00502	
91.60	0.00511	0.00488	
96.60	0.00495		

Table VI-23. M_W=84,400; σ_H latex; pH=4.0; C_{Ao}=0.01 mg/L; latex=0.00025%.

Replicate "C"	Concentration of PAAm, mg/L		
	Field Strength, volts/cm		
Time, seconds	11.8	20.2	28.0
6.60	0.00868	0.00802	0.00860
11.60	0.00827	0.00787	0.00794
16.60	0.00765	0.00757	0.00743
21.60	0.00747	0.00733	0.00715
26.60	0.00705	0.00697	0.00678
31.60	0.00709	0.00672	0.00651
36.60	0.00689	0.00647	0.00629
41.60	0.00665	0.00629	0.00607
46.60	0.00637	0.00607	0.00584
51.60	0.00610	0.00600	0.00563
56.60	0.00607	0.00572	0.00550
61.60	0.00589	0.00558	0.00534
66.60	0.00575	0.00539	0.00511
71.60	0.00555	0.00525	0.00505
76.60	0.00537	0.00521	0.00495
81.60	0.00537	0.00500	0.00482
86.60	0.00511	0.00494	
91.60	0.00506	0.00487	
96.60	0.00505		

Table VI-24. M_W=84,400; σ_H latex; pH=4.0; C_{Ao}=0.01 mg/L; latex=0.00025%.

Replicate "D"	Concentration of PAAm, mg/L		
	Field Strength, volts/cm		
Time, seconds	11.8	20.2	28.0
6.60	0.00806	0.00809	0.00824
11.60	0.00799	0.00779	0.00784
16.60	0.00771	0.00745	0.00739
21.60	0.00747	0.00711	0.00713
26.60	0.00711	0.00698	0.00676
31.60	0.00693	0.00666	0.00658
36.60	0.00681	0.00650	0.00626
41.60	0.00660	0.00626	0.00607
46.60	0.00647	0.00601	0.00582
51.60	0.00633	0.00581	0.00562
56.60	0.00605	0.00560	0.00549
61.60	0.00593	0.00539	0.00532
66.60	0.00574	0.00531	0.00514
71.60	0.00566	0.00523	0.00504
76.60	0.00550	0.00513	0.00488
81.60	0.00542	0.00502	0.00483
86.60	0.00523	0.00491	
91.60	0.00512	0.00487	
96.60	0.00502		

Table VI-25. M_W=84,400; σ_H latex; pH=4.0; C_{Ao}=0.03 mg/L; latex=0.00075%.

Replicate "A"	Concentration of PAAm, mg/L		
	Field Strength, volts/cm		
Time, seconds	11.8	20.2	28.0
5.10		0.02265	0.02253
7.10	0.02294	0.02177	0.02087
9.10	0.02187	0.02121	0.01990
11.10	0.02074	0.01958	0.01871
13.10	0.02005	0.01846	0.01796
15.10	0.01894	0.01804	0.01705
17.10	0.01788	0.01742	0.01645
19.10	0.01760	0.01660	0.01614
21.10	0.01683	0.01610	0.01532
23.10	0.01641	0.01570	0.01505
25.10	0.01615	0.01543	0.01441
27.10	0.01556	0.01484	0.01430
29.10	0.01523	0.01446	
31.10	0.01493	0.01433	
33.10	0.01430	0.01375	
35.10	0.01447		
37.10	0.01432		

Table VI-26. M_W=84,400; σ_H latex; pH=4.0; C_{Ao}=0.03 mg/L; latex=0.00075%.

Replicate "B"	Concentration of PAAm, mg/L		
	Field Strength, volts/cm		
Time, seconds	11.8	20.2	28.0
5.10		0.02248	0.02253
7.10	0.02226	0.02190	0.02087
9.10	0.02168	0.02027	0.01990
11.10	0.02060	0.01971	0.01871
13.10	0.02005	0.01859	0.01796
15.10	0.01888	0.01787	0.01705
17.10	0.01835	0.01724	0.01645
19.10	0.01751	0.01683	0.01614
21.10	0.01722	0.01601	0.01532
23.10	0.01637	0.01561	0.01505
25.10	0.01601	0.01498	0.01441
27.10	0.01559	0.01489	0.01430
29.10	0.01511	0.01453	
31.10	0.01480	0.01452	
33.10	0.01460	0.01415	
35.10	0.01435		
37.10	0.01431		

Table VI-27. M_W=84,400; σ_H latex; pH=4.0; C_{Ao}=0.03 mg/L; latex=0.00075%.

Replicate "C"	Concentration of PAAm, mg/L		
	Field Strength, volts/cm		
Time, seconds	11.8	20.2	28.0
5.10		0.02273	0.02273
7.10	0.02262	0.02195	0.02096
9.10	0.02190	0.02033	0.01977
11.10	0.02060	0.01975	0.01900
13.10	0.02007	0.01878	0.01804
15.10	0.01894	0.01773	0.01725
17.10	0.01769	0.01717	0.01653
19.10	0.01728	0.01665	0.01603
21.10	0.01697	0.01609	0.01544
23.10	0.01635	0.01556	0.01506
25.10	0.01591	0.01511	0.01456
27.10	0.01559	0.01480	0.01425
29.10	0.01511	0.01453	
31.10	0.01491	0.01426	
33.10	0.01441	0.01375	
35.10	0.01437		
37.10	0.01395		

Table VI-28. M_W=84,400; σ_H latex; pH=4.0; C_{Ao}=0.03 mg/L; latex=0.00075%.

Replicate "D"	Concentration of PAAm, mg/L		
	Field Strength, volts/cm		
Time, seconds	11.8	20.2	28.0
5.10		0.02276	0.02273
7.10	0.02265	0.02177	0.02096
9.10	0.02203	0.02047	0.01977
11.10	0.02021	0.01947	0.01900
13.10	0.02003	0.01851	0.01804
15.10	0.01863	0.01770	0.01725
17.10	0.01818	0.01715	0.01653
19.10	0.01776	0.01644	0.01603
21.10	0.01734	0.01620	0.01544
23.10	0.01648	0.01546	0.01506
25.10	0.01598	0.01496	0.01456
27.10	0.01559	0.01475	0.01425
29.10	0.01486	0.01454	
31.10	0.01487	0.01415	
33.10	0.01454	0.01401	
35.10	0.01447		
37.10	0.01401		

Table VI-29. M_W=84,400; σ_H latex; pH=4.0; C_{Ao}=0.04 mg/L; latex=0.00100%.

Replicate "A"	Concentration of PAAm, mg/L		
	Field Strength, volts/cm		
Time, seconds	11.8	20.2	28.0
7.50			0.02567
8.50	0.02732	0.02563	0.02440
9.50	0.02849	0.02499	0.02364
10.50	0.02606	0.02426	0.02289
11.50	0.02422	0.02333	0.02210
12.50	0.02374	0.02263	0.02136
13.50	0.02387	0.02159	0.02079
14.50	0.02221	0.02125	0.02050
15.50	0.02199	0.02111	0.01996
16.50	0.02159	0.02011	0.01932
17.50	0.02075	0.01982	0.01901
18.50	0.02024	0.01970	0.01886
19.50	0.02045	0.01942	0.01846
20.50	0.01991	0.01929	
21.50	0.01999	0.01818	
22.50	0.01911	0.01898	
23.50	0.01949	0.01752	
24.50	0.01881	0.01756	
25.50	0.01853		

Table VI-30. M_W=84,400; σ_H latex; pH=4.0; C_{Ao}=0.04 mg/L; latex=0.00100%.

Replicate "B"	Concentration of PAAm, mg/L		
	Field Strength, volts/cm		
Time, seconds	11.8	20.2	28.0
7.50			0.02648
8.50	0.02635	0.02596	0.02537
9.50	0.02582	0.02486	0.02364
10.50	0.02663	0.02415	0.02293
11.50	0.02445	0.02333	0.02212
12.50	0.02370	0.02259	0.02140
13.50	0.02319	0.02176	0.02100
14.50	0.02264	0.02107	0.02054
15.50	0.02204	0.02100	0.02026
16.50	0.02197	0.02031	0.01918
17.50	0.02148	0.01986	0.01875
18.50	0.02051	0.01957	0.01896
19.50	0.01995	0.01916	0.01900
20.50	0.01982	0.01938	
21.50	0.01951	0.01886	
22.50	0.01928	0.01881	
23.50	0.01866	0.01817	
24.50	0.01896	0.01780	
25.50	0.01858		

Table VI-31. M_W=84,400; σ_H latex; pH=4.0; C_{Ao}=0.04 mg/L; latex=0.00100%.

Replicate "C"	Concentration of PAAm, mg/L		
	Field Strength, volts/cm		
Time, seconds	11.8	20.2	28.0
7.50			0.02584
8.50	0.02565	0.02613	0.02436
9.50	0.02582	0.02449	0.02383
10.50	0.02422	0.02374	0.02278
11.50	0.02424	0.02327	0.02203
12.50	0.02298	0.02219	0.02121
13.50	0.02259	0.02143	0.02106
14.50	0.02228	0.02143	0.02060
15.50	0.02166	0.02062	0.01933
16.50	0.02117	0.02027	0.01967
17.50	0.02064	0.01973	0.01903
18.50	0.02031	0.01947	0.01892
19.50	0.02036	0.01898	0.01870
20.50	0.01962	0.01876	
21.50	0.01913	0.01846	
22.50	0.01960	0.01788	
23.50	0.01936	0.01799	
24.50	0.01832	0.01915	
25.50	0.01858		

Table VI-32. M_W=84,400; σ_H latex; pH=4.0; C_{Ao}=0.05 mg/L; latex=0.00125%.

Replicate "A"	Concentration of PAAm, mg/L		
	Field Strength, volts/cm		
Time, seconds	11.8	20.2	28.0
3.60			0.03542
4.60	0.03508	0.03701	0.03316
5.60	0.03511	0.03388	0.03172
6.60	0.03530	0.03099	0.03045
7.60	0.03206	0.03075	0.02882
8.60	0.03096	0.02999	0.02842
9.60	0.03024	0.02828	0.02738
10.60	0.02953	0.02747	0.02596
11.60	0.02801	0.02716	0.02582
12.60	0.02736	0.02632	0.02454
13.60	0.02692	0.02567	0.02450
14.60	0.02600	0.02491	0.02381
15.60		0.02450	
16.60	0.02463	0.02432	
17.60	0.02481	0.02385	

Table VI-33. M_W=84,400; σ_H latex; pH=4.0; C_{Ao}=0.05 mg/L; latex=0.00125%.

Replicate "B"	Concentration of PAAm, mg/L		
	Field Strength, volts/cm		
Time, seconds	11.8	20.2	28.0
3.60			0.03542
4.60	0.03818	0.03429	0.03313
5.60	0.03530	0.03320	0.03166
6.60	0.03398	0.03163	0.03061
7.60	0.03329	0.03053	0.02859
8.60	0.03075	0.03040	0.02825
9.60	0.02961	0.02845	0.02729
10.60	0.02849	0.02757	0.02685
11.60	0.02826	0.02716	0.02553
12.60		0.02626	0.02452
13.60		0.02552	0.02452
14.60	0.02598	0.02459	0.02377
15.60	0.02562	0.02471	
16.60	0.02454	0.02479	
17.60	0.02452	0.02391	

Table VI-34. M_W=84,400; σ_H latex; pH=4.0; C_{Ao}=0.05 mg/L; latex=0.00125%.

Replicate "C"	Concentration of PAAm, mg/L		
	Field Strength, volts/cm		
Time, seconds	11.8	20.2	28.0
3.60			0.03542
4.60	0.03398	0.03342	0.03320
5.60	0.03654	0.03461	0.03245
6.60	0.03368	0.03307	0.03045
7.60	0.03192	0.03035	0.02914
8.60	0.03177	0.02961	0.02808
9.60	0.03014	0.02968	0.02736
10.60	0.02966	0.02794	0.02640
11.60	0.02826	0.02642	0.02555
12.60	0.02810	0.02647	0.02493
13.60	0.02630	0.02549	0.02448
14.60	0.02605	0.02475	0.02426
15.60		0.02477	
16.60		0.02416	
17.60		0.02401	

Table VI-35. M_W=84,400; σ_H latex; pH=4.0; C_{Ao}=0.05 mg/L; latex=0.00125%.

Replicate "D"	Concentration of PAAm, mg/L		
	Field Strength, volts/cm		
Time, seconds	11.8	20.2	28.0
3.60			0.03542
4.60	0.03719	0.03422	0.03316
5.60	0.03365	0.03388	0.03194
6.60	0.03254	0.03172	0.03051
7.60	0.03230	0.03056	0.02885
8.60	0.03014	0.02923	0.02825
9.60	0.02999	0.02842	0.02734
10.60	0.02817	0.02731	0.02641
11.60	0.02801	0.02647	0.02563
12.60	0.02711	0.02600	
13.60		0.02540	0.02450
14.60	0.02575	0.02475	0.02395
15.60	0.02553	0.02414	
16.60		0.02381	
17.60	0.02453	0.02387	

Table VI-36. M_W=154,000; σ_H latex; pH=4.0; C_{Ao}=0.02 mg/L; latex=0.00050%.

Replicate "A"	Concentration of PAAm, mg/L		
	Field Strength, volts/cm		
Time, seconds	11.8	20.0	28.0
5.10	0.01489	0.01565	0.01533
8.60	0.01521	0.01521	0.01400
12.10	0.01447	0.01431	0.01397
15.60	0.01402	0.01343	0.01299
19.10	0.01365	0.01310	0.01240
22.60	0.01308	0.01242	0.01200
26.10	0.01285	0.01189	0.01148
29.60	0.01227	0.01141	0.01105
33.10	0.01181	0.01106	0.01067
36.60	0.01135	0.01081	0.01041
40.10	0.01116	0.01043	0.01007
43.60	0.01068	0.01028	0.00970
47.10	0.01060	0.00995	
50.60	0.01050	0.00975	
54.10	0.01018	0.00956	
57.60	0.00988		

Table VI-37. M_W=154,000; σ_H latex; pH=4.0; C_{Ao}=0.02 mg/L; latex=0.00050%.

Replicate "B"	Concentration of PAAm, mg/L		
	Field Strength, volts/cm		
Time, seconds	11.8	20.0	28.0
5.10	0.01659	0.01556	0.01548
8.60	0.01491	0.01506	0.01429
12.10	0.01484	0.01458	0.01374
15.60	0.01426	0.01366	0.01286
19.10	0.01369	0.01298	0.01248
22.60	0.01313	0.01249	0.01193
26.10	0.01264	0.01200	0.01134
29.60	0.01214	0.01145	0.01115
33.10	0.01182	0.01121	0.01070
36.60	0.01151	0.01092	0.01020
40.10	0.01146	0.01039	0.00997
43.60	0.01091	0.01028	0.00972
47.10	0.01086	0.01014	
50.60	0.01037	0.00980	
54.10	0.01019	0.00961	
57.60	0.00996		

Table VI-38. M_W=154,000; σ_H latex; pH=4.0; C_{Ao}=0.02 mg/L; latex=0.00050%.

Replicate "C"	Concentration of PAAm, mg/L		
	Field Strength, volts/cm		
Time, seconds	11.8	20.0	28.0
5.10	0.01597	0.01645	0.01585
8.60	0.01519	0.01495	0.01463
12.10	0.01470	0.01421	0.01361
15.60	0.01417	0.01361	0.01302
19.10	0.01355	0.01291	0.01243
22.60	0.01323	0.01252	0.01181
26.10	0.01277	0.01184	0.01134
29.60	0.01206	0.01149	0.01091
33.10	0.01182	0.01112	0.01068
36.60	0.01152	0.01073	0.01033
40.10	0.01109	0.01052	0.01011
43.60	0.01078	0.01021	0.00968
47.10	0.01063	0.01004	
50.60	0.01048	0.00981	
54.10	0.01011	0.00965	
57.60	0.00979		

Table VI-39. M_W=154,000; σ_H latex; pH=4.0; C_{Ao}=0.02 mg/L; latex=0.00050%.

Replicate "D"	Concentration of PAAm, mg/L		
	Field Strength, volts/cm		
Time, seconds	11.8	20.0	28.0
5.10	0.01519	0.01537	0.01512
8.60	0.01556	0.01508	0.01467
12.10	0.01470	0.01412	0.01373
15.60	0.01439	0.01350	0.01294
19.10	0.01373	0.01308	0.01247
22.60	0.01300	0.01237	0.01177
26.10	0.01262	0.01204	0.01129
29.60	0.01220	0.01140	0.01093
33.10	0.01180	0.01123	0.01067
36.60	0.01142	0.01079	0.01025
40.10	0.01101	0.01049	0.00984
43.60	0.01118	0.01022	0.00969
47.10	0.01060	0.01004	
50.60	0.01025	0.00979	
54.10	0.01015	0.00952	
57.60	0.00977		

Table VI-40. M_W=18,200; σ_H latex; pH=4.0; C_{Ao}=0.02 mg/L; latex=0.00050%.

Replicate "A"	Concentration of PAAm, mg/L		
	Field Strength, volts/cm		
Time, seconds	11.8	20.0	28.0
5.35	0.01447	0.01411	0.01493
6.85	0.01510	0.01426	0.01357
8.35	0.01374	0.01399	0.01322
9.85	0.01412	0.01323	0.01257
11.35	0.01330	0.01271	0.01251
12.85	0.01236	0.01194	0.01181
14.35	0.01212	0.01160	0.01131
15.85	0.01167	0.01118	0.01090
17.35	0.01109	0.01072	0.01046
18.85	0.01086	0.01046	0.01018
20.35	0.01053	0.01005	0.01010
21.85	0.01050	0.01000	0.00953
23.35	0.01005	0.00974	0.00951
24.85	0.00963	0.00955	

Table VI-41. M_W=18,200; σ_H latex; pH=4.0; C_{Ao}=0.02 mg/L; latex=0.00050%.

Replicate "B"	Concentration of PAAm, mg/L		
	Field Strength, volts/cm		
Time, seconds	11.8	20.0	28.0
5.35	0.01507	0.01561	0.01476
6.85	0.01512	0.01408	0.01345
8.35	0.01351	0.01397	0.01349
9.85	0.01403	0.01319	0.01292
11.35	0.01285	0.01262	0.01226
12.85	0.01277	0.01232	0.01199
14.35	0.01220	0.01173	0.01134
15.85	0.01159	0.01115	0.01078
17.35	0.01108	0.01060	0.01051
18.85	0.01066	0.01060	0.01014
20.35	0.01074	0.01014	0.00996
21.85	0.01020	0.00990	0.00970
23.35	0.01019	0.00989	0.00959
24.85	0.00990	0.00961	

Table VI-42. M_W=18,200; σ_H latex; pH=4.0; C_{Ao}=0.02 mg/L; latex=0.00050%.

Replicate "C"	Concentration of PAAm, mg/L		
	Field Strength, volts/cm		
Time, seconds	11.8	20.0	28.0
5.35	0.01507	0.01474	0.01486
6.85	0.01428	0.01440	0.01409
8.35	0.01457	0.01330	0.01304
9.85	0.01329	0.01294	0.01286
11.35	0.01308	0.01256	0.01237
12.85	0.01283	0.01214	0.01170
14.35	0.01200	0.01171	0.01134
15.85	0.01202	0.01118	0.01084
17.35	0.01129	0.01093	0.01048
18.85	0.01090	0.01050	0.01004
20.35	0.01061	0.01028	0.00968
21.85	0.01019	0.00988	0.00957
23.35	0.01000	0.00979	0.00961
24.85	0.00992	0.00976	

Table VI-43. M_W=18,200; σ_H latex; pH=4.0; C_{Ao}=0.02 mg/L; latex=0.00050%.

Replicate "D"	Concentration of PAAm, mg/L		
	Field Strength, volts/cm		
Time, seconds	11.8	20.0	28.0
5.35	0.01578	0.01462	0.01450
6.85	0.01393	0.01387	0.01377
8.35	0.01370	0.01376	0.01313
9.85	0.01400	0.01302	0.01272
11.35	0.01266	0.01269	0.01205
12.85	0.01258	0.01189	0.01183
14.35	0.01194	0.01166	0.01124
15.85	0.01129	0.01143	0.01084
17.35	0.01113	0.01075	0.01042
18.85	0.01088	0.01058	0.01001
20.35	0.01038	0.01029	0.00992
21.85	0.01025	0.00981	0.00975
23.35	0.00995	0.00966	0.00950
24.85	0.00989	0.00958	

Table VI-43. M_W=154,000; σ_H latex; pH=10; C_{Ao}=0.10 mg/L; latex=0.00050%.

Replicate "A"	Concentration of PAAm, mg/L		
	Field Strength, volts/cm		
Time, seconds	11.6	19.6	27.8
7.50		0.08941	0.08915
10.50	0.08845	0.08773	0.08727
13.50	0.08559	0.08467	0.08461
16.50	0.08515	0.08203	0.08187
19.50	0.08187	0.08026	0.07968
22.50	0.08056	0.07743	0.07701
25.50	0.07800	0.07546	0.07485
28.50	0.07684	0.07394	0.07334
31.50	0.07564	0.07182	0.07234
34.50	0.07263	0.07007	0.06938
37.50	0.07174	0.06973	0.06812
40.50	0.07048	0.06831	0.06677
43.50	0.06885	0.06563	0.06595
46.50	0.06812	0.06487	0.06476
49.50	0.06784	0.06385	0.06362
52.50	0.06697	0.06216	0.06203
55.50	0.06615	0.06266	0.06228
58.50	0.06498	0.06139	0.06100
61.50	0.06290	0.06165	0.06139

Table VI-45. M_W=154,000; σ_H latex; pH=10; C_{Ao}=0.10 mg/L; latex=0.00050%.

Replicate "B"	Concentration of PAAm, mg/L		
	Field Strength, volts/cm		
Time, seconds	11.6	19.6	27.8
7.50		0.08885	0.08902
10.50	0.08781	0.08803	0.08637
13.50	0.08556	0.08474	0.08352
16.50	0.08436	0.08330	0.08135
19.50	0.08187	0.07950	0.07889
22.50	0.07936	0.07769	0.07605
25.50	0.07775	0.07510	0.07414
28.50	0.07605	0.07327	0.07219
31.50	0.07552	0.07144	0.07007
34.50	0.07299	0.07007	0.06973
37.50	0.07174	0.06903	0.06706
40.50	0.07007	0.06774	0.06646
43.50	0.06885	0.06667	0.06487
46.50	0.06858	0.06454	0.06385
49.50	0.06706	0.06531	0.06385
52.50	0.06716	0.06302	0.06302
55.50	0.06465	0.06126	0.06241
58.50	0.06326	0.06253	0.06191
61.50	0.06241	0.06100	0.06019

Table VI-46. M_W=154,000; σ_H latex; pH=10; C_{Ao}=0.10 mg/L; latex=0.00050%.

Replicate "C"	Concentration of PAAm, mg/L		
	Field Strength, volts/cm		
Time, seconds	11.6	19.6	27.8
7.50		0.08902	0.08932
10.50	0.08792	0.08737	0.08702
13.50	0.08734	0.08634	0.08415
16.50	0.08436	0.08275	0.08135
19.50	0.08163	0.08017	0.07865
22.50	0.07995	0.07805	0.07611
25.50	0.07884	0.07634	0.07374
28.50	0.07558	0.07459	0.07249
31.50	0.07401	0.07234	0.07086
34.50	0.07347	0.07128	0.06912
37.50	0.07189	0.06938	0.06765
40.50	0.06998	0.06981	0.06697
43.50	0.06930	0.06765	0.06498
46.50	0.06885	0.06552	0.06397
49.50	0.06784	0.06408	0.06290
52.50	0.06531	0.06476	0.06139
55.50	0.06687	0.06216	0.06152
58.50	0.06476	0.06290	0.06266
61.50	0.06314	0.06216	0.06073

Table VI-47. M_W=154,000; σ_H latex; pH=10; C_{Ao}=0.10 mg/L; latex=0.00050%.

Replicate "D"	Concentration of PAAm, mg/L		
	Field Strength, volts/cm		
Time, seconds	11.6	19.6	27.8
7.50		0.09100	0.08932
10.50	0.08818	0.08752	0.08682
13.50	0.08607	0.08471	0.08405
16.50	0.08457	0.08359	0.08110
19.50	0.08249	0.08069	0.07913
22.50	0.08073	0.07775	0.07645
25.50	0.07913	0.07594	0.07434
28.50	0.07673	0.07447	0.07204
31.50	0.07440	0.07361	0.07007
34.50	0.07320	0.07128	0.06920
37.50	0.07174	0.06990	0.06812
40.50	0.06990	0.06912	0.06605
43.50	0.06938	0.06687	0.06552
46.50	0.06726	0.06595	0.06338
49.50	0.06605	0.06520	0.06350
52.50	0.06574	0.06531	0.06266
55.50	0.06615	0.06362	0.06216
58.50	0.06605	0.06191	0.06203
61.50	0.06420	0.06191	0.06100

Table VI-48. M_W=82,400; σ_H latex; pH=10; C_{Ao}=0.10 mg/L; latex=0.00050%.

Replicate "A"	Concentration of PAAm, mg/L		
	Field Strength, volts/cm		
Time, seconds	11.6	19.6	27.8
6.0	0.08873	0.08965	0.08752
8.0	0.08898	0.08682	0.08748
10.0	0.08685	0.08563	0.08454
12.0	0.08549	0.08286	0.08316
14.0	0.08341	0.08110	0.08110
16.0	0.08206	0.08008	0.07898
18.0	0.08102	0.07780	0.07651
20.0	0.07908	0.07497	0.07516
22.0	0.07785	0.07256	0.07327
24.0	0.07528	0.07212	0.07204
26.0	0.07401	0.07104	0.07064
28.0	0.07144	0.06998	0.06947
30.0	0.07227	0.06812	0.06876
32.0	0.06973	0.06784	0.06755
34.0	0.06998	0.06774	0.06746
36.0	0.06990	0.06574	0.06677
38.0	0.06956	0.06605	0.06615
40.0	0.06420	0.06646	0.06465
42.0	0.06765	0.06373	0.06487

Table VI-49. M_W=82,400; σ_H latex; pH=10; C_{Ao}=0.10 mg/L; latex=0.00050%.

Replicate "B"	Concentration of PAAm, mg/L		
	Field Strength, volts/cm		
Time, seconds	11.6	19.6	27.8
6.0	0.08979	0.09038	0.08857
8.0	0.08607	0.08563	0.08699
10.0	0.08741	0.08525	0.08433
12.0	0.08436	0.08271	0.08214
14.0	0.08256	0.08021	0.08021
16.0	0.07999	0.07850	0.07820
18.0	0.07999	0.07668	0.07673
20.0	0.07570	0.07491	0.07427
22.0	0.07414	0.07340	0.07306
24.0	0.07306	0.07112	0.07112
26.0	0.07277	0.07112	0.06973
28.0	0.07204	0.06956	0.06903
30.0	0.07007	0.06849	0.06876
32.0	0.06903	0.06774	0.06755
34.0	0.06765	0.06774	0.06552
36.0	0.06840	0.06605	0.06408
38.0	0.06563	0.06520	0.06302
40.0	0.06774	0.06431	0.06465
42.0	0.06509	0.06338	0.06278

Table VI-50. M_W=82,400; σ_H latex; pH=10; C_{Ao}=0.10 mg/L; latex=0.00050%.

Replicate "C"	Concentration of PAAm, mg/L		
	Field Strength, volts/cm		
Time, seconds	11.6	19.6	27.8
6.0	0.08624	0.08991	0.08784
8.0	0.08741	0.08600	0.08733
10.0	0.08553	0.08624	0.08464
12.0	0.08464	0.08260	0.08214
14.0	0.08199	0.08106	0.07990
16.0	0.08077	0.07898	0.07785
18.0	0.07835	0.07695	0.07622
20.0	0.07840	0.07634	0.07453
22.0	0.07576	0.07421	0.07313
24.0	0.07388	0.07241	0.07144
26.0	0.07292	0.07159	0.07048
28.0	0.07089	0.06964	0.06821
30.0	0.07072	0.06885	0.06784
32.0	0.06903	0.06765	0.06677
34.0	0.06921	0.06626	0.06552
36.0	0.06938	0.06646	0.06498
38.0	0.06903	0.06584	0.06431
40.0	0.06531	0.06408	0.06397
42.0	0.06774	0.06431	0.06326

Table VI-51. M_W=82,400; σ_H latex; pH=10; C_{Ao}=0.10 mg/L; latex=0.00050%.

Replicate "D"	Concentration of PAAm, mg/L		
	Field Strength, volts/cm		
Time, seconds	11.6	19.6	27.8
6.0	0.08702	0.08975	0.08784
8.0	0.08728	0.08723	0.08752
10.0	0.08566	0.08436	0.08481
12.0	0.08447	0.08301	0.08305
14.0	0.08237	0.08143	0.08081
16.0	0.08090	0.07908	0.07830
18.0	0.07870	0.07645	0.07640
20.0	0.07775	0.07522	0.07453
22.0	0.07459	0.07313	0.07241
24.0	0.07347	0.07263	0.07120
26.0	0.07347	0.07056	0.06998
28.0	0.07167	0.07015	0.06774
30.0	0.06990	0.06774	0.06821
32.0	0.06947	0.06831	0.06584
34.0	0.06840	0.06687	0.06626
36.0	0.06755	0.06793	0.06314
38.0	0.06765	0.06563	0.06454
40.0	0.06656	0.06385	0.06373
42.0	0.06755	0.06442	0.06373

Table VI-52. M_W=18,200; σ_H latex; pH=10; C_{Ao}=0.10 mg/L; latex=0.00050%.

Replicate "A"	Concentration of PAAm, mg/L		
	Field Strength, volts/cm		
Time, seconds	11.6	19.6	27.8
4.875	0.08426	0.08637	0.08405
6.125	0.08734	0.08305	0.08026
7.375	0.08461	0.08380	0.07845
8.625	0.07903	0.08052	0.07769
9.875	0.07959	0.07706	0.07534
11.125	0.07759	0.07738	0.07299
12.375	0.07440	0.07466	0.07167
13.625	0.07485	0.07277	0.07032
14.875	0.07453	0.07256	0.06912
16.125	0.06812	0.06998	0.06867
17.375	0.07048	0.06903	0.06784
18.625	0.07089	0.06834	0.06563
19.875	0.06803	0.06667	0.06454
21.125	0.07007	0.06716	0.06487
22.375	0.06595	0.06552	
23.625	0.06626	0.06465	
24.875	0.06687		
26.125	0.06476		

Table VI-53. M_W=18,200; σ_H latex; pH=10; C_{Ao}=0.10 mg/L; latex=0.00050%.

Replicate "B"	Concentration of PAAm, mg/L		
	Field Strength, volts/cm		
Time, seconds	11.6	19.6	27.8
4.875	0.08651	0.08600	0.08316
6.125	0.08433	0.08658	0.08069
7.375	0.08457	0.08226	0.08043
8.625	0.08069	0.08135	0.07775
9.875	0.07668	0.07941	0.07453
11.125	0.07913	0.07570	0.07292
12.375	0.07870	0.07401	0.07174
13.625	0.07414	0.07361	0.07023
14.875	0.07128	0.07227	0.06981
16.125	0.07151	0.06990	0.06840
17.375	0.06981	0.06938	0.06726
18.625	0.06938	0.06938	0.06667
19.875	0.06755	0.06726	0.06542
21.125	0.06716	0.06726	0.06408
22.375	0.06765	0.06498	
23.625	0.06667	0.06563	
24.875	0.06542		
26.125	0.06476		

Table VI-54. M_W=18,200; σ_H latex; pH=10; C_{Ao}=0.10 mg/L; latex=0.00050%.

Replicate "C"	Concentration of PAAm, mg/L		
	Field Strength, volts/cm		
Time, seconds	11.6	19.6	27.8
4.875	0.08498	0.08498	0.08498
6.125	0.08590	0.08377	0.08123
7.375	0.08308	0.08249	0.07954
8.625	0.08123	0.08017	0.07743
9.875	0.08143	0.07743	0.07528
11.125	0.07558	0.07695	0.07401
12.375	0.07434	0.07434	0.07263
13.625	0.07334	0.07306	0.07007
14.875	0.07277	0.07256	0.06821
16.125	0.07089	0.06938	0.06912
17.375	0.07072	0.06849	0.06697
18.625	0.06964	0.06793	0.06716
19.875	0.06784	0.06746	0.06677
21.125	0.06840	0.06615	0.06716
22.375	0.06716	0.06784	
23.625	0.06139	0.06465	
24.875	0.06476		
26.125	0.06191		

Table VI-55. M_W=18,200; σ_H latex; pH=10; C_{Ao}=0.10 mg/L; latex=0.00050%.

Replicate "D"	Concentration of PAAm, mg/L		
	Field Strength, volts/cm		
Time, seconds	11.6	19.6	27.8
4.875	0.08744	0.08512	0.08191
6.125	0.08829	0.08634	0.08073
7.375	0.08443	0.08218	0.07820
8.625	0.08282	0.07850	0.07738
9.875	0.07922	0.07825	0.07617
11.125	0.07472	0.07669	0.07421
12.375	0.07478	0.07434	0.07174
13.625	0.07478	0.07263	0.07081
14.875	0.07204	0.07197	0.06894
16.125	0.07174	0.06947	0.06849
17.375	0.06990	0.06912	0.06784
18.625	0.06973	0.06765	0.06626
19.875	0.06930	0.06716	0.06574
21.125	0.06849	0.06840	0.06615
22.375	0.06867	0.06646	
23.625	0.06656	0.06253	
24.875	0.06755		
26.125	0.06765		

Table VI-56. M_W=82,400; σ_H latex; pH=4.0; C_{Ao}=0.02 mg/L; latex=0.00050%; I=0.050.

Replicate "A"	Concentration of PAAm, mg/L		
	Field Strength, volts/cm		
Time, seconds	11.6	15.6	20.0
5.60	0.01454	0.01453	0.01502
9.60	0.01367	0.01424	0.01362
13.60	0.01359	0.01370	0.01286
17.60	0.01274	0.01307	0.01233
21.60	0.01268	0.01261	0.01206
25.60	0.01207	0.01216	0.01177
29.60	0.01183	0.01191	0.01129
33.60	0.01154	0.01180	0.01109

Table VI-57. M_W=82,400; σ_H latex; pH=4.0; C_{Ao}=0.02 mg/L; latex=0.00050%; I=0.050.

Replicate "B"	Concentration of PAAm, mg/L		
	Field Strength, volts/cm		
Time, seconds	11.6	15.6	20.0
5.60	0.01477	0.01443	0.01468
9.60	0.01379	0.01389	0.01443
13.60	0.01346	0.01357	0.01339
17.60	0.01284	0.01293	0.01234
21.60	0.01260	0.01237	0.01202
25.60	0.01221	0.01208	0.01160
29.60	0.01188	0.01162	0.01141
33.60	0.01158	0.01141	0.01107

Table VI-58. M_w=82,400; σ_H latex; pH=4.0; C_{Ac}=0.02 mg/L; latex=0.00050%; I=0.050.

Replicate "C"	Concentration of PAAm, mg/L		
	Field Strength, volts/cm		
Time, seconds	11.6	15.6	20.0
5.60	0.01431	0.01486	0.01556
9.60	0.01349	0.01429	0.01514
13.60	0.01311	0.01361	0.01346
17.60	0.01268	0.01330	0.01298
21.60	0.01233	0.01265	0.01270
25.60	0.01216	0.01231	0.01200
29.60	0.01185	0.01169	0.01165
33.60	0.01153	0.01169	0.01131

Table VI-59. M_W=82,400; σ_H latex; pH=4.0; C_{Ao}=0.02 mg/L; latex=0.00050%; I=0.050.

Replicate "D"	Concentration of PAAm, mg/L		
	Field Strength, volts/cm		
Time, seconds	11.6	15.6	20.0
5.60	0.01455	0.01482	0.01482
9.60	0.01374	0.01380	0.01443
13.60	0.01336	0.01313	0.01390
17.60	0.01275	0.01280	0.01337
21.60	0.01242	0.01229	0.01273
25.60	0.01200	0.01197	0.01214
29.60	0.01175	0.01170	0.01172
33.60	0.01163	0.01163	0.01136

Table VI-60. M_W=82,400; σ_L latex; pH=4.0; C_{Ao}=0.02 mg/L; latex=0.00050%.

Replicate "A"	Concentration of PAAm, mg/L		
	Field Strength, volts/cm		
Time, seconds	12.8	21.6	30.6
8.50	0.00909		0.00929
11.50	0.00906	0.00893	0.00890
14.50	0.00906	0.00901	0.00890
17.50	0.00892	0.00885	0.00875
20.50	0.00881	0.00878	0.00863
23.50	0.00871	0.00867	0.00854
26.50	0.00870	0.00863	0.00848
29.50	0.00860	0.00852	0.00838
32.50	0.00852	0.00849	0.00837
35.50	0.00847	0.00838	0.00830
38.50	0.00845	0.00837	0.00829
41.50	0.00840	0.00834	
44.50	0.00841	0.00831	
47.50	0.00840	0.00832	
50.50	0.00835	0.00831	
53.50	0.00836		
56.50	0.00836		
59.50	0.00833		

Table VI-61. M_W=82,400; σ_L latex; pH=4.0; C_{Ao}=0.02 mg/L; latex=0.00050%.

Replicate "B"	Concentration of PAAm, mg/L		
	Field Strength, volts/cm		
Time, seconds	12.8	21.6	30.6
8.50	0.00939		0.00900
11.50	0.00913	0.00912	0.00892
14.50	0.00904	0.00897	0.00883
17.50	0.00886	0.00881	0.00868
20.50	0.00886	0.00871	0.00858
23.50	0.00875	0.00862	0.00855
26.50	0.00869	0.00856	0.00848
29.50	0.00858	0.00849	0.00838
32.50	0.00852	0.00845	0.00835
35.50	0.00852	0.00838	0.00832
38.50	0.00846	0.00837	0.00832
41.50	0.00842	0.00833	
44.50	0.00835	0.00833	
47.50	0.00837	0.00828	
50.50	0.00837	0.00831	
53.50	0.00838		
56.50	0.00836		
59.50	0.00833		

Table VI-62. M_W=82,400; σ_L latex; pH=4.0; C_{Ao}=0.02 mg/L; latex=0.00050%.

Replicate "C"	Concentration of PAAm, mg/L		
	Field Strength, volts/cm		
Time, seconds	12.8	21.6	30.6
8.50	0.00916		0.00908
11.50	0.00901	0.00908	0.00890
14.50	0.00909	0.00891	0.00884
17.50	0.00895	0.00882	0.00874
20.50	0.00883	0.00870	0.00867
23.50	0.00871	0.00863	0.00858
26.50	0.00867	0.00854	0.00848
29.50	0.00862	0.00847	0.00838
32.50	0.00858	0.00842	0.00841
35.50	0.00850	0.00838	0.00831
38.50	0.00845	0.00837	0.00830
41.50	0.00843	0.00834	
44.50	0.00839	0.00829	
47.50	0.00839	0.00828	
50.50	0.00836	0.00830	
53.50	0.00839		
56.50	0.00837		
59.50	0.00834		

Table VI-63. M_W=82,400; σ_L latex; pH=4.0; C_{Ao}=0.02 mg/L; latex=0.00050%.

Replicate "D"	Concentration of PAAm, mg/L		
	Field Strength, volts/cm		
Time, seconds	12.8	21.6	30.6
8.50	0.00903		0.00907
11.50	0.00899	0.00904	0.00893
14.50	0.00896	0.00897	0.00888
17.50	0.00882	0.00889	0.00879
20.50	0.00881	0.00872	0.00862
23.50	0.00867	0.00861	0.00854
26.50	0.00863	0.00856	0.00849
29.50	0.00860	0.00851	0.00838
32.50	0.00851	0.00844	0.00835
35.50	0.00848	0.00838	0.00832
38.50	0.00851	0.00836	0.00832
41.50	0.00847	0.00834	
44.50	0.00842	0.00831	
47.50	0.00841	0.00831	
50.50	0.00839	0.00833	
53.50	0.00840		
56.50	0.00837		
59.50	0.00833		

Table VI-64. M_W=82,400; σ_M latex; pH=4.0; C_{Ao}=0.02 mg/L; latex=0.00050%.

Replicate "A"	Concentration of PAAm, mg/L		
	Field Strength, volts/cm		
Time, seconds	12.8	21.6	30.6
11.5	0.00847	0.00839	0.00835
16.0	0.00827	0.00824	0.00824
20.5	0.00822	0.00818	0.00803
25.0	0.00811	0.00807	0.00791
29.5	0.00802	0.00787	0.00777
34.0	0.00795	0.00773	0.00759
38.5	0.00779	0.00760	0.00744
43.0	0.00770	0.00747	0.00737
47.5	0.00757	0.00735	0.00697
52.0	0.00744	0.00721	0.00686
56.5	0.00733	0.00715	
61.0	0.00723	0.00705	
65.5	0.00720	0.00695	
70.0	0.00708		
74.5	0.00692		

Table VI-65. M_W=82,400; σ_M latex; pH=4.0; C_{Ao}=0.02 mg/L; latex=0.00050%.

Replicate "B"	Concentration of PAAm, mg/L		
	Field Strength, volts/cm		
Time, seconds	12.8	21.6	30.6
11.5	0.00829	0.00859	0.00832
16.0	0.00839	0.00829	0.00821
20.5	0.00820	0.00810	0.00806
25.0	0.00811	0.00798	0.00789
29.5	0.00806	0.00781	0.00774
34.0	0.00790	0.00771	0.00759
38.5	0.00779	0.00756	0.00742
43.0	0.00764	0.00741	0.00731
47.5	0.00757	0.00728	0.00696
52.0	0.00742	0.00716	0.00688
56.5	0.00729	0.00715	
61.0	0.00726	0.00694	
65.5	0.00712	0.00696	
70.0	0.00700		
74.5	0.00693		

Table VI-66. M_W=82,400; σ_M latex; pH=4.0; C_{Ao}=0.02 mg/L; latex=0.00050%.

Replicate "C"	Concentration of PAAm, mg/L		
	Field Strength, volts/cm		
Time, seconds	12.8	21.6	30.6
11.5	0.00876	0.00826	0.00826
16.0	0.00839	0.00827	0.00819
20.5	0.00833	0.00814	0.00807
25.0	0.00815	0.00807	0.00794
29.5	0.00803	0.00787	0.00774
34.0	0.00792	0.00773	0.00757
38.5	0.00779	0.00764	0.00745
43.0	0.00766	0.00747	0.00734
47.5	0.00753	0.00735	0.00693
52.0	0.00738	0.00726	0.00687
56.5	0.00732	0.00715	
61.0	0.00721	0.00707	
65.5	0.00717	0.00689	
70.0	0.00701		
74.5	0.00701		

APPENDIX VII

SUMMARY OF REGRESSION RESULTS - PERIKINETIC EXPERIMENTS

Table VII1. Summary of *m* values.

		REPLICATES					
	Filename	1	2	3	4	Mean	St.Dev
Mw 4	50FINL'	0.0371	0.0363	0.0394	0.0410	0.0385	0.0025
Mw 4	109FINL'	0.0364	0.0404	0.0375	0.0394	0.0384	0.0021
Mw 4	12FINL'	0.0461	0.0459	0.0530	0.0441	0.0473	0.0045
Mw 10	109FNL'	0.0032	0.0031	0.0036	0.0033	0.0033	0.0003
Mw 10	50FNL'	0.0030	0.0031	0.0038	0.0038	0.0034	0.0005
Mw 10	12FNL'	0.0057	0.0050	0.0030	0.0047	0.0046	0.0013
PAAm Conc	060FINL'	0.0393	0.0383	0.0383	0.0367	0.0382	0.0012
Lat Conc	0005FNL'	0.0380	0.0421	0.0409	0.0412	0.0406	0.0020
Lat Conc	0015FNL'	0.0384	0.0221	0.0318	0.0351	0.0319	0.0081
Lat Conc	0020FNL'	0.0702	0.0766	0.0712	0.0570	0.0688	0.0096
Sys Conc	02FINAL	0.0283	0.0339	0.0364	0.0408	0.0349	0.0060
Sys Conc	06FINL'	0.0407	0.0414	0.0380	0.0401	0.0401	0.0017
Sys Conc	08FINL"	0.0446	0.0384	0.0346		0.0392	0.0062
Sys Conc	10FINL'	0.0454	0.0424	0.0437	0.0376	0.0423	0.0039
Lat CD	76LOWFNL	0.0738	0.0774	0.0771	0.0739	0.0756	0.0023
Lat CD	76MEDFINAL	0.0425	0.0420	0.0433		0.0426	0.0008
Ion Str	I05FNL33	0.0316	0.0308	-0.0038	-0.0004	0.0145	0.0223

Table VII2. Summary of R^2 values.

		REPLICATES					
	Filename	1	2	3	4	Mean	St.Dev
Mw 4	50FINL'	0.9949	0.9959	0.9931	0.9926	0.9941	0.0018
Mw 4	109FINL'	0.9933	0.9951	0.9961	0.9934	0.9945	0.0016
Mw 4	12FINL'	0.9835	0.9866	0.9867	0.9888	0.9864	0.0025
Mw 10	109FNL'	0.9845	0.9867	0.9866	0.9906	0.9871	0.0029
Mw 10	50FNL'	0.9670	0.9855	0.9857	0.9807	0.9797	0.0101
Mw 10	12FNL'	0.9659	0.9779	0.9654	0.9579	0.9668	0.0095
PAAm Conc	060FINL'	0.9782	0.9854	0.9727	0.9820	0.9796	0.0063
Lat Conc	0005FNL'	0.9854	0.9690	0.9894	0.9931	0.9842	0.0123
Lat Conc	0015FNL'	0.9957	0.9918	0.9935	0.9972	0.9946	0.0027
Lat Conc	0020FNL'	0.9819	0.9785	0.9861	0.9911	0.9844	0.0063
Sys Conc	02FINAL	0.9948	0.9924	0.9949	0.9937	0.9940	0.0013
Sys Conc	06FINL'	0.9932	0.9956	0.9959	0.9928	0.9944	0.0018
Sys Conc	08FINL"	0.9747	0.9779	0.9585		0.9703	0.0128
Sys Conc	10FINL'	0.9829	0.9773	0.9767	0.9919	0.9822	0.0081
Lat CD	76LOWFNL	0.9515	0.9518	0.9595	0.9467	0.9524	0.0061
Lat CD	76MEDFINAL	0.9787	0.9794	0.9799		0.9793	0.0008
Ion Str	I05FNL33	0.9476	0.9776	0.9368	0.9641	0.9565	0.0207

Table VII3. Summary of $\ln(C_{Ao}/C_{So})$ values.

		REPLICATES					
	Filename	1	2	3	4	Mean	St.Dev
Mw 4	50FINL'	0.415	0.404	0.423	0.414	0.414	0.009
Mw 4	109FINL'	0.437	0.430	0.438	0.432	0.434	0.004
Mw 4	12FINL'	0.376	0.372	0.377	0.383	0.377	0.005
Mw 10	109FNL'	0.597	0.602	0.603	0.602	0.601	0.003
Mw 10	50FNL'	0.615	0.612	0.616	0.616	0.615	0.002
Mw 10	12FNL'	0.623	0.619	0.631	0.627	0.625	0.006
PAAm Conc	060FINL'	0.811	0.815	0.821	0.827	0.819	0.008
Lat Conc	0005FNL'	1.160	1.118	1.128	1.155	1.140	0.024
Lat Conc	0015FNL'	-0.048	-0.050	-0.048	-0.048	-0.049	0.001
Lat Conc	0020FNL'	-0.245	-0.251	-0.252	-0.253	-0.250	0.004
Sys Conc	02FINAL	0.405	0.101	0.402	0.412	0.330	0.176
Sys Conc	06FINL'	0.399	0.399	0.397	0.398	0.398	0.001
Sys Conc	08FINL"	0.341	0.352	0.382		0.358	0.026
Sys Conc	10FINL'	0.410	0.410	0.417	0.424	0.415	0.008
Lat CD	76LOWFNL	1.805	1.810	1.819	1.865	1.825	0.032
Lat CD	76MEDFINAL	1.068	1.064	1.064		1.065	0.003
Ion Str	I05FNL33	0.502	0.494	0.486	0.496	0.495	0.008

APPENDIX VIII

ORTHOKINETIC DATA

Table VIII-1. Summary of Orthokinetic Data.

Time, s	Concentration of PAAm, Average of Four, mg/L			
	M_W= 154,000		M_W= 18,200	
	N_{Re}= 4000	N_{Re}= 800	N_{Re}= 4000	N_{Re}= 800
0.0	0.0200			
3.1	0.0170			
6.4	0.0157			
9.3	0.0154			
12.7	0.0145			
0.0		0.0200		
8.0		0.0166		
15.4		0.0157		
24.7		0.0149		
31.5		0.0146		
46.3		0.0127		
0.0			0.0200	
1.8			0.0191	
4.4			0.0175	
6.4			0.0169	
8.0			0.0156	
9.3			0.0151	
11.5			0.0136	
0.0				0.0200
4.0				0.0178
8.0				0.0167
13.3				0.0156
17.0				0.0136
22.0				0.0128